UNIVERSITÀ
DEGLI STUDI
DI PADOVA

Sede Amministrativa: Università degli Studi di Padova

Dipartimento di Scienze Farmaceutiche

SCUOLA DI DOTTORATO DI RICERCA IN: Biologia e Medicina della Rigenerazione
INDIRIZZO: Ingegneria dei Tessuti e Trapianti
CICLO XXIV

TITOLO TESI

STEM CELLS IN MOLECULAR AND REGENERATIVE MEDICINE

Direttore della Scuola: Ch.mo Prof. Maria Teresa Conconi
Coordinatore d'indirizzo: Ch.mo Prof. Maria Teresa Conconi
Supervisore: Ch.mo Prof. Pier Paolo Parnigotto
Correlatore: Ch.mo Dr. Joost Martens

Dottorando: Amit Mandoli

TABLE OF CONTENTS

RIASSUNTO

Le cellule staminali sono una popolazione cellulare con la particolare capacità di moltiplicarsi indefinitamente autorinnovandosi e di differenziarsi in cellule mature di qualsiasi altro tessuto attraverso il processo di differenziazione. In particolare l'utilizzo delle cellule staminali adulte costituisce una promettente applicazione nel campo della medicina rigenerativa, la riparazione dei tessuti e la terapia genica. Le cellule staminali adulte da midollo osseo (BMCs) comprendono due popolazioni cellulari: le cellule staminali ematopoietiche (HSCs), dalle quali originano tutte le cellule mature del sangue, e le cellule staminali mesenchimali (MSCs) che possono differenziare in osteoblasti, condrociti, adipociti, miociti, tenociti e cellule stromali di supporto per l'ematopoiesi. In condizioni normali l'autorinnovamento della popolazione staminale è strettamente regolato sia da segnali estrinseci che intrinseci ed un'alterazione di questo equilibrio può portare all'instaurarsi di un cancro.

In questa tesi abbiamo analizzato due differenti aspetti delle cellule staminali: le cellule staminali che danno origine a leucemia nella leucemia mieloide acuta (AML) e l'utilizzo delle cellule staminali nella medicina rigenerativa.

Nella prima parte del lavoro abbiamo approfondito il meccanismo molecolare dell' AML-ETO, risultato della traslocazione genica t(8:21) che viene associata alla trasformazione leucemica. La leucemia mieloide acuta (AML) è definita come un gruppo eterogeneo di disordini clonali causati dalla trasformazione maligna di cellule staminali o progenitori staminali di derivazione midollare, che mostrano un aumento della capacità proliferativa così come un differenziamento aberrante che porta ad una insufficienza ematopoietica (per esempio: granulocitopenia, trombocitopenia o anemia). Questi tipi di leucemia sembrano essere il risultato dell'acquisizione di riarrangiamenti cromosomici e mutazioni geniche multiple da parte delle cellule ematopoietiche multipotenti o di progenitori cellulari più differenziati e indirizzati verso una linea cellulare specifica, che risultano così trasformati in cellule staminali leucemiche o cellule inizianti la leucemia, che mantengono la capacità di autorinnovamento. L' AML è solitamente considerata una malattia delle cellule staminali e comunemente presenta alterazioni sia a livello genetico che epigenetico. L' AML è la forma più comune di leucemia acuta che colpisce soprattutto la popolazione adulta e la sua incidenza aumenta con l'età. Gli attuali approcci terapeutici hanno come target le cellule staminali leucemiche e la popolazione leucemica per intero. E' quindi di cruciale importanza riuscire a

determinare e caratterizzare l'esatto meccanismo molecolare coinvolto nella trasformazione leucemica per lo sviluppo di nuovi bersagli terapeutici. I pazienti affetti da AML che manifestano la traslocazione t(8:21) hanno una prognosi intermedia e l'identificazione di ampi eventi genici in questo subset delle AML è clinicamente rilevante in quanto potrebbe portare alla comprensione dei meccanismi molecolari della progressione della malattia.

A questo scopo sono stati analizzati i pattern di legame al DNA di AML1-ETO nelle cellule di linea AML e nei blasti di AML. Abbiamo dimostrato che AML1-ETO lega preferenzialmente le regioni che contengono le sequenze di consenso RUNX1/AML1 e ETS e che i siti di legame di AML1-ETO si sovrappongono invariabilmente a quelli di HEB e parzialmente a quelli di CBFβ, RUNX1/AML1 così come accade per i fattori ETS, quali ERG e FLI1. Le successive analisi sulle cellule t(8;21) e t(15;17) (un'altra traslocazione associata con l' AML) hanno evidenziato il legame di fattori ETS specifici per questi tipi cellulari e il legame preferenziale di AML1-ETO ai siti di legame per i fattori ETS specifici per il tipo cellulare. Inoltre è stato anche scoperto che il legame di un fattore ETS, ERG, correla con un segnale di acetilazione istonica "attiva".

Presi insieme questi risultati suggeriscono che i fattori ETS demarcano i siti regolatori ematopoietici che forniscono un target per la regolazione epigenetica (aberrante) da parte delle proteine di oncofusione.

Nella seconda parte di questa tesi è stata testata la possibilità di ottenere *in vitro* un esofago ingegnerizzato composto da matrice acellulare esofagea e cellule staminali mesenchimali (MSCs) che potesse essere impiantato *in vivo*.

Le cellule staminali mesenchimali (MSCs) nei vertebrati sono precursori multipotenti di molte linee cellulari di origine mesodermica e vengono ottenute per la maggior parte dal midollo osseo. Alcune caratteristiche delle MSCs, inclusa la capacità di migrare verso i siti di infiammazione, la facilità di trasduzione e la perdita di immunogenicità, suggeriscono che queste cellule possano essere potenzialmente utilizzabili nella medicina rigenerativa. I probabili usi terapeutici includono la possibilità di rigenerare un tessuto danneggiato, agendo come veicolo per il trasporto di transgeni terapeutici, di supportare altri tipi cellulari per il riparo tessutale, e di modulare la reazione immunitaria dell'ospite nei confronti delle cellule o dei tessuti co-trapiantati. L'uso delle MSCs permette di evitare i problemi di natura etica e morale associati

all'utilizzo delle cellule staminali di origine embrionale; inoltre le MSCs hanno già dimostrato la loro efficacia in studi preliminari che prevedevano la loro applicazione in ingegneria tessutale.

I materiali artificiali e i tessuti autologhi utilizzati per la ricostruzione dell'esofago spesso comportano complicazioni come stenosi e rottura dell'impianto nei follow-up a lungo termine. Nel presente studio è stata valutata l'adesione delle MSCs ad una matrice acellulare di esofago per la costruzione di un tessuto esofageo ingegnerizzato. Le MSCs sono state isolate da midollo osseo di coniglio, caratterizzate, espanse *in vitro* e seminate su una matrice esofagea di coniglio.

Le matrici acellulari ottenute attraverso un metodo detergente-enzimatico non presentavano marker per il complesso maggiore di istocompatibilità. Inoltre supportavano l'adesione cellulare e in non più di 24 ore dalla semina lo scaffold appariva completamente coperto dalle MSCs sia in condizione statica che in bioreattore.

Complessivamente questi risultati suggeriscono che i tessuti ingegnerizzati composti da matrice acellulare omologa e MSCs autologhe possono rappresentare un promettente approccio per il riparo di danni all'esofago.

SUMMARY

Stem Cells are rare cells with the crucial ability to self-renew and to generate mature cells of any tissue through differentiation. Adult stem cells hold great promise for regenerative medicine, tissue repair, and gene therapy. Adult bone marrow cells (BMCs) include two populations of bone marrow stem cells (BMCs): hematopoietic stem cells (HSCs), which give rise to all mature lineages of blood, and mesenchymal stem cells (MSCs), which can differentiate into osteoblasts, chondrocytes, adipocytes, myocytes, tenocytes, and haematopoiesis supporting stromal cells. Under normal condition these stem cells are tightly regulated by both intrinsic and extrinsic signals and malfunctioning in this balance can result in cancer. In this thesis we focused on two different aspects of stem cells: the leukemia stem/initiating cells in acute myeloid leukemia (AML) and the usage of stem cells in regenerative medicine.

In the first part we focused on the molecular mechanism of AML-ETO, a results from the t(8:21) translocation which has been associated with leukemic transformation. Acute myeloid leukaemia (AML) is defined as a heterogeneous group of clonal disorders caused by malignant transformation of a bone marrow-derived self-renewing stem or progenitor cell, which demonstrates an enhanced proliferation as well as aberrant differentiation resulting in haematopoietic insufficiency (i.e. granulocytopenia, thrombocytopenia or anaemia). These leukaemias are suggested to result from the acquisition of chromosomal rearrangements and multiple gene mutations in either a hematopoietic multipotent cell or a more differentiated, lineage-restricted progenitor cell that is transformed in a so-called leukaemic stem or initiating cell, which keeps the ability to self-renewal. AML is generally regarded as a stem cell disease and is commonly altered both at the epigenetic as well as the genetic level. AML is the most common acute leukemia affecting adults, and its incidence increases with age. Therapies based on the current knowledge target the bulk leukemic population and spare the leukemic stem cells. It is therefore critical to determine and characterize the exact molecular mechanism involved in leukemic transformation for the development of novel therapeutic targets. AML patients harboring the t(8:21) translocation has intermediate prognosis and the identification of genome wide events in this subset of AML is clinically relevant and would lead to the understanding of molecular mechanism of disease progression.

To this end we analyzed the DNA binding pattern of AML1-ETO in AML cell lines and in primary AML blasts. We demonstrate that AML1-ETO preferentially binds regions that contain RUNX1/AML1 and ETS core consensus sequences and that the AML1-ETO binding sites invariably consist of HEB and partially CBFβ, RUNX1/AML1 as well as of ETS factors such as ERG and FLI1. Subsequent analysis in t(8;21) and t(15;17) (another AML associated translocation) cells revealed cell type specific ETS factor binding and preferential AML1-ETO binding to the cell type specific ETS factor binding sites. In addition, we uncovered that binding of the ETS factor ERG correlates with the 'active' histone acetylation mark.
Together our results suggest that ETS factors demarcate hematopoietic regulatory sites that provide a target for (aberrant) epigenetic regulation by oncofusion proteins.
In the second part we attempted to evaluate the possibility to obtain in vitro an implantable tissue-engineered esophagus composed of acellular esophageal matrix and Mesenchymal stem cells (MSCs).

Mesenchymal Stem Cells (MSCs) are multipotent precursors to many mesodermal cell lineages in vertebrate animals and are most often obtained from bone marrow. Certain attributes of MSCs, including migration toward sites of inflammation, ease of transduction, and lack of immunogenicity, suggest these cells may be potentially useful for regenerative medicine. Putative therapeutic uses include regeneration of damaged tissue, acting as a vessel for delivering a therapeutic transgene, support of other cell types for tissue repair, and modulating the immune reaction to co-transplanted cells or tissues. The use of MSCs in tissue engineering approaches avoids the moral and technical issues associated with the use of those from embryonic source and MSCs have already demonstrated their efficacy in preliminary tissue engineering application.
Artificial materials and autologous tissues used for esophageal reconstruction often induce complications like stenosis and leakage at long-term follow-up. In the present study we attempted to evaluate the adhesion of MSCs on acellular esophageal matrix for esophagus tissue engineering. MSCs were isolated from rabbit bone marrow, characterized, expanded in vitro, and seeded onto rabbit acellular esophageal matrix.
Acellular matrices obtained by detergent-enzymatic method did not present any major histocompatibility complex marker. Moreover, they supported cell adhesion, and in as much as

just after 24 h from seeding, the scaffold appeared completely covered by MSCs in static as well as in bioreactor.

Collectively, these results suggest that patches composed of homologous esophageal acellular matrix and autologous MSCs may represent a promising tissue engineering approach for the repair of esophageal injuries.

PART I: Role of oncofusion proteins AML-ETO in Acute Myeloid Leukemia (AML).

CHAPTER 1 INTRODUCTION

E-twenty-six (ETS) specific transcription factors are a family of more than 20 helix-loop-helix domain transcription factors that have been implicated in a myriad of cellular processes, amongst which hematopoiesis (Sharrocks et al., 1997). The hallmark ETS factor protein involved in hematopoietic development is SPI1 (PU.1), which activates gene expression during myeloid and B-lymphoid cell development. Other ETS factors include the two closely related proteins ERG and FLI1, which both play crucial roles in hematopoietic development (Kruse et al., 2009; Taoudi et al., 2011) and multiple forms of cancer (Martens, 2011; Lessick and Ladanyi, 2011).

1.1 Hematopoiesis and hematopoietic stem cells

Hematopoiesis is the formation and development of blood cells. This is a continuous process throughout life where millions of blood cells are produced each hour which ensures the daily production of the over a thousand billion (1×10^{12}) blood cells needed for the survival of an adult (Ogawa, 1993). In cases of stress, such as bleeding or infection, the production increases even further to maintain homeostasis and can there by compensate stress (Kaushansky, 2006). The blood consists of a mixture of many different cell types as well as blood plasma -a liquid containing nutrients, proteins and growth factors. The blood cells are generally divided into red and white blood cells. The red blood cells (erythrocytes) have the important function of oxygen delivery from the lungs to all parts of the body. The white blood cells, myeloid or lymphoid, comprise the cellular part of the immune system with the function to fight infectious or other harmful agents, but also to clear dead cells from the body. Blood platelets (thrombocytes) are formed from megakaryocytes and are crucial in preventing bleedings from damaged blood vessels. Most mature cells in the blood system are relatively short lived. Apart from some types of lymphocytes, like memory B-cells which can survive for years, most blood cells have a life-span ranging from a few days to a few months. Therefore, progenitors are required to continuously fill up all the mature cell populations. The general progenitor is the hematopoietic stem cell (HSC).

HSCs are rare cells present in the bone marrow (BM) which are defined by their ability to self-renew as well as giving rise to differentiated cells of all blood lineages. These highly self renewing HSCs which are also termed long-term repopulating HSCs (LT-HSCs) are at the top of the hierarchy in the stem cell model of the hematopoietic system and are defined by their ability to provide life-long hematopoiesis in the host. LT-HSCs give rise to progeny cells that sequentially lose self-renewal capacity while gaining the capacity to proliferate extensively. Short-term HSCs (ST-HSC) have limited self-renewal capacity but are still multipotent. The MPP, or multipotential progenitor, is a cell downstream of the LT and ST-HSCs that has the same multilineage differentiation capacity, but is not defined as a stem cell as it lacks self-renewal ability (Morrison et al., 1997; Weissman, 2000). Up to this point all cells have the ability to differentiate to all mature lineages. From here on, progenitors become stepwise more restricted towards a specific lineage in the hematopoietic system (Figure 1). Mixed populations consisting of both HSCs and progenitor populations can be referred to as hematopoietic stem and progenitor cells (HSPC). The next step in differentiation involves a lineage choice and a restriction in potential as, according to the commonly accepted classical model of hematopoiesis, either a common myeloid progenitor (CMP) or a common lymphoid progenitor (CLP) is formed.

The CMP can give rise to two oligopotential cell types, the megakaryocytic/erythroid (MEP) and granulocyte/monocyte (GMP) progenitors, each retaining the ability to differentiate to platelets and red cells, or granulocytes, macrophages, and dendritic cells, respectively (Akashi et al., 1999; Akashi et al., 2000). The lymphoid branch of the hematopoietic tree arises at the level of the CLP, which has the potential to form B, T, natural killer (NK), and dendritic (DC) lymphoid cells (Kondo et al., 1997). However, this model has been challenged, and it is now thought that megakaryocytic/erythroid progenitors deviate already at the level of ST-HSCs while a lymphoid primed multipotent progenitor (LMPP) gives rise to lymphoid and myeloid cells.

Normal hematopoietic development is critically dependent on a tightly regulated balance between HSCs self renewal and differentiation. Studies suggest that the decision of these HSCs to differentiate or self-renew is regulated by both intrinsic and extrinsic signals (O'Reilly et al., 1997; Van Den Berg et al., 1998; Bhardwaj et al., 2001; Antonchuk et al., 2002; Reya and Clevers, 2005). The balance between these mechanisms determines whether cells remain quiescent, proliferate, differentiate, self-renew, or undergo apoptosis (Domen and Wessman, 1999; Domen et al., 2000; Orkin and Zon, 2002). In normal conditions, the majority of HSCs are

quiescent and mainly the more committed progenitors are proliferating and produce mature blood cells (Hao et al., 1996). Malfunctioning in this balance can result in leukemia or other hematological malignancies (Warner et al., 2004).

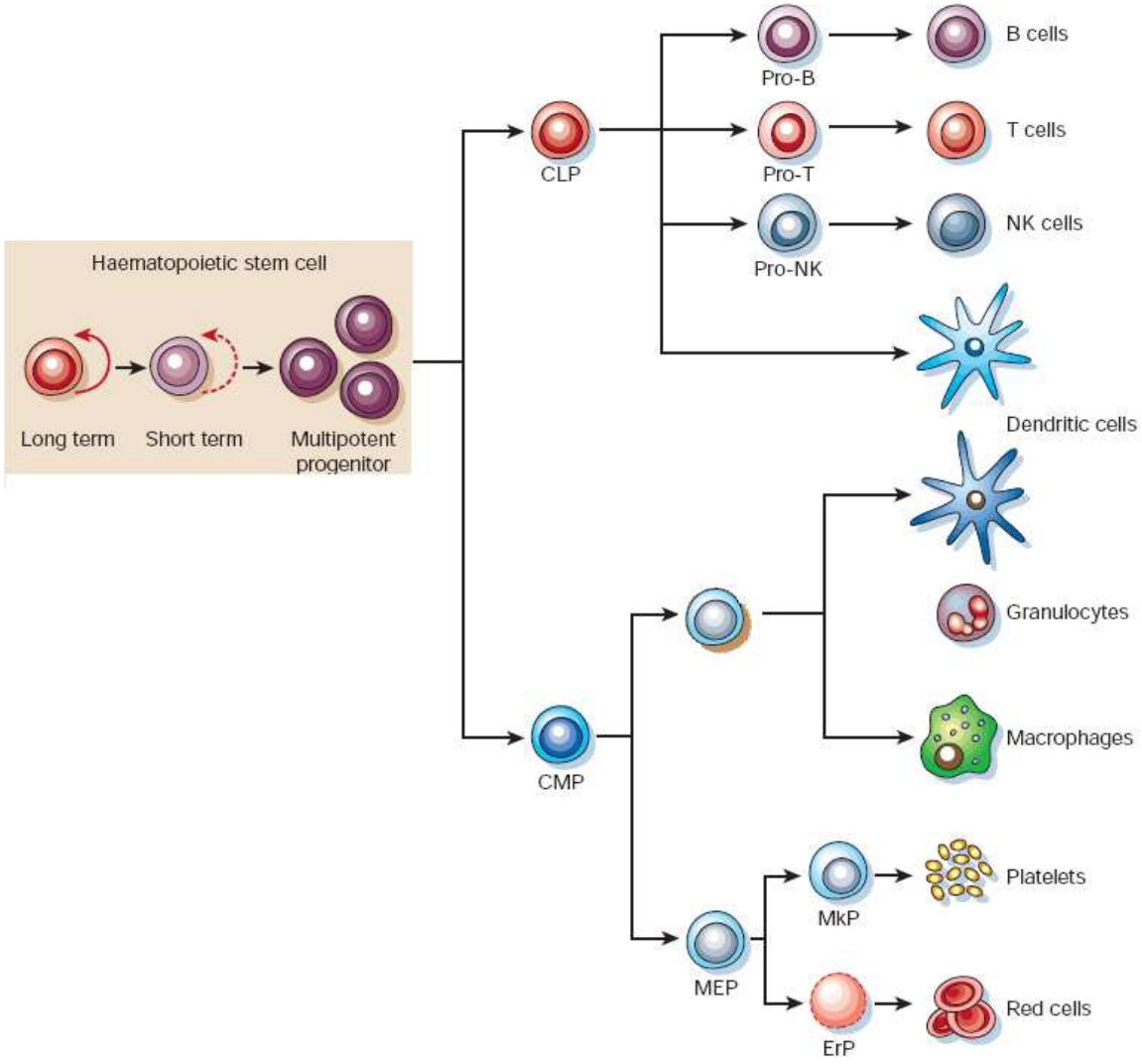

Figure 1. The hematopoietic hierarchy. Schematic drawing of the hematopoietic tree showing involved cell types and their hierarchical relationships The hematopoietic hierarchy consists of the hematopoietic stem cells (HSC), the multipotent progenitors (MPPs) and the more downstream progenitors, the common myeloid and the common lymphoid progenitor (CMP and CLP, respectively). Collectively, these give rise to all the mature cells of the hematopoietic lineage (adapted from Reya et al., 2001).

1.2 Cancer stem cells

A marked functional heterogeneity is observed among tumor cells with regards to proliferative potential and tumorigenicity. It has been consistently demonstrated that only a small subset of cells within the bulk cancerous population in solid tumors has tumor initiating ability (Buick and Pollak, 1984; Mackillop et al., 1983) as well as substantial proliferative potential (Mendelsohn, 1962; Wantzin and Killmann, 1977). This heterogeneity can be explained by two different models. One model, termed the stochastic model, proposes that every cell within a blast cell population possesses an equal but low probability of being able to initiate the tumor by entering the cell cycle (Till et al., 1964). This model assumes that a cell capable of extensive proliferation, necessary to initiate and sustain tumor growth, ultimately undergoes many more divisions than a cell lacking this ability. Therefore, the majority of cells are unable to regrow the tumor because the cumulative probability of undergoing the required number of cell divisions is very low (Reya et al., 2001). The other model, the hierarchical model, proposes that not all cells within the tumor are malignant but only a defined subset of these neoplastic cells can give rise to the bulk tumor. The hierarchical model is also called the cancer stem cell (CSC) model because the group of cells responsible for this maintenance of the tumor has stem cell-like characteristics (Schwarz and Melendez, 2011; Lane et al., 2009; Bonnet and Dick, 1997) (Figure 2). Increasing evidences support the CSC hypothesis and the overlap between SCs and CSCs has been found to be very close (Reya et al., 2001). Normal SCs have the ability to proliferate life-long, are immortal and are mostly resistant to drugs by multiple mechanisms. SCs can divide asymmetrically and produce two cells: a daughter SC and a progenitor cell that can differentiate into different lineages but cannot self-renew. SCs have specific markers and are able to differentiate into certain tissues and cells due to the microenvironment and other factors. CSCs are quite similar to these criteria. CSCs have the ability to proliferate and self-renew and are heterogeneous. The CSC develops along the differentiation path similar as normal SCs and finally the tumor comprises of tumor initiating cells (CSCs) and of abundant non-tumor initiating cells. CSCs express specific markers, often also found on SCs and importantly CSCs are often more resistant to drugs then the bulk of the tumor (Reya et al., 2001; Soltysova et al., 2005; McCulloch and Till, 2005). Other evidences for the existence of CSCs arise from *in vitro* and *in vivo* experiments. When myeloma cells were extracted from mouse ascites, separated from normal hematopoietic

cells and used in clonal colony-formation assays, only 1-10,000 to 1-100 cells were able to form colonies (Park et al., 1971). When leukemic cells were transplanted in mice assays, only 1-4% of cells could form spleen colonies (Reya et al., 2001; Soltysova et al., 2005; McCulloch and Till, 2005; Park et al., 1971; Bergsagel and Valeriote, 1968). This *in vivo* assay suggests two possible causes explaining the small percentages of cells forming colonies. Either these 1-4% cells are the only cells that have clonogenic capacity, or the probability of proliferation was low and these cells were the only cells that did proliferate while in theory all cells could have proliferated. Bonnet et al. proves that the first possibility is the most plausible one by showing that cells with the CD34+/CD38- phenotype are the cells that are able to proliferate and initiate leukemia. This population of cells represent 0.2% of the human leukemia population (Bonnet and Dick, 1997).

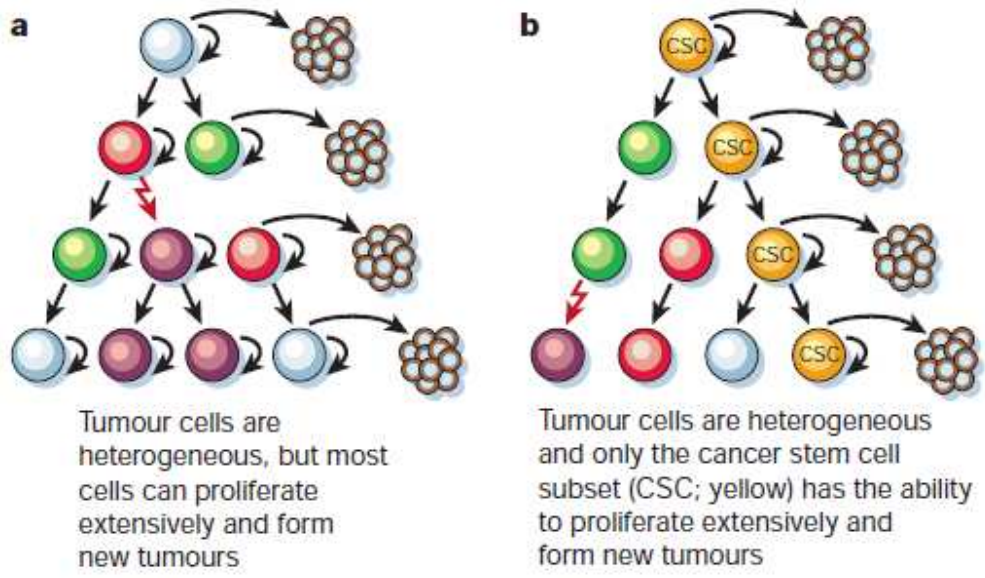

Figure 2. Two models of cancer development. Two general models of heterogeneity in solid cancer cells. **a**, Cancer cells of many different phenotypes have the potential to proliferate extensively, but any one cell would have a low probability of exhibiting this potential in an assay of clonogenicity or tumorigenicity. **b**, Most cancer cells have only limited proliferative potential, but a subset of cancer cells consistently proliferate extensively in clonogenic assays and can form new tumours on transplantation. The model shown in b predicts that a distinct subset of cells is enriched for the ability to form new tumours, whereas most cells are depleted of this ability. Existing therapeutic approaches have been based largely on the model shown in a, but the failure of these therapies to cure most solid cancers suggests that the model shown in b may be more accurate (adapted from Reya et al., 2001).

Thus, cancer stem cells are defined as the specific cell population inside a tumor which has the capacity for self-renewal, the potential to develop into any cell in the overall tumor population, and the proliferative ability to drive continued expansion of the population of malignant cells. (Zou, 2007). A study from 1964 has shown that cancer cells develop more or less according to normal development where it has shown that single teratocarcinoma cells can develop into different types of tissues and differentiate into tumorigenic and nontumorigenic cells (Kleinsmith and Pierce, 1964). Another study has shown that cancer cells are derived from the differentiation of malignant initiating cells, later to be called CSCs, in order to develop a tumor (Pierce and Wallace, 1971). Several studies have demonstrated that the CSC hypothesis holds true in human tumors (Al-Hajj et al., 2003; Passegue et al., 2003; Singh et al., 2003). It is not known whether CSCs really arise from SCs, however it is possible that deregulation of the normal SCs give rise to the development of cancer (Zou et al, 2007). Tumorigenesis starts either with transformation of a multipotent SC which leads to uncontrolled self-renewal or transformation of a more downstream progenitor cell leading to acquired self-renewal of a cell that did not have self renewal capacity (Wang and Dick, 2005).

1.3 Acute myeloid leukemia

Acute myeloid leukaemia (AML) is defined as a heterogeneous group of clonal disorders caused by malignant transformation of a bone marrow-derived self-renewing stem or progenitor cell, which demonstrates an enhanced proliferation as well as aberrant differentiation resulting in haematopoietic insufficiency (i.e. granulocytopenia, thrombocytopenia or anaemia) (Estey and Dohner, 2006). These leukaemias are suggested to result from the acquisition of chromosomal rearrangements and multiple gene mutations in either a hematopoietic multipotent cell or a more differentiated, lineage-restricted progenitor cell, that is transformed in a so-called leukaemic stem cell, which keeps the ability to self-renewal. AML is generally regarded as a stem cell disease. AML is the most common acute leukemia affecting adults, and its incidence increases with age. AML accounts for 15 to 20 percent of acute leukaemia in children and 80 percent of acute leukaemia in adults, and it is slightly more common in males (Espey et al., 2007; Garcia et al., 2007; Jemal et al., 2008). In adults, the median age at presentation is about 70 years, with three men affected for every two women (Estey et al., 2006). With approximately 1% of cancer deaths

worldwide AML is a relatively rare disease. Still, its incidence is expected to increase as the population ages. The early signs of AML include fever, weakness and fatigue, loss of weight and appetite, and aches and pains in the bones or joints. Other signs of AML include tiny red spots in the skin, easy bruising and bleeding, frequent minor infections, and poor healing of minor cuts. As an acute leukemia, AML progresses rapidly and is typically fatal within weeks or months if left untreated. However, acute myeloid leukemia is a potentially curable disease, although only a minority of patients are cured with current therapies.

1.3.1 Leukemia stem cells

It is likely that leukemia arises through the acquisition of defects in the HSCs. The concept of tumorigenic LSCs has emerged from findings that only a small subset of leukemic cells is capable of extensive proliferation *in vitro* and *in vivo*. By using non-obese diabetic mice with severe combined immunodeficiency disease (NOD/SCID mice) it was shown that cells that are able to initiate leukemia (the SCID leukemia-initiating cells or SL-ICs) have the ability to proliferate, self-renew, and differentiate via asymmetrical division. The cells identified by Bonnet as the leukemia initiating cells reside in the CD34+CD38- immunophenotypic compartment (Bonnet and Dick., 1997). Further, it was demonstrated that the malignant clone is hierarchically organized similar to the normal hematopoietic system, where the CD34+/CD38- cells are higher in the hierarchy than the CD34+/CD38+ cells. The frequency of the tumor initiating cells was approximately 1 per million AML blasts, establishing that very few AML cells had LSC capacity. A similar role for the CD34+CD38- compartment in leukemogenesis was suggested for ALL, chronic myeloid leukemia (CML) and the myelodysplastic syndrome (MDS) (Cabaleda et al., 2000; Holyoake et al., 2001; Nilsson et al., 2002).

However, the view that LSCs reside selectively in the CD34+/CD38- population was recently challenged (Tussing et al., 2008). It was demonstrated that anti-CD38 antibodies have an inhibitory effect on engraftment of cord blood (CB) cells as well as on CD38+ AML cells. When this inhibitory effect is blocked, the CD34+/CD38+ fraction can engraft from certain AML samples, although future studies will be needed to gain further insight into the LSC frequency within the CD34+/CD38+ population. Furthermore, it was recently suggested that in AMLs with

the NPM mutation, the CD34- compartment might also contain LSC activity (Wierenga et al., 2006).

These studies stress that leukemia initiating transformation and progression associated genetic events occur at the level of these primitive CD34+/CD38- cells. This parallels the hierarchy in normal BM in which a rare population of CD34+/CD38- cells have stem cell characteristics (Larochelle et al., 1996), supporting the hypothesis that malignant transformation take place in normal HSC (Figure 3). However, there is still uncertainty whether the transformation to LSC occurs in the normal stem cell or the normal progenitor cell. Recent studies in mice models have shown that AML specific oncoproteins can transform both committed progenitors and HSC into LSC (Cozzio et al., 2003; Huntly et al., 2004; Krivtsov et al., 2006; Deshpande et al., 2006). It has been demonstrated that occurrence of a mutation of the HSC is not strictly necessary, i.e. mutation of more committed progenitors may also be sufficient to transform into LSCs (Lavau et al., 2000). Mutations may confer self-renewal properties to progenitors that are normally quiescent and lead to second mutations and a subsequent transformed phenotype. Taken together, cumulative data suggests that LSCs may arise from mutations occurring in either the HSC or committed progenitor compartments, at least in murine models of disease (Deshpande et al., 2006; Lavau et al., 2000).

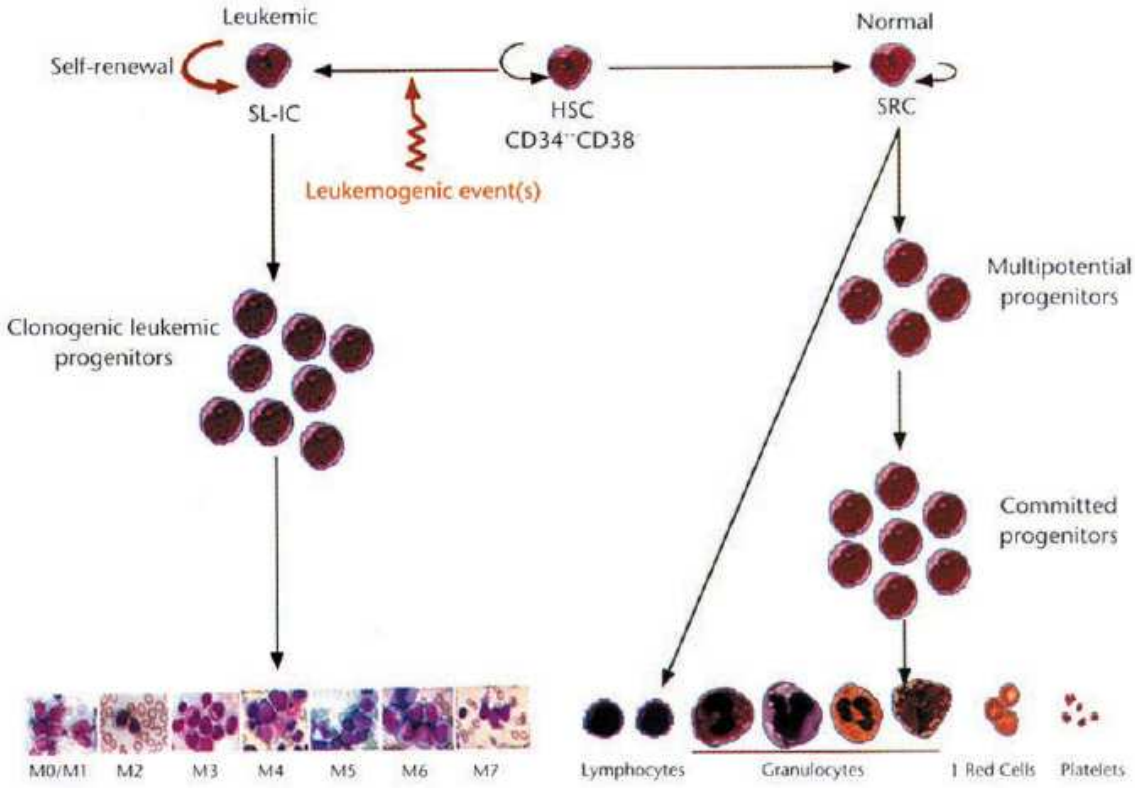

Figure 3. Acute myelogenous leukaemia forms a stem-cell hierarchy. In human normal hematopoiesis a CD34+/CD38- hematopoietic stem cell (HSC) gives rise to the SCID repopulating cell (SRC) which is capable of self renewal and the production of all form of mature blood cells through the subsequent differentiation into multipotential progenitors and committed CD34+/CD38- hematopoietic progenitors. In AML leukemic transformation of the HSC leads to the occurrence of a SCID leukemia initiating cell (SL-IC) that is capable of self-renewal and produces both the clonogenic blast cells that form the bulk of the tumor, similar to the hierarchy in normal bone marrow (adapted from Bonnet and Dick, 1997).

1.3.2 Classification of AML

The clinical signs and symptoms of AML are diverse and nonspecific, but they are usually directly caused by leukaemic infiltration of the bone marrow, with resultant cytopenia (Descheler and Lubbert, 2006). AML is considered to be a heterogeneous group of disorders with variable underlying abnormalities and clinical behaviour, including responses to treatment. Therefore, classification of the disease is important and several classification systems exist to subdivide AML.

The most commonly used method of classification is developed by the French-American-British (FAB) group that used the morphologic variability and cytochemical criteria to determine degree of commitment and differentiation of the cell lineage. Acute myeloid leukemia has been divided into 8 subtypes, M0 through to M7 under the FAB (French-American-British) classification system, based on the type of cell from which the leukemia developed and degree of maturity (Kuriyama, 2003). Although the FAB classification is useful in identifying certain biologic subtypes, it does not include all subtypes (Table1).

Recurring, non-random cytogenetic abnormalities are common in haematological malignancies, and their recognition has paved the way for the identification and therapeutic exploitation of the clonal molecular lesions that are uniquely associated with specific subtypes of AML. Appreciation of the prognostic importance of these cytogenetic and molecular genetic abnormalities has provided the major thrust for the emergence of new genetically based leukaemia classifications. In this way, and to the extent that the molecular pathogenesis of AML has been clarified, patients are characterized by one of a series of recurring genetic abnormalities with prognostic implications (Grimwade et al., 1998; Sahin et al. 2007). Therefore, a new classification of leukaemia combining morphology, cytochemistry, molecular genetics, and clinical features was proposed by the World Health Organization (WHO) (Harris et al., 1999; WHO, 2008) shown in Table 2.

FAB subtype	Common name and % of case	Associated translocations and rearrangements	Genes involved
M0	Acute myeloblastic leukemia with minimal differentiation (3%)	t(9,22)(q34,q11), Del(5q), del(7q), +8, +13, t(12;13)(p13;q14)	ABL, BCR, EGR1,IRF1,CSF1, CDK6 ETV6, TTL
M1	Acute myeloblastic leukemia without maturation (15-20%)	+6 (or trisomy 6), +4	
M2	Acute myeloblastic leukemia with maturation (25-30%)	+4 t(8;21)(q22;q22), t(6;9)(p23;q34) t(7;11)(p15;p15)	 AML1, ETO, DEK, CAN(NUP214) HOXA9, NUP98
M3	Acute promyelocytic leukemia (5-10%)	t(15,17)(q22,q12) t(11,17)(q23,q12) t(11,17)(q13,q12) t(5,17)(q23,q12)	PML,RARa, PLZF,RARa, NuMa,RARa, NPM1,RARa
M4	Acute myelomonocytic leukemia (25-30%)	+22, +4, t(6;9)(p23;q34) Inv(16)(p13,q22) t(10,11)(p11.2,q23) t(10,11)(p12,q23) t/3;7)(q26;q21)	 DEK, CAN MYH11,CBFb, ABI1,MLL, AF10,MLL EVI1, CDK6
M5	Acute monocytic leukemia (2-9%)	t(9;11)(p22,q23) t(10,11)(p11.2,q23) t(10,11)(p12,q23)	AF9,MLL ABI1,MLL, AF10,MLL
M6	Erythroleukemia (3-5%)	Del(5q), Del(7q)	EGR1,IRF1,CSF1R, ASNS,EPO,ACHE,MET
M7	Acute megakaryocytic leukemia (3-12%)	Del(5q), Del(7q), t(1,22)(p13,q13) t(11,12)(p15,p13)	EGR1,IRF1,CSF1R, ASNS,EPO,ACHE,MET, OTT,MAL, NUP98,JARID1A

Table 1. The French-American-British (FAB) classification of AML and associated genetic abnormalities (adapted from Bennett et al., 1976).

Acute myeloid leukemia with recurrent genetic abnormalities ***AML with balanced translocations/inversions*** Acute myeloid leukaemia with t(8;21)(q22;q22); RUNX1-RUNXT1(AML1-ETO) Acute myeloid leukaemia with inv(16)(p13q22) or t(16;16)(p13;q22);CBFB-MYH11 Acute promyelocytic leukaemia with t(15;17)(q22;q21);PML-RARA Acute myeloid leukaemia with t(9;11)(p22;q23);MLL-MLLT3(MLL-AF9) Acute myeloid leukaemia with t(6;9)(p23;q34);DEK-NUP124 Acute myeloid leukaemia with inv(3)(q21q26.2) or t(3;3)(q21;q26.2);RPN1-EVI1 Acute myeloid leukaemia (megakaryoblastic) with t(1;22)(p13;q13);RBM15-MKL1 ***AML with gene mutations*** Mutations affecting FLT3, NPM1, CEBPA, KIT, MLL, WT1, NRAS, and KRAS
Acute myeloid leukemia with myelodisplasia-related changes Acute leukaemia with 20% or more peripheral blood or bone marrow blasts with morphological features of myelodysplasia or a prior history of a myelodysplastic syndrome (MDS) or myelodysplastic/myeloproliferative neoplasm (MDS/MPN), or MDS- related cytogenetic abnormalities, and absence of the specific genetic abnormalities of AML with recurrent genetic abnormalities.
Therapy-related myeloid neoplasms Therapy-related acute myeloid leukaemia (t-AML), myelodysplastic syndrome (t-MDS) and myelodysplastic/myeloproliferative neoplasms (t-MDS/MPN) occurring as late complications of cytotoxic chemotherapy and/or radiation therapy administered for a prior neoplastic or non-neoplastic disorder.
Acute myeloid leukemia, not otherwise specified. Acute myeloid leukaemia with minimal differentiation Acute myeloid leukaemia without maturation Acute myeloid leukaemia with maturation Acute myelomonocytic leukaemia Acute monoblastic and monocytic leukaemia Acute erythroid leukaemia Acute megakaryoblastic leukaemia Acute basophilic leukaemia Acute panmyelosis with myelofibrosis
Myeloid sarcoma Tumour mass consisting of myeloid blasts with or without maturation, occurring at an anatomical site other than the bone marrow.
Myeloid proliferations related to Down syndrome
Transient abnormal myelopoiesis ***Myeloid leukaemia associated with Down syndrome*** ***Blastic plasmacytoid dendritic cell neoplasm*** Clinically aggressive tumour derived from the precursors of plasmacytoid dendritic cells, with a high frequency of cutaneous and bone marrow involvement and leukaemic dissemination.

Table 2. The World Health Organization (WHO) classification of acute myeloid leukaemia Chromosomal rearrangements in AML.

1.3.3 Chromosomal rearrangements in AML

In AML, somatic mutations usually results from recurrent balanced rearrangements, most often a chromosomal translocation, that originates from a rearrangement of a critical region of a proto-oncogene, but also from deletions of single chromosomes, such as 5q- or 7q-; gain or loss of whole chromosomes (+8 or -7); or chromosome inversions, such as inv(3), inv(16), or inv(8) (Mitelman et al., 2007). In addition, it appears that certain genomic loci are associated with specific subtypes of leukaemia. For example, more than 60 different recurring translocations target the MLL gene locus on chromosome 11q23 and are generally associated with a myelomonocytic or monocytic AML phenotype (FAB M4 or M5) (Meyer et al., 2009). As another example, five different translocations target the retinoic acid receptor locus (RARA), including the t(15;17)(q22;q21), which is the most common, with all being associated with the APL phenotype (FAB M3) (Lo-Coco et al., 2008).

Of the more than 749 balanced chromosome aberrations identified in leukaemia, the majority result in the formation of fusion genes (Mitelman et al., 2009). Fusion of portions of two genes usually does not prevent the process of transcription and translation, thus the fusion gene encodes a fusion protein that, because of its abnormal structure, can disrupt normal cell pathways and predispose to malignant transformation.

The mutant protein product is often a transcription factor or a key element in the transcription machinery that disrupts the regulatory sequences controlling growth rate, survival, differentiation and maturation of blood cell progenitors (Downing, 2003; Renneville et al., 2008). For instance, translocations that target the core-binding factor (CBF), a heterodimeric transcriptional complex essential for haematopoiesis, result in expression of dominant negative inhibitors of normal CBF function, such as the RUNX1- RUNX1T1 (AML1-ETO) fusion protein, leading to impaired hematopoietic differentiation (Mrózek et al., 2008). Most of these abnormalities have prognostic implications, allowing the classification of patients by risk group (Table 3).

Translocation	Prognosis	FAB	Oncofusion-protein	Occurence
t(8;21)	Favorable	M2	AML1-ETO	10% of AML
t(15;17)	Favorable	M3	PML-RARα	10% of AML
inv(16)	Favorable	M4	CBFβ-MYH11	5% of AML
der(11q23)	Variable	M4/M5	MLL-fusions	4% of AML
t(9;22)	Adverse	M1/M2	BCR-ABL1	2% of AML
t(6;9)	Adverse	M2/M4	DEK-CAN	<1% of AML
t(1;22)	Intermediate	M7	OTT-MAL	<1% of AML
t(8;16)	Adverse	M4/M5	MOZ-CBP	<1% of AML
t(7;11)	Intermediate	M2/M4	NUP98-HOXA9	<1% of AML
t(12;22)	Variable	M4/M7	MN1-TEL	<1% of AML
inv(3)	Adverse	M1/M2/M4/M6/M7	RPN1-EVI1	<1% of AML
t(16;21)	Adverse	M1/M2/M4/M5/M7	FUS-ERG	<1% of AML

Table 3. AML-associated oncofusion proteins (adapted from Martens and Stunnenberg, 2010).

1.3.4 Gene mutations in AML

Although gene rearrangements as a result of chromosomal translocations are key events in leukaemogenesis, they are usually not sufficient to cause AML. Additional genetic abnormalities, including mutations that affect genes that contribute to cell proliferation, such as FLT3, KIT, and RAS mutations affecting other genes involved in myeloid differentiation, such as CEBPA, and mutations affecting genes implicated in cell cycle regulation or apoptosis such as TP53 and NPM1, also constitute major events in AML pathogenesis with relevant prognostic implications (Mrósek et al., 2007; Renneville et al., 2008).

Mutations in FLT3 gene, including both point mutations within the kinase domain and internal tandem duplications (ITDs), are among the most common genetic changes seen in AML, occurring in 25 to 45 percent of cases and, in the case of FLT3-ITD mutations, are associated with a poor prognosis, particularly in those cases with loss of the remaining wild-type FLT3 allele (Mrósek et al., 2007; Renneville et al., 2008). Mutations of NPM1 , which is also a fusion partner in gene fusions generated by recurrent chromosome translocations such as the t(2;5)(p23;q35) in anaplastic large-cell lymphoma, the t(3;5)(q25;q35) in AML, and the t(5;17)(q35;q21) in APL (Morris et al., 1994; Yoneda- Kato et al., 1996; Redner et al., 1996), have been found nearly exclusively in *de novo* AML, with an incidence of approximately 30% in adults (and 2-6% in children), thus becoming the most frequent genetic lesions in adult *de novo*

AML (Renneville et al., 2008). NPM1 mutations occur predominantly in cytogenetically normal (CN) patients, and are associated with a significantly improved outcome in the absence of FLT3 - ITD mutation (Mrósek et al., 2007; Renneville et al., 2008). An improved outcome is also associated with CEBPA mutations, which are particularly common in AML cases with a normal karyotype. CEBPA mutations are associated with significantly better event-free survival, disease-free survival and overall survival (Preudhomme et al., 2002; Barjesteh et al., 2003). In contrast, the partial tandem duplication of the MLL gene (MLL-PTD), the first gene mutation shown to affect prognosis in AML, particularly in CN patients, was shown to be associated with significantly shorter complete remission duration (Döhner et al., 2002). The same seems to be true for the BAALC and ERG genes, whose over-expression is associated in both cases with an adverse prognosis, particularly in CN AML (Marcucci et al., 2005; Baldus et al., 2006).

1.4 The two-hit model of leukemogenesis

A lot of the commonly occurring leukemia-associated fusion genes have been shown to be insufficient for transformation. In human leukemia, there are numerous cases in which a chromosomal translocation, co-expressed with an activating mutation or with an aberrant expression of proto-oncogenes, is detected. These observations favour a pathogenic model of AML, in which the interaction of at least two different groups of genetic alterations are necessary for disease development (Gilliland, 2002) (Figure 4). These oncogenic events can be divided in two classes according to the two-hit model of leukaemogenesis (Kelly and Gilliland, 2002; Speck and Gilliland, 2002). In this model, there is a cooperation between gene rearrangements and mutations that confer a proliferative and/or survival advantage and those that impair hematopoietic differentiation (Kelly and Gilliland, 2002; Fröhling et al., 2005; Kosmider and Moreau-Gachelin, 2006; Moreau-Gachelin, 2006; Renneville et al., 2008). Class I mutations represented by activating mutations of cell-surface receptors such as RAS, or tyrosine kinases such as FLT3, result in enhanced proliferative and/or survival advantage for hematopoietic progenitors, leading to clonal expansion of the affected haematopoietic progenitors (Fröhling et al., 2005; Kosmider and Moreau- Gachelin, 2006; Moreau-Gachelin, 2006; Renneville et al., 2008).

The second type of lesion, class II mutations (represented by core-binding-factor gene rearrangements, resulting from the t(8;21), inv(16), or t(16;16), or by the PML–RARA and MLL gene rearrangements) are associated with impaired hematopoietic differentiation (Fröhling et al., 2005; Kosmider and Moreau-Gachelin, 2006; Moreau-Gachelin, 2006; Renneville et al., 2008).

Support for this model comes from the studies in mouse showing that class I and II mutations by themselves can only produce a myeloproliferative disorder but do not cause AML (Renneville et al., 2008). Only when both classes of mutations are present, their cumulative effect can develop AML. In a conditionally expressing AML1-ETO mouse model, only mice which had been treated additionally with the mutagen ENU developed AML, while the non treated group showed only minimal hematopoietic abnormalities (Higuchi et al., 2002). A very similar observation was reported with an hMRP8-AML1-ETO transgenic mouse model and a murine retroviral AML1-ETO model (de Guzman et al., 2002; Yuan et al., 2001). AML1-ETO co-expressed with tyrosine kinase FLT3-LM (Schessl et al., 2005) or Wilms tumour (WT1), a proto-oncogene, could induce full blown leukemia (Nishida et al., 2006) in murine bone marrow transplantation models. Similarly, the TEL/PDGFRβ fusion gene cooperates with AML1/ETO in inducing AML in mice (Grisolano et al., 2003). Similarly translocation t(15;17) PML-RARα, commonly found in acute pro-myelocytic leukemias, is known to co-operate with BCL2 (Wuchter et al., 1999) or with activating FLT3 mutations (Kelly et al., 2002; Reilly, 2002) in inducing leukemia. These data clearly show that additional cooperating mutations are crucial for the pathogenesis of most frequent sub-types of AML.

Additional support for the two-hit model comes from demonstration that class I and class II lesions occur together more commonly than do two class I or two class II lesions (Dash and Gilliland, 2001; Care et al., 2003; Downing, 2003; Valk et al., 2004b; Cammenga et al., 2005; Cairoli et al., 2006; Schnittger et al., 2006; Renneville et al., 2008). This model, however, cannot easily explain the -5/-7 AML but could be modified to account for the role of epigenetic factors (Egger et al., 2004). Specifically, various putative tumour suppressor genes are hypermethylated and thus silenced in AML, and because hypermethylation, once present, is permanent, it is functionally equivalent to a genetic mutation (Toyota et al., 2001). Many of the identified gene mutations that affect proliferation or differentiation pathways represent potential targets for the development of new drugs (Figure 4). Class I mutations can be molecularly targeted with FLT3 -specific inhibitors, or with farnesyltransferase inhibitors, which preclude localization of RAS to

the plasma membrane. Class II mutations might be targeted by compounds that restore normal haematopoietic differentiation, as in the use of all-trans-retinoic acid (ATRA) for the treatment of acute promyelocytic leukaemia that is associated with the PML–RARA fusion, and potentially by histone deacetylase (HDAC) inhibitors (Renneville et al., 2008).

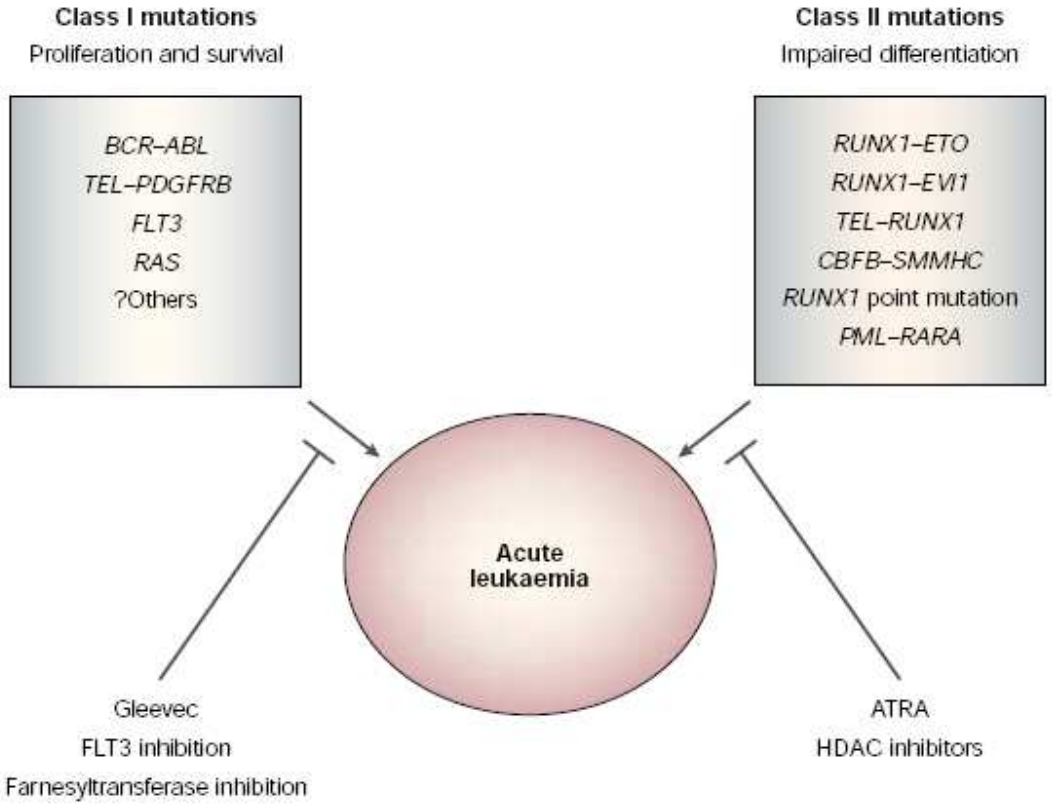

Figure 4. Two hit model of leukaemogenesis. The Class I mutations which are involved in proliferation and Class II mutations which result in impaired differentiation cooperate with each other in inducing leukemia (adapted from Speck and Gilliland, 2002).

1.5 CBF family of transcription factors

The core binding factors (CBFs) are heterodimeric transcription factors which activate and repress transcription of key regulators of growth, survival and differentiation pathways. These are frequent targets of mutations and re-arrangements in human AMLs and ALLs. The CBF family

consists of three distinct DNA binding CBFα units: RUNX1, RUNX2, RUNX3 and a common non DNA binding CBFβ subunit that is encoded by CBFβ.

AML1. RUNX1 or AML1 was the first mammalian CBF gene to be cloned. All RUNX proteins contain a runt homology DNA binding domain at the N-terminus which is highly homologous to the drosophila Runt protein which is involved in segmentation and sex determination (Romana et al., 1995). Runx1 (and by extension CBFβ) is required for the differentiation of definitive hematopoietic progenitors and HSCs from a hemogenic endothelium in the mouse embryo (Miyoshi et al., 1991; Mukouyama et al., 2000). Besides the RUNT domain AML1 also contains a transactivation domain (Meyers et al., 1995) and a nuclear matrix attachment signal (NMTS) (Zeng et al., 1998). Mutations in the AML1 gene were shown to be associated with a number of malignant and premalignant conditions including acute myelogenous leukemia, childhood acute lymphocytic leukemia, familial platelet disorder, and myelodysplastic syndromes (Speck and Gilliland, 2002). AML1 is involved in many different chromosomal translocations, the most common ones being t(8;21)(q22;q22) (Downing et al., 1993; Erickson et al., 1992) and inv(16)(p13;q22) which account for approximately 15% of adult AML (Martens and Stunnenberg., 2010). The TEL-AML1 translocation is observed in 20–25% of pediatric ALL (Liu et al., 1993). The AML1 gene generates three different spliced isoforms, AML1a, AML1b, and AML1c, where AML1a differs from AML1b and AML1c by the lack of a C-terminus (Miyoshi et al., 1995).

ETO. ETO (also called MTG8 or CBFA2T1) is best known as the fusion partner of AML1 in leukemia carrying the t(8;21) translocation (Miyoshi et al., 1993). The ETO gene is located on chromosome 8q22. Earlier studies have revealed that ETO interacts with nuclear co-repressor proteins and have shown that these interactions enable it to play a critical role as transcriptional repressor by interacting with co-repressors like NCOR, SMRT, Sin3 and various other HDACs. It also acts as a negative regulator of AML1 transcriptional regulation (Gelmetti et al., 1998; Lutterbach et al., 1998; Wang et al., 1998)

AML1-ETO. AML1-ETO was first reported by Janet D. Rowley in a leukemic patient. Approximately 10% of AML cases carry the t(8;21) translocation, which involves the AML1

(RUNX1) and ETO genes, and express the resulting AML1-ETO fusion protein. The resulting fusion yields 177 amino acids (aa) of AML1 with its N-terminal region containing the Runt domain (RHD) and 575 amino acids of the entire reading frame of ETO. Due to its similarities with drosophila nervy proteins, ETO has four domains named nervy homology domains (NHR1-4). It has 50% to 70% sequence homology with the drosophila homologue. The NHR1 domain is also known as TAF domain and resembles the TATA binding associated factors in humans as well as drosophila (TAF110) (Erickson, 1994), which indicates its role as a transcription factor. NHR2 is known as 'Hydrophobic Heptad Repeats' (HHR), essential for hetero- and homodimerizations (Gelmetti, 1998). NHR3 contains the predicted coiled-coil structure (Minucci et al., 2000) and NHR4 a myeloid-Nervy-DEAF1 homology domain (MYND) with two predicted zinc-finger motifs which are involved in protein–protein interaction ((Erickson et al., 1994; Gross and McGinnis, 1996). The fusion protein AML1-ETO is suggested to function as a transcriptional repressor by recruiting NCoR/SMRT/HDAC complexes to DNA through its ETO moiety (Davis et al., 2003). Moreover, it has been shown that AML1-ETO blocks AML1-dependent transactivation in various promoter reporter assays, suggesting it may function as a dominant negative regulator of wild-type AML1 (Meyers et al., 1995; Uchida et al., 1997; Frank et al., 1995). AML1- ETO was recently hypothesized to target DNA through E-box motifs as a result of physical interactions with transcription factors of the E-protein family, in particular HEB/TCF12 (Gardini et al., 2008; Zhang et al., 2004). Furthermore it has been shown that ETS factors interact with AML1-ETO and thus play a major role in leukemogenesis in t(8;21) leukemia.

1.6 E-twenty-six (ETS) factors

E-twenty-six (ETS) specific factors are a family of more than 20 helix–loop–helix domain transcription factors that have been implicated in a myriad of cellular processes, amongst which (aberrant) hematopoiesis (Sharrocks et al., 1997). The hallmark ETS factor involved in hematopoiesis is encoded by the PU.1 (SPI1) gene and represents an ETS-domain transcription factor that is a master regulator of gene expression during myeloid and B-lymphoid cell development. Other ETS factors include the two closely related proteins ERG and FLI1, which both play crucial roles in hematopoietic development (Kruse et al., 2009; Taoudi et al., 2011) and multiple forms of cancer (Martens, 2011; Lessick and Ladanyi, 2011).

PU.1. PU.1 is a key differentiation regulator that, in concert with transcriptional partners, can modulate the expression of numerous genes expressed in hematopoietic cells (Burda et al., 2010) including known cell-surface proteins (CD11b, CD16, CD18 and CD64), cytokines and their respective receptors (G-CSF, GM-CSF and M-CSF) and many other gene targets. The requirement of PU.1 during hematopoiesis has been addressed by various experimental approaches (reviewed in Burda et al., 2010). Collectively these studies revealed an important and crucial role of PU.1 as a primary transcriptional determinant of hematopoietic cell fate and emphasize the potential consequences on hematopoiesis of aberrant regulation of this ETS factor.

ERG. ERG emerged as a central player in blood development in a genetic screen for hematopoietic regulators in mice (Loughran et al., 2008; Kruse et al., 2009). This screen revealed the necessity of ERG in establishing definitive hematopoiesis and for hematopoietic stem cell maintenance. The importance of ERG in blood development was further confirmed when it was shown that ERG is involved in megakaryopoiesis and T-cell development, that ERG is required for ESC differentiation toward the endothelial fate and that it regulates angiogenesis and endothelial apoptosis (Anderson et al., 1999; Lefebvre et al., 2005; Kruse et al., 2009; Nikolova-Krstevski et al., 2009; Birdsey et al., 2008; Stankiewicz and Crispino, 2009). Finally, a role for ERG in growth promotion of hematopoietic cells was suggested in experiments showing that forced expression of ERG in adult bone marrow cells induces expansion of T, erythroid and precursor B cells (Tsuzuki et al., 2011). The growth promoting effects of ERG in all these studies suggest that aberrant regulation of ERG could play an important role in development of leukemia and other cancers. Indeed, shRNA mediated silencing of ERG in a panel of 10 leukemic cell lines attenuated growth (Tsuzuki et al., 2011), suggesting a crucial role of ERG in maintaining a proliferative state.

FLI1. Fli1 is a phosphoprotein, closely related to ERG and plays a central role in hematopoiesis. Compared to ERG, which has a half life of 21 hours FLi1 has a relatively short half life of 100 min (Zhang et al., 2005). Fli1 is mutated in a number of cancers, including Ewing's sarcoma and erythroleukemia (Delattre et al., 1992). Genetic manipulation in mice (Hart et al., 2000; Spyropoulos et al., 2000) and mutation in humans (Hart et al.,2000; Raslova et al., 2004) have revealed multiple roles for FLi1 in hematopoiesis, including the production of megakaryocytes

and platelets, and a requirement for Fli1 in normal HSC and megakaryocyte homeostasis (Kruse et al., 2009). Indeed, Fli1 is implicated in the regulation of important stem cell genes, emphasizing its role within the hematopoietic stem cell compartment (Pimanda et al., 2007; Gottgens et al., 2002).

1.7 ETS factors and oncofusion proteins

Recently, SPI1 (PU.1) was identified as a binding partner of the PML-RARα oncofusion protein complex in an inducible overexpression model (Wang et al., 2010). The PML-RARα oncofusion protein is the result of a translocation involving the PML gene on chromosome 15 and the retinoic acid receptor α (RARα) on chromosome 17 (de The et al., 1990; Kakizuka et al., 1991). Numerous studies have shown that at the molecular level PML-RARα aberrantly regulates chromatin through recruitment of histone deacetylases (HDACs) (Martens et al., 2010; Lin et al., 1998; Grignani et al., 1998). Although the genomic regions targeted by the PML-RARα oncofusion protein have recently been identified (Martens et al., 2010), genomic binding analysis of AML1-ETO has thus far only been studied using an inducible AML1-ETO cell line (Gardini et al., 2008).

1.8 Aim of the study

Significant progress has been made toward a detailed characterization of chromosomal translocations/rearrangements in AML; however, in most cases the exact molecular mechanism of leukemic transformation is not known. Studies suggested that cancer is stem cell disease and it is epigenetic as well as genetic disease and therapies based on the current knowledge target the bulk leukemic population and spare the leukemic stem cells. It is therefore critical to determine and characterize the exact molecular mechanism involved in leukemic transformation for the development of novel therapeutic targets. AML patients harboring the t(8:21) translocation has intermediate prognosis and the identification of genome wide events in this subset of AML is clinically relevant and would lead to the understanding of disease progression. The purpose of this study is to establish genome wide binding profile of the AML-ETO oncofusion protein to gain further insight into genetic as well as epigenetic mechanisms by which AML-ETO affects

normal hematopoiesis and facilitate leukemic transformation into leukemic stem cells with following objectives:

- To identify Genome wide binding profile of AML-ETO cell lines and patients
- To identify the role of other factors in AML-ETO leukemogenesis
- To identify epigenetic association with t(8:21) blast

CHAPTER 2 MATERIALS AND METHODS

2.1 IN VITRO EXPERIMENTS

2.1.1 Cell culture. Kasumi-1 (Asou et al., 1991), SKNO-1 (Matozaki et al., 1995) and U937 AML1 ETO (UAE) cells (Alcalay et al., 2003) were routinely cultured in RPMI 1640 supplemented with 10% FCS at 37 °C. AML1-ETO expression in UAE cells was induced by treatment for 5 hours with 1 mM zinc. 293T and MCF7 cells were cultured in DMEM supplemented with 10% FCS at 37 °C. K562-ERG cells were cultured in RPMI with 10% FCS, 500 µg/ml G418 and 1 µg/ml puromycin at 37 °C. ERG expression in K562-ERG cells was induced by treatment for 72 hours with 1 µg/ml doxycyclin.

2.1.2 Transfection. 293T, MCF7 and K562-ERG cells were transfected with pcDNA ERG or AML1-ETO expression constructs using lipofectamine (Invitrogen) according to the manufacturers protocol. Cells were harvested 24 hours after transfection. Protein lysates were tested by western blotting using antibodies against AML1-ETO (AE), TBP (Diagenode), KAP1 (Abcam) and ERG (sc-353, Santa Cruz) and subsequently used for ChIP experiments.

2.1.3 Protein extraction and Western Blot. Nuclear fractions were harvested as described (Nancy et al1991). Briefly cells were washed with cold PBS, resuspended in cold hypotonic lysis buffer and incubated on ice for 10 minutes. Cytoplasmic fraction was yielded after centrifugation for 10 second. The pellet was suspended in hypertonic buffer, incubated on ice for 20 min and centrifuged for 2 min at 4^{o}C and supernatant (nuclear fraction) was stored. Nuclear fractions were mixed with 5x sample buffer and separated on 8% sodium dodecyl sulfate-polyacrylamide gel electrophoresis, transferred to nitrocellulose membrane (Bio-Rad), blocked in 5% nonfat dry milk in Tris(tris(hydroxymethyl)aminomethane) buffered saline with 0.1% Tween 20 (TBS-T) for 1 hour at room temperature, and then incubated with primary antibodies in TBS-T (with 5 % nonfat dry milk) overnight at 4°C. AML-ETO was detected with rabbit polyclonal antibody against AML-ETO, TBP, KAP1 and ERG (1:1000) followed by an IgG-HRP-conjugated secondary antibody against rabbit (Dako). Proteins were visualized using ECL (GE healthcare).

2.1.4 CHIP. For ChIP cells were crosslinked with 1% formaldehyde for 20 min at room temperature, quenched with 1.25 M glycine and washed with three buffers: (1) PBS, (ii) buffer of composition 0.25% Triton X 100,10mM EDTA, .5 mM EGTA, 20mM HEPES pH 7.6 and (iii)

0.15 M NaCl, 10mM EDTA, .5 mM EGTA, 20mM HEPES pH 7.6. Cells were then suspended in ChIP incubation buffer (.15% SDS, 1% Triton X 100, 150mM NaCl, 10mM EDTA, .5 mM EGTA, 20mM HEPES pH 7.6) and sonicated using a Bioruptor sonicator (Diagenode) for 20 min at high power, 30 sec ON, 30 seconds OFF. Sonicated chromatin was centrifuged at maximum speed for 10 min and then incubated overnight at 4°C in incubation buffer supplemented with .1% BSA with protein A/G-Sepharose beads (Santa Cruz) and 1µg of antibody. Beads were washed sequentially with four different wash buffers at 4°C: two times with solution of composition 0.1% SDS, 0.1% DOC, 1% Triton, 150 mM NaCl, HEG, one time with the solution same as before but with 500 mM NaCl, one time with solution of composition 0.25 M LiCl, 0.5% DOC, 0.5% NP-40, HEG and two times with HEG. Precipitated chromatin was eluted from the beads with 400 µl of elution buffer (1% SDS, 0.1 M NaHCO3) at room temperature for 20 minutes. Protein-DNA crosslinks were reversed at 65°C for 4 hours in the presence of 200mM NaCl, after which DNA was isolated by qiagen column.

Chips were performed using specific antibodies to ETO, HEB, ERG, FLI1 (Santa Cruz), H3K9K14ac, AML1-ETO, ETO, CBFα, RNAPII (Diagenode), RUNX1, FLI1 (Abcam) and H4panAc (Millipore) and analyzed by quantitative PCR (qPCR) or ChIP-seq.

2.1.5 qPCR. ChIP experiments were analyzed by qPCR with specific primers using SYBR Green mix (Biorad) with MyiQ machine (Biorad). Relative occupancy was calculated as fold over background, for which the second exon of the Myoglobin gene or the promoter of the H2B gene was used. Primers for qPCR were designed with Primer 3. PCR efficiency of primers was calculated with series of 10-times dilutions and accepted when found to be reliable (20.15). Primer sequences are available in appendix1.

2.1.6 RE-CHIP. For re-Chip experiment, chromatin was first incubated overnight at 4 °C with first antibodies (either ERG or AML-ETO) as for regular ChIPs. After standard washing, elution was performed with 1% SDS (30 min, 37 °C). Eluate was diluted with Incubation buffer with protease inhibitors and incubated overnight with second antibodies (AML-ETO or ERG) and protein-A/G beads (Santa Cruz) at 4°C. The subsequent steps were performed as for regular ChIPs followed by qPCR.

2.1.7 Co-immunoprecipitation. Co-immunoprecipitation experiments were performed as before (Martens et al., 2002) in assay buffer (0.1% NP-40, 250 mM NaCl, 50 mM Tris-HCl (pH 7.5) containing a mixture of protease inhibitors). SKNO-1 protein lysates were incubated overnight

with ERG or IgG antibodies and prot A/G beads (Santa Cruz), washed 4 times in assay buffer and tested using western blotting for the presence of AML1-ETO or RNAPII (Diagenode).

2.1.8 GST-fusion proteins. GST fusion protein-coated beads and GST fusion proteins were prepared as previously reported (Martens et al., 2002). GST fusion proteins were constructed by PCR amplification of different AML1-ETO domains in pGEX-2T using the BamHI and EcoRI restriction sites. Expression of GST and GST-fusion proteins was induced by IPTG treatment for 3 hours.

GST-constructs (with corresponding AML1-ETO amino acid sequence):

1 RHD/AML (aa 1-183)

2 PST1 (aa 172-271)

3 NHR1 (aa 257-395)

4 PST2 (aa 396-481)

5 NHR2 (aa 467-579)

6 NHR3 (aa 565-662)

7 NHR4PST (aa 663-752)

2.1.9 MethylCap^{TM}. Pull down experiments were performed using GST fused to the MBD domain of MeCP2 (Diagenode). DNA was isolated from blast cells, sonicated to generate fragments of approximately 400 bp and pulled down with GST-MBD coated paramagnetic beads and the IP-STAR robot (Diagenode). After washing with 200 mM NaCl, the bound methylated DNA was eluted using 700 mM NaCl and used for high-throughput DNA sequencing (Brinkman et al., 2010).

2.1.10 Illumina high throughput sequencing. End repair was performed using the precipitated DNA of ~ 6 million cells (3-4 pooled biological replicas) using Klenow and T4 PNK. A 3' protruding A base was generated using Taq polymerase and adapters were ligated. The DNA was loaded on gel and a band corresponding to ~300 bp (ChIP fragment + adapters) was excised. The DNA was isolated, amplified by PCR and used for cluster generation on the Illumina 1G genome analyzer. The 32 bp tags were mapped to the human genome HG18 using the eland program allowing 1 mismatch. For each base pair in the genome the number of overlapping sequence reads was determined and averaged over a 10 bp window and visualized in the UCSC genome browser (http://genome.ucsc.edu).

2.1.11 Patients' AML blasts and normal CD34+ hematopoietic cells. t(8;21) AML blasts from peripheral blood or bone marrow from de novo AML patients were studied after informed consent was obtained in accordance with the Declaration of Helsinki. The protocol was approved by the Ethical Review Board of the University Medical Center Groningen, the Netherlands. AML mononuclear cells were isolated by density gradient centrifugation and AML CD34+ cells were selected as described (Schepers et al., 2007). Percentages of CD34+ cells in the mononuclear AML cell fraction for patient 186 were 25%, for 229 were 38% and for 12 were 32%. Normal CD34+ cells were obtained from donors following written informed consent. APL blasts were obtained from a patient with newly diagnosed AML having t(15;17). The sample consisted of more than 80% bone marrow invasion and was a typical FAB M3 expressing the Bcr1 PML-RARα variant. Normal karyotype AML blasts were obtained from patients with newly diagnosed AML FAB M0/M1 and FAB M2. These studies were approved by the S.U.N. Ethical Committee (7028032003).

2.1.12 RNA-Seq. Total RNA was extracted from SKNO-1 cells with the RNeasy kit and on-column DNase treatment (Qiagen) and the concentration was measured with a Qubit fluorometer (Invitrogen). 250 ng of total RNA was treated by Ribo-Zero rRNA Removal Kit (epicentre) to remove ribosomal RNAs according to manufacturer instructions. 16 µl of purified RNA was fragmented by addition of 4 µl 5x fragmentation buffer (200 mM Tris acetate pH 8.2, 500 mM potassium acetate and 150 mM magnesium acetate) and incubated at 94°C for exactly 90 seconds. After ethanol precipitation first strand cDNA was synthesized from the fragmented RNA with SuperscriptIII (Invitrogen) using random hexamers. First strand cDNA was purified by Qiagen mini elute columns and second strand cDNA was prepared in the presence of dUTP instead of dTTP. Double stranded cDNA was purified by Qiagen mini elute columns and used for Illumina sample prepping and sequenced according to the manufacturars instructions. A total of 16,178,852 RNA-seq reads were uniquely mapped to HG18 and used for bioinformatic analysis. RPKM (reads per kilobase of gene length per million reads) (Mortazavi et al. 2008) values for RefSeq genes were computed using tag counting scripts and used to analyze the expression level of AML1-ETO and RUNX1/AML1 target genes in SKNO-1 cells. The Mann-Whitney U test was used to statistically address the difference between AML1-ETO and RUNX1 target genes.

2.2 Bioinformatic analysis

2.2.1 Identification of AML1-ETO binding sites in Kasumi-1 and SKNO-1. AML1-ETO peaks in SKNO-1 and Kasumi-1 cells were detected using MACS (Zhang et al., 2008) at a p-value cut off for peak detection of 10^{-8}. To identify high confidence binding sites, i.e., the strongest fraction of binding events in both these cell lines we employed a regression analysis in which each binding site is evaluated for its relative tag density in both cell lines. For this, in each resulting peak region the number of tags for AML1-ETO in Kasumi-1 and SKNO-1 cells was counted. Subsequently all regions were tested for relative AML1-ETO tag densities (tag density at peak divided by total number of tags in all peaks), sorted and visualized in a dot plot. The data points of the dot plot were subsequently used for regression analysis, with resulting regression curves, plus cut off values shown in figures 6B and 7F. To increase visibility, dots representing the individual data points were removed. A cut off value was set at 0,00010 (>14 tags/kb), which represent in Kasumi-1 cells a binding site composed of 14 tags in a window of 1 kb and 6.2 million tags sequenced in total.

2.2.2 Quantitative PCR validation of AML1-ETO binding sites. High confidence AML1-ETO peaks from Kasumi-1/SKNO-1 cells were divided in three categories: high, middle, low. From each of these categories 10 peaks were selected and subsequently validated in ChIP-qPCR experiments using the primer pairs below. The resulting occupancy levels for each of the three categories was plotted in a boxplot and compared to the number of tags within each high, middle or low peak region.

2.2.3 Peak detection. Peaks were generally identified using MACS (Zhang et al., 2008). Random genomic regions were selected using the complete human genome sequence and the Rand function of Perl to identify sets of random genomic positions. These random positions were subsequently extended to 1 kb.

2.2.4 Tag counting. Tags within a given region were counted and adjusted to present the number of tags within a 1 kb region. Subsequently the percentage of these tags as a measure of the total number of sequenced tags of the sample was calculated. For the heatmap display in Figures 6C, 9C and 13B a cut off was used of 3 % tags/kb (10-4), which represent a peak of 1000 bp width and composed of 30 tags or more with 10 million tags sequenced (or 15 tags with 5 million tags sequenced). In Figure 19E and 19F the average tag density per bin of H3ac or DNAme from two

patients (pz229 and pz186) was determined. In Figure 11C a t-test was used to show statistical difference between AML1-ETO occupancy before and after dox treatment of K562-ERG cells. For box plots the middle dot represents the median value, the bottom and top of the box are the 25th and 75th percentile and the ends of the whiskers represent the 9th and the 91st percentile.

2.2.5 Peak distribution analysis. To determine genomic locations of binding sites peak files were analyzed using a script that annotates binding sites according to all RefSeq genes. With this tool every binding site is annotated either as promoter (-500 bp to the Transcription Start Site), non promoter CpG island, intron, exon or intergenic (everything else).

2.2.6 Accessibility mapping. To examine whether ERG bound to accessible sites we used public available DNAseI accessibility data from K562 cells (GEO series GSE29692) and the DNAseI hotspots as can be found under the 'regulation' tracks in the UCSC browser.

2.2.7 Motif analysis. To identify the motifs underlying the AML1-ETO peaks gimmemotifs (van Heeringen and Veenstra, 2011) was used. Briefly, gimmemotifs is a de novo motif prediction pipeline combining three motif prediction tools, MotifSampler (Thijs et al., 2001), Weeder (Pavesi et al., 2004) and MDmodule (Liu et al., 2002). Gimmemotifs was run on 20% of randomly selected 200-bp peak sequences (centered at the peak summit as reported by MACS) and position weight matrices (PWMs) were generated. The 'large' analysis setting was used for Weeder. MDmodule and MotifSampler were each used to predict 10 motifs for each of the widths between 6 and 20. The significance of the predicted motifs was determined by scanning the remaining 80% of the peak sequences and two different backgrounds: a set of random genomic sequences with a similar genomic distribution as the peak sequences and a set of random sequences generated according to a 1st order Markov model, matching the dinucleotide frequency of the peak sequences. P-values were calculated using the hypergeometric distribution with the Benjamin-Hochberg multiple testing correction. All motifs with a p-value <0.001 and an absolute enrichment of at least >1.5-fold compared to both backgrounds were determined as significant.

To count motifs in ERG binding sites we derived the weight matrix of different consensus binding sites for various proteins involved in hematopoiesis from Jaspar (http://jaspar.genereg.net/). All ERG binding sites were subsequently examined for the presence or absence of these motifs using a script that scans for homology of the matrix within the DNA sequence underlying the ERG binding site (pwmscan.py)(see also van Heeringen et al., 2010) using a threshold score of 0.9 (on a scale from 0 to 1). Due to the different composition and

length of the motifs the resulting homology scores could not be directly compared and needed to be normalized. For this we calculated the lower (no homology) and higher (complete homology) scores for each individual motif with the script pwm_scores.py, and used these scores to rank each motif score within an ERG binding site to a scale from 0 to 1. These ranked values were subsequently displayed in a heatmap in which red means a high score for a particular motif (and thus the presence of a motif) and green a low score (and the absence of the motif).

For the motif count distribution analysis in Figure 11F the Chi-square test was used to show a statistical significant change in the pattern.

2.2.8 Identification of AML1-ETO binding sites in patients cells. Peaks in patient samples 12, 186 and 229 were detected using MACS (Zhang et al., 2008) at a p-value cutoff for peak detection of 10-6. Resulting peaks files were overlapped and common peaks identified in all three patient samples were selected for further analysis.

2.2.9 Expression analysis. Expression of ETS factors in AML samples was examined in the dataset published by (Valk et al., 2004) using oncomine (www.oncomine.com). ETS factor candidate proteins were selected based on levels of expression and change in expression in AML as compared to control cells (CD34+ and bone marrow).

For expression analysis of the AML1-ETO high confidence binding sites identified in patient samples the AML1-ETO binding sites were coupled to their nearest ENSEMBL gene. Expression of these genes was evaluated through usage of a published data set (Valk et al., 2004) on 22 t(8;21) AMLs, 18 t(15;17), 3 normal CD34+ cells and 46 non AML1-ETO FAB M2 AMLs. For this, the corresponding affymetrix ID for each ENSEMBL gene was identified and corresponding expression changes of non AML1-ETO FAB M2 AMLs versus normal CD34+ cells, AML1-ETO AMLs versus normal CD34+ cells and t(15;17) AMLs versus normal CD34+ cells were determined and used as log2 values in hierarchical clustering.

For expression analysis in U937AE cells all 9,635 AML1-ETO peaks were assigned to their nearest ENSEMBL gene. For each AML1-ETO target gene RNAPII occupancy was measured as described previously (Nielsen et al., 2008; Welboren et al., 2009; Martens et al., 2010). Briefly, the number of sequence tags within ENSEMBL gene bodies (+500 bp to end of gene) was counted for all genes of the normalized RNAPII tracks generated in uninduced and zinc induced U937 AML1-ETO cells and presented as % tags/kb. The ratio of uninduced versus induced was

determined and a cut off of the median plus/minus 1x standard deviation was used to select genes that show increased or decreased RNAPII occupancy.

Expression of ERG and FLI1 in SKNO-1, UAE and NB4 cells was examined using RNA-seq (data not shown) and analyzing RPKM values. This revealed that SKNO-1 cells express both ERG and FLI1 to equal level, while in UAE and NB4 cells FLI1 is highest expressed.

CHAPTER 3 RESULTS

3.1 Identification of AML1-ETO binding sites in Kasumi-1 and SKNO-1 leukemic cells

To identify new targets of the AML1-ETO oncofusion protein we developed a specific antibody against the fusion point of AML1-ETO. This antibody (AE) recognizes the fusion of AML1-ETO protein in western blot analysis (Figure 5A) and shows specificity in chromatin immunoprecipitation (ChIP) and AML1-ETO domain analysis experiments (Figure 5B, C). The AE antibody was used in ChIP-seq experiments in the AML1-ETO expressing leukemic cell lines Kasumi-1 and SKNO-1. AML1-ETO peaks were detected at regions that have been previously described as AML1-ETO targets such as *JUP* (Muller-Tidow et al., 2004), *JAG1* (Alcalay et al.,) *CSF1R* (Follows et al., 2003), *FUT7* and *OGG1* (Gardini et al., 2008) and numerous targets for which the AML1-ETO binding sites have not been described before, such as for *AXIN1*, *RARα*, *RARγ, RXRα* the leukemia associated genes *TAL1* and *MLL,* and the hematopoietic regulators *RUNX1* and *SPI1* (Figure 6A), suggesting that AML1-ETO influences many factors involved in hematopoietic differentiation. We used MACS (Zhang et al., 2008) at a p-value cut off of 10^{-8} to identify all AML1-ETO binding regions in SKNO-1 and Kasumi-1 cells, counted the number of AML1-ETO tags for each identified AML1-ETO binding region in both cell lines and calculated for each binding region the relative tag density i.e. density at one region divided by average density at all regions. Regression curve analysis (Figure 6B) revealed a set of 2,754 genomic regions at a cut off of 0.00010 (>14 tags/kb) to which AML1-ETO binds with high confidence. These binding sites were verified using two additional antibodies that recognize different domains within the AML1-ETO protein (Figure 5C, Figure 7A-C) as well as with ChIP-qPCR experiments (Figure 8 A,B) suggesting that our high confidence binding sites represent a set of *bona fide* AML1-ETO targets.

3.2 AML1-ETO co-localizes with HEB, AML1/RUNX1 and CBFβ

Although AML1-ETO has been reported to bind DNA as a homodimer or oligomer (Minucci et al., 2000; Wichmann et al., 2010), more recent findings in a zinc inducible AML1-ETO overexpressing cell line, indicate that RUNX1/AML1 can be present at AML1-ETO binding sites (Gardini et al., 2008). In addition, the E-box protein HEB as well as the core binding factor CBFβ (the heterodimer partner of wildtype RUNX1/AML1) are thought to be co-localizing with

AML1-ETO through interaction with the ETO and AML part, respectively (Gardini et al., 2008; Zhang et al., 2004; Roudaia et al., 2009; Kwok et al., 2009). To further substantiate our AML1-ETO binding results and to investigate whether AML1-ETO, RUNX1, CBFβ and HEB co-localize at a genome-wide level we performed ChIP-seq experiments with specific RUNX1 (recognizing the C-terminus of RUNX1 and not AML1-ETO), HEB and CBFβ antibodies which, using MACS at a p-value cut off of 10^{-6}, yielded 23,278 RUNX1, 27,501 HEB and 11,227 CBFβ peaks, respectively (Figure 8C). At the vast majority of AML1-ETO binding sites we detected enrichments of both RUNX1/AML1 and HEB (Figure 6A), while CBFβ enrichment was only detected at a subset of AML1-ETO binding sites. Quantitation of RUNX1, HEB and CBFβ tag densities at AML1-ETO peaks revealed enrichments of both RUNX1/AML1 and HEB at all high confidence AML1-ETO binding sites, while CBFβ enrichment was only detected at a subset (~41%) of AML1-ETO binding sites (Figure 6C).

Interestingly, the distribution of the 2,754 high confidence AML1-ETO binding sites differs with that of the 23,278 RUNX1/AML1 sites as AML1-ETO localizes predominantly to non-promoter regions (Figure 6D), whereas RUNX1 localizes preferentially to promoter regions. In addition, RNA-seq analysis of AML1-ETO target genes in SKNO-1 cells revealed that these are significantly lower expressed then RUNX1 target genes (Figure 8D). Together these results suggest that AML1-ETO targets enhancer sites rather than promoter elements and that AML1-ETO might act as a transcriptional repressor of RUNX1 target genes.

3.3 Colocalization of ERG and FLI1 with AML1-ETO

Motif analysis of the AML1-ETO binding sites revealed the presence of the RUNX1 motif in 99% of our binding sites (Figure 9A). Interestingly, in conjunction with the RUNX1 motif we found the ETS factor core motif GGAAG in nearly all (99%) of the binding sites (Figure 9A), suggesting that ETS family members might bind similar genomic regions as AML1-ETO. As the ETS factor family harbors over 20 representatives that each bind the GGAAG core consensus we investigated which ETS candidate might interplay with the AML1-ETO complex. Analysis of published expression data (Valk et al., 2004) revealed that 3 ETS proteins, TEL, FLI1 and ERG, are highly expressed in AML cells with t(8;21), identifying these as prime candidates to be colocalizing with AML1-ETO.

ChIP-seq analysis in SKNO-1 cells revealed enrichment of FLI1 and ERG at the AML1-ETO binding sites at the *BCL2* and *FLT3* genes (Figure 9B), while the presence of TEL could not be addressed due to lack of a suitable ChIP-seq grade antibody. Quantitation of ERG and FLI1 tag densities at AML1-ETO peaks revealed high levels of ERG and FLI1 at ~79% of AML1-ETO binding sites (Figure 9C), while the remaining sites showed either ERG or FLI1 colocalization. We also observed colocalization of ERG and FLI1 at numerous other genomic regions that are not occupied by AML1-ETO. Overlapping the 26,931 ERG and 20,884 FLI1 binding regions confirmed this observation and suggested that ERG and FLI1 bind similar genomic loci (Figure 9D).

Our AML1-ETO/ERG colocalization results extend a recent study that showed interaction of AML1 and ERG co-occupancy of similar genomic regions in the mouse model cell line HPC-7 (Wilson et al., 2010). Indeed, re-ChIP analysis confirmed occupancy of AML1-ETO and ERG at similar genomic regions in SKNO-1 cells. 5 binding sites were selected and validated for AML1-ETO/ERG binding by using either ERG antibodies in the first round of ChIP followed by a second round using AML1-ETO and no antibodies (Figure 10A) or AML1-ETO antibodies in the first round of ChIP followed by a second round using ERG and no antibodies (Figure 10B). Also direct interaction of endogenous AML1-ETO and ERG confirmed by co-immunoprecipitation experiments (Figure 9E). Moreover, transfection of ERG and AML1-ETO in the MCF7 breast cancer cell line, which does not endogenously express these proteins (Figure 10C), revealed colocalization of both proteins to the same genomic regions (Figure 10D, E), suggesting that colocalization of AML1-ETO and ERG does not need the contribution of other hematopoietic-specific factors.

3.4 ETS factors demarcate AML1-ETO binding sites

To investigate whether ETS factors are co-recruited by AML1-ETO or facilitates AML1-ETO binding we extended our analysis to an inducible U937 cell line (UAE) that upon zinc addition expresses AML1-ETO (Figure 10F) (Alcalay et al., 2003). Genome-wide profiling of AML-ETO after 5 hours zinc induction revealed numerous binding sites, such as at the *SKI* and *NFE2* genes (Figure 9F and Figure 10G). Using MACS we identified 9,635 AML1-ETO binding sites in zinc-treated UAE cells (Figure 9G, left). Interestingly, the high confidence binding sites identified in the two AML model cell lines only partially overlapped with those found in UAE cells (Figure

10H), suggesting that the AML1-ETO binding repertoire is dependent on the cell type in which it is expressed.

We wondered whether in UAE cells AML1-ETO target genes are transcriptional active or silent. Therefore we performed expression analysis using RNAPII occupancy as readout (Martens et al., 2010), focusing on genes that have AML1-ETO binding within a genomic region covering the complete gene (introns and exons) and its putative regulatory up- and downstream regions (-25kb to TSS and 3'UTR to +25 kb) upon zinc induction. Interestingly, of the 7,523 genes that have AML1-ETO binding 829 have decreases in RNAPII occupancy (median fold change 1 ± standard deviation) whereas 241 have increased occupancy (Figure 10I), suggesting that AML1-ETO can act as a transcriptional repressor, but its effect is context dependent, in line with previous reports that showed that AML1-ETO can function both as a transcriptional activator as well as a repressor (reviewed in e.g. Peterson and Zhang, 2004).

ChIP-seq experiments in UAE cells, which express high levels of FLI1, revealed that FLI1 is already present at the AML1-ETO binding sites before expression of the oncofusion protein at for example the *SKI* and *NFE2* genes (Figure 9F and Figure 10G), suggesting that ETS factors demarcate potential AML1-ETO binding sites. Quantitation of FLI1 tag densities at AML1-ETO peaks confirmed the observation that AML1-ETO binding sites are predefined by FLI1 binding (Figure 9G, right). Together, these results suggest that ETS factors might represent proteins that facilitate AML1-ETO binding.

3.5 ETS factors facilitate AML1-ETO binding

To further investigate the interplay of AML1-ETO and ETS factors, we utilized a dox-inducible ERG K562 cell line (Mochmann et al., 2011), which shows lower ERG expression before treatment and increased ERG expression after 72 hours dox treatment (Figure 11A). We transfected these cells 24 hours before harvesting with an expression vector that results in abundant expression of the AML1-ETO protein (Figure 11A). We used ChIP-seq and MACS at a p-value cut off of 10^{-6} to identify all ERG binding sites before and after dox induction and identified 10,642 and 15,855 binding events before and after ERG induction, respectively (Figure 12A). Interestingly, we detect 7,037 new ERG binding sites that appear after dox treatment (Figure 12A), for example at the SPI1 promoter and the TAF12 enhancer region (Figure 11B and 12B). Comparison with public DNAseI-seq data in K562 cells (see UCSC 'regulation' tracks)

revealed that the vast majority of new ERG binding sites, similar as the ERG binding sites present before dox induction, localize to accessible regions (Figure 12C), although, in comparison to ERG binding sites before dox induction, more intronic and intergenic regions then promoter are targeted (Figure 12D).

Subsequent AML1-ETO ChIP-seq analysis revealed that AML1-ETO was recruited to the TAF12 and SPI1 regions upon dox induction (Figure 12B and 11B). Of the 7,037 new ERG binding sites, 6,178 harbor low levels of ERG before induction while 859 do not show ERG binding in the uninduced state (Figure 12E and 11C). Interestingly, at the 6,178 'increased' ERG binding sites AML1-ETO is localized before dox induction and moderately increased (Figure 11C), while at the 859 'new' ERG binding regions AML1-ETO is recruited only after dox treatment (Figure 12E). Together these results suggest that AML1-ETO is localized to regions that harbor the ERG protein and that ERG facilitates AML1-ETO binding.

3.6 PML-RARα also colocalizes with ETS factors

To investigate whether ETS factors are also present at PML-RARα binding sites ChIP-seq was performed using specific antibodies against FLI1 in the PML-RARα expressing leukemic cell line NB4. This revealed colocalization at many genomic regions such as the PRAM1 and GALNAC4S-6ST genes (Figure 13A). Counting the FLI1 tags within a previously defined set of 2,722 PML-RARα binding regions (Martens et al., 2010) revealed increased FLI1 binding at 71% of PML-RARα peaks (Figure 13B). As recently also the ETS factor SPI1 (PU.1) was identified as a binding partner of the PML-RARα oncofusion protein complex (Wang et al., 2010), these results suggest that, as for AML1-ETO, the PML-RARα oncofusion protein preferentially colocalizes with ETS factors.

We used MACS at a p-value of 10^{-6} to identify all FLI1 binding sites in NB4 cells and compared those with the FLI1 binding sites observed in the t(8;21) cell lines. Only 13% of t(8;21) FLI1 peaks overlapped with FLI1 peaks in NB4 cells (Figure 13C), which we interpret as cell type specificity of ETS factor binding in line with a role of ETS factors in demarcating regulatory sites during differentiation.

In agreement with the oncofusion protein/ETS factor cell specific binding we find AML1-ETO and PML-RARα binding to many non-overlapping regions. Still a set of 594 regions, which includes key regulators of hematopoiesis such as RUNX1 and SPI1, could be identified to which

both AML1-ETO and PML-RARα bind. As these regions are potential common contributors for transformation we performed functional analysis of the associated genes using KEGG pathway analysis (Figure 14A). This revealed enrichment for genes involved in various signaling pathways, cell death and leukemogenesis.

3.7 Decreased acetylation at genomic regions upon AML1-ETO binding

Similar to PML-RARα (Martens et al., 2010), AML1-ETO has been suggested to be a modulator of H3 acetylation via recruitment of HDACs to target genes (Gelmetti et al., 1998; Amann et al., 2001). In contrast, AML1-ETO has also been reported to colocalize with the HAT p300 (Wang et al., 2011), where p300 is involved in acetylation of AML1-ETO residues. To investigate the link between AML1-ETO binding and histone (de)acetylation we performed ChIP-seq experiments in a U937 cell line expressing zinc inducible AML1-ETO. Genome-wide profiling of H3ac and H4ac revealed decreased acetylation at many of the Zn-induced AML1-ETO binding sites, such as those found at the *TNFRSF8* and *FGGY* genes (Figure 13D and 14B). In contrast, the analysis also revealed alternative histone acetylation patterns, such as at the *UBASH3B* gene for which a decrease in H3ac and a moderate increase in H4ac was detected (Figure 14C). To substantiate these findings we counted the number of H3ac and H4ac tags within all the AML1-ETO target regions before and after zinc induction and identified four groups (Figure 13E and 14D). The largest group (n=3,082) showed decreases in both H3ac and H4ac, while in other groups only H4ac (n=2,272) or H3ac decreased (n= 2,104) or H3ac and H4ac moderately increased (n=2,177). Together, these results reveal that at a very large number (77%) AML1-ETO binding sites induce decreases in H3 and/or H4 acetylation and suggest that AML1-ETO recruits HDAC activities to its binding sites.

3.8 AML1-ETO binding sites in AML primary patient blasts

To examine whether the high confidence AML1-ETO binding sites found in Kasumi-1 and SKNO-1 cells are present in patient AML cells with t(8,21) we performed ChIP-seq using the AE antibody. We obtained AML1-ETO peaks at similar genomic regions in these primary AML blasts (n=3) as in Kasumi-1 and SKNO-1 cells, for example at the *ITGB2* and *OGG1* genes (Figure 15A). We performed MACS at a p-value cutoff of 10^{-6} to identify all AML1-ETO binding sites and detected 4,475 sites in patient 12, 12,344 in patient 186 and 8,234 in patient

229. Comparing these sites with those obtained in the t(8;21) cell lines revealed that 45% of the 2,754 Kasumi-1/SKNO-1 AML1-ETO peaks overlapped with those from patient 12, 58% with the binding sites detected in patient 186 and 46% with those from patient 229.

Overlapping the binding regions of the three patients samples (Figure 15B) revealed a common set of 2,898 regions. As these AML common regions likely represent the key binding sites for AML1-ETO induced oncogenic transformation we performed functional analysis of the associated genes using GO annotation clustering (Figure 16A). This revealed high enrichment scores (>3) for genes involved in cell death, structural processes and hematopoietic differentiation.

AML1-ETO has been reported to be involved in transcriptional activation as well as in repression (Peterson and Zhang, 2004). To examine the transcription level of AML1-ETO target genes all common AML1-ETO binding sites were assigned to their closest genes and correlated with published expression datasets from human progenitor $CD34^+$ cells and AML1-ETO, PML-RARα and non AML1-ETO expressing FAB M2 AMLs (Valk et al., 2004). Although transcriptional changes were in general not dramatic (Figure 12B), ~50% of AML1-ETO target genes are lower expressed in t(8;21) compared to normal $CD34^+$ cells, while the remaining genes display increased expression levels. Interestingly, the set of genes that is lower expressed in t(8;21) cells is higher expressed in non AML1-ETO M2 cells and partially higher expressed in t(15;17) cells.

To examine whether the ETS factor colocalization binding results in SKNO-1 cells could be validated in primary AML blasts carrying t(8,21) we performed ChIP-seq using the ERG antibody with cells from an AML patient (pz12) that harbors t(8;21). We again found colocalization of ERG and AML1-ETO at similar genomic regions in primary patient cells, for example at the *SPI1* gene (Figure 15C). Using MACS we identified 18,342 ERG binding sites in this patient and confirmed that the majority of the 2,898 common AML1-ETO binding sites identified in the AML cells colocalized with ERG (Figure 15D), corroborating and extending the AML1-ETO/ETS factor colocalization to primary patient blasts.

3.9 Distinct ERG distribution in normal $CD34^+$ and AML1-ETO expressing cells

As our results suggest that ETS factors such as ERG flag AML1-ETO docking sites we wondered whether the ERG highlighted regions are laid down in normal hematopoietic $CD34^+$ cells that have the potential to differentiate towards both the myeloid and lymphoid lineage (Figure 17A)

(Morrison et al., 1995). Therefore, ChIP-seq was performed to determine the ERG binding profile in normal $CD34^+$ human progenitors. Our analysis revealed ERG binding at nearly 25,000 binding regions, such as at the *CAMK1* transcription start site and on the *SPI1* gene (Figure 17B). Motif analysis of the sequences underlying ERG binding sites in $CD34^+$ cells confirmed the presence of the ETS factor core motif, validating our binding sites as genuine ETS binding. Moreover, it revealed the presence of multiple consensus sequences for hematopoietic regulators such as RUNX1, TAL1, nuclear receptor half sites and AP1 factors (Figure 17C). Interestingly, recognition motifs for E2A (in 6,637 ERG binding sites) and C/EBP (in 8,388 ERG binding sites), two proteins specifying lymphoid and myeloid lineages, respectively, were also enriched in mostly non-overlapping subpopulations of $CD34^+$ ERG binding regions, suggesting indeed that ERG binding sites in normal $CD34^+$ cells predefine regulatory sites for differentiation towards both the myeloid and lymphoid lineage.

Comparison of the CD34+ ERG binding sites with those detected in t(8;21) blasts revealed the presence of ERG at many common sites such as at the SPI1 downstream region (Figure 17B). However, also differential ERG binding sites were detected such as observed at the OGG1 promoter and the *SPI1* gene (Figure 17B). Of the ERG binding sites detected in $CD34^+$ only 40% overlapped with those in t(8;21) cells (Figure 17D) suggesting that ERG profiles are cell type specific. To even further extend this observation we compared ERG binding sites detected in normal $CD34^+$ cells and t(8;21) cells with those present in patient cells that harbor the t(15;17) translocation (Figure 17E) confirming that ERG profiles are to a large extend cell type specific.

Motif analysis of the 8,376 newly gained ERG binding sites in t(8;21) cells revealed no major shifts in the presence of consensus sequences for ETS, RUNX1, TAL1, nuclear receptor half sites and AP1 factors as compared to normal $CD34^+$ cells (Figure 18A), although less C/EBP and E2A consensus sequences were found. However, we noticed that a large fraction of AML1-ETO protein targets newly gained ERG binding sites (Figure 17D), which becomes even more apparent when examining AML1-ETO binding in t(8;21) cell lines (Figure 18B), where 69% of AML1-ETO protein targets ERG binding sites that are specific for SKNO-1 cells in the comparison with $CD34^+$ cells. Together these results suggest that AML1-ETO preferentially target cell type specific ETS factor bound genomic regions.

Despite that all ERG binding sites have a RUNX1 consensus sequence AML1-ETO binds only to a subset, suggesting that these regions harbor additional molecular characteristics. We

hypothesized that targeting of AML1-ETO could be dependent on the number of RUNX1 sequences underlying the ERG binding regions. Counting the number of RUNX1 motifs in ERG only binding sites in comparison with those that bound also AML1-ETO revealed a statistical significant difference (p-value $1.8x10^{-5}$) in the distribution of the number of binding sites. While most overlapping AML1-ETO and ERG binding sites have 2 to 4 consensus RUNX1 motifs (Figure 17F, right), other ERG binding sites have generally 1 (Figure 17F, left). These results suggest that the underlying DNA template supports the binding of oligomerized AML1-ETO protein in line with previous reports (Minucci et al., 2000; Wichmann et al., 2010).

3.10 ERG binding sites have defined epigenetic marking in CD34$^+$ cells

To investigate whether oncofusion proteins could alter the epigenetic make-up of ERG binding sites, we correlated the epigenetic modifications at these genomic regions. To this aim, we performed ChIP-seq for H3K9K14ac in normal CD34$^+$ cells and included 9 previously published histone modification profiles of hematopoietic progenitor cells (Cui et al., 2009) in our analysis. This revealed a strong correlation of ERG binding sites with H3K9K14ac (Figure 19A) while other modifications are not, or enriched only in subsets of ERG binding regions, such as H3K4me3, which is specifically enriched at ERG binding sites located at promoters. Indeed, at the ERG binding sites that are present at the *p300* promoter and the *SOX10* exon we detect H3 acetylation in normal CD34$^+$ cells (Figure 19B). The ERG site at the *p300* promoter is still present in t(8;21) cells while ERG binding and H3K9K14ac are lost at the *SOX10* gene.

To extend these observations we examined H3K9K14ac at all ERG peaks that are maintained in t(8;21) AML blasts in comparison with unique ERG binding sites in normal CD34$^+$ cells. These results show that ERG peaks present in normal CD34$^+$ and t(8;21) AML cells have high levels of H3K9K14ac both in normal CD34$^+$ cells and in AML cells (Figure 19C), while ERG peaks that are unique for normal CD34$^+$ cells do only have increased H3K9K14ac in normal CD34$^+$ cells but not in t(8;21) AML cells. Together these results reveal an intimate connection of ERG binding and H3 acetylation.

To investigate whether AML1-ETO recruits histone deacetylation activities to ERG binding sites in patient samples we analyzed in t(8;21) blasts from 2 patients (pz186 and pz229) the H3ac and DNAme levels at all ERG binding sites. For this, we ranked the ERG binding sites according to AML1-ETO tag density (Figure 19D) and divided the ERG binding sites in 10 bins of equal size.

For most bins we observe an inverse correlation between H3ac levels and DNA methylation (Figure 19E and 19 F). In contrast, bins 9 and 10, which have the highest AML1-ETO tag count and represent the high confidence AML1-ETO/ERG binding sites, show reduced levels of H3ac, despite low levels of DNAme. This analysis suggests that reduced H3ac is a hallmark of ERG sites occupied by AML1-ETO. Together these results imply that a major molecular strategy of the oncofusion protein AML1-ETO involves targeting of histone deacetylation activities to hematopoietic regulatory sites bound by ERG.

3.11 FIGURES

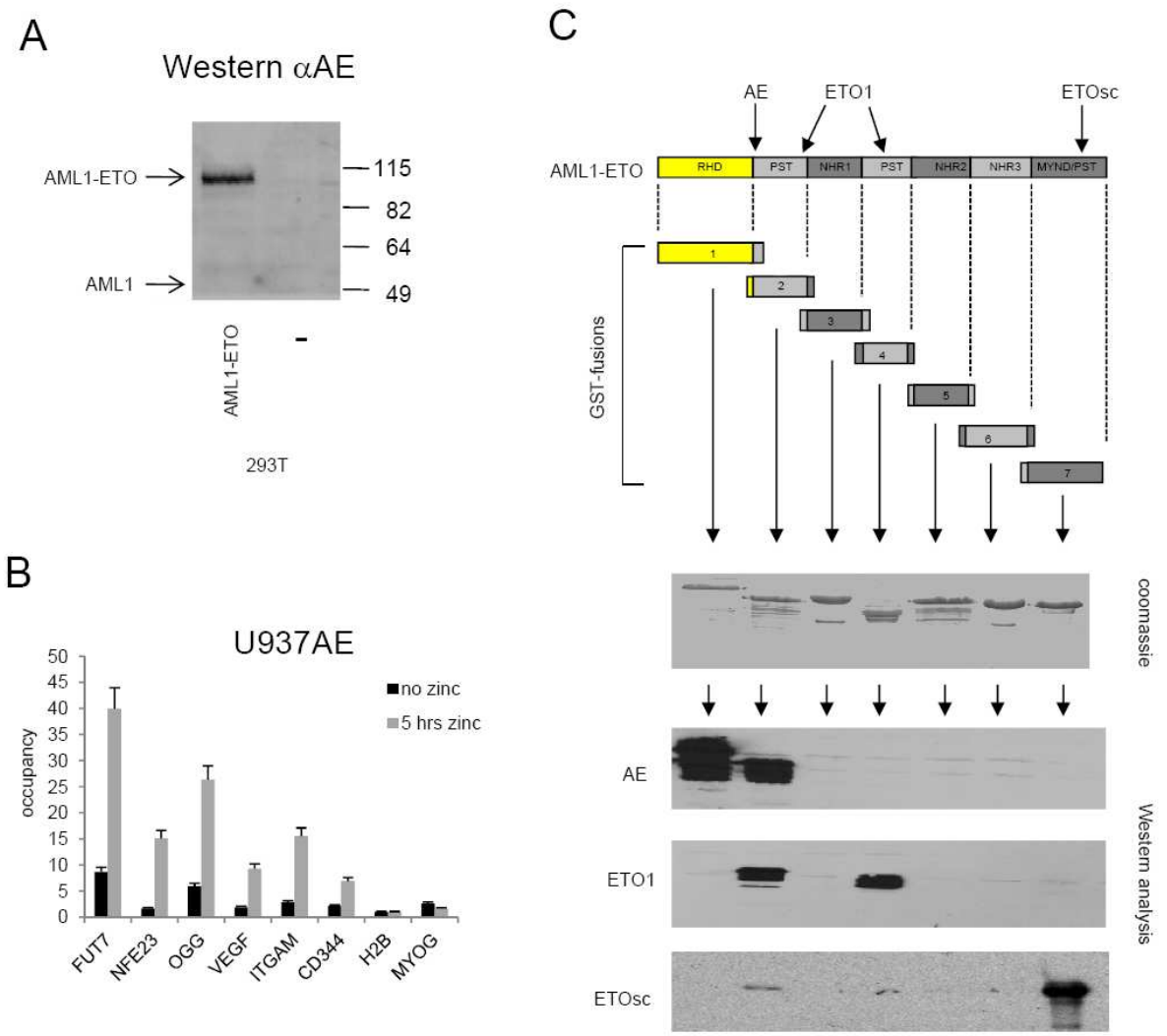

Figure 5. Analysis of the AML1-ETO recognizing antibody AE. **A**. 293T cells were transfected with full length AML1-ETO or control vector and protein extracts were analyzed for the presence of AML1-ETO in Western using the AE antibody. Only a signal was detected at the expected height of the AML1-ETO protein. **B**. ChIP analysis using the AE antibody and 6 previously described AML1-ETO binding sites in the AML1-ETO zinc inducible U937 cell line UAE. **C**. Analysis of the recognition capacity of the AE, ETO1 (Diagenode) and ETOsc (Santa Cruz) antibodies towards GST fusion domains of AML1-ETO. The fusion point of AML1-ETO is present both in GST fusion product 1 and 2, peptides that were used for generating the ETO1 antibody were present in GST fusion 2 and 4 while the Santa Cruz ETO antibody (ETOsc) was developed against a peptide present in GST fusion 7. RHD, Runt-Homology Domain; PST, Proline-Serine-Threonine-rich region; NHR, Nervy Homology Region; MYND, Myeloid-Nervy-Deaf domain. The RUNX1/AML1 part of AML1-ETO is highlighted in yellow.

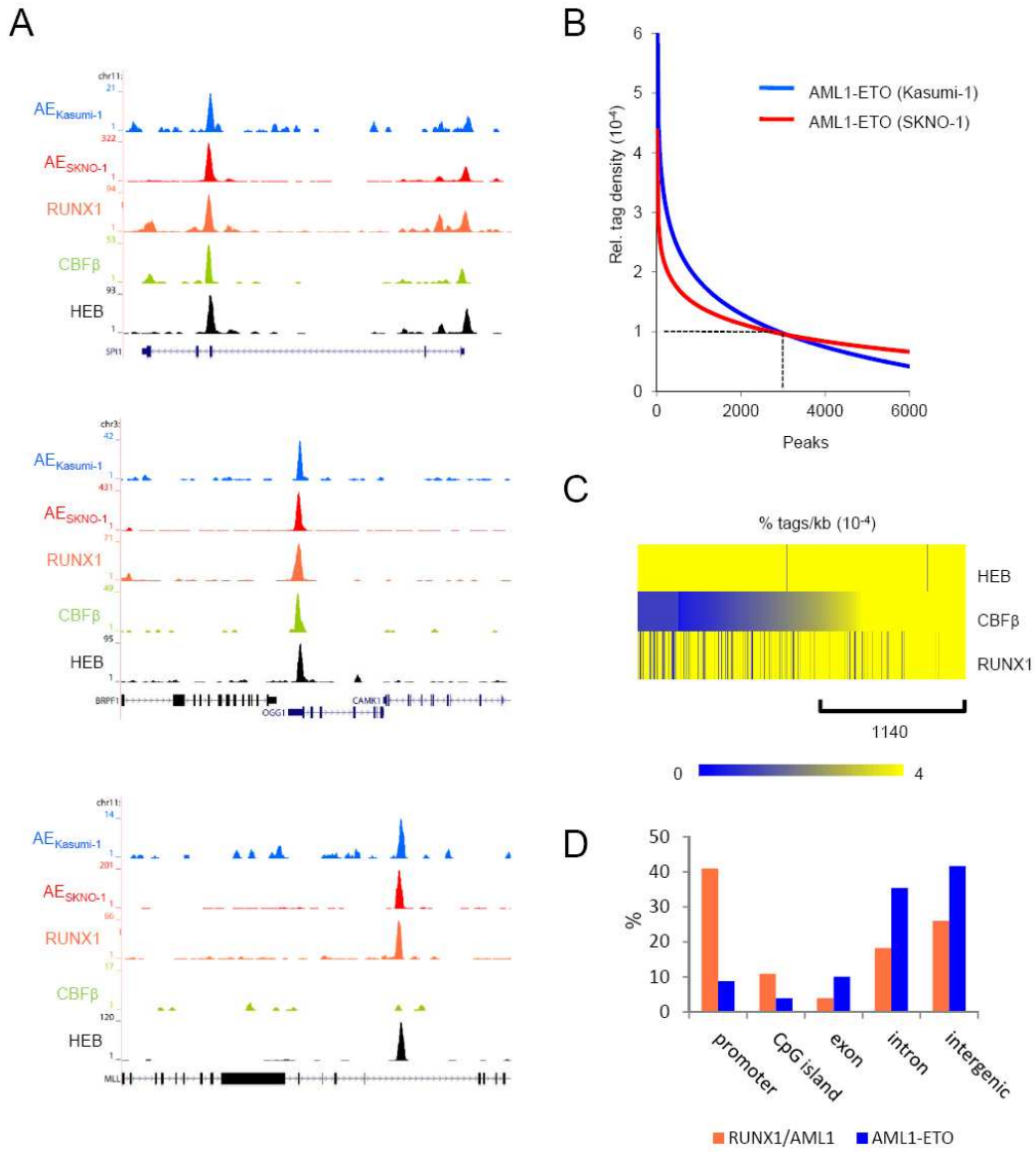

Figure 6. AML1-ETO, RUNX1, CBFβ and HEB colocalization to genomic regions. **A**. Overview of the *OGG1*, *SPI1*, and *MLL* AML1-ETO binding sites. In blue the Kasumi-1 AML1-ETO (AE) ChIP-seq data is plotted, in red the SKNO-1 AML1-ETO (AE), in orange the RUNX1, in green the CBFβ and in black the HEB data. **B**. AML1-ETO binding sites detected by ChIP-seq in leukemic Kasumi-1 and SKNO-1 cells. AML1-ETO peaks were called using MACS (p-value 10^{-8}) after which relative AML1-ETO density in Kasumi-1 or SKNO-1 cells was determined at these peaks. Results were sorted according to relative tag density and the top 6000 peaks displayed in a regression curve. A cut off was set at a relative tag density of 0.0001 (14 tags/kb). **C**. Heat map displaying HEB, CBFβ and RUNX1 tag densities at the 2,754 high confidence AML1-ETO binding sites. **D**. Distribution of the AML1-ETO and RUNX1/AML1 binding site locations relative to RefSeq genes. Locations of binding sites are divided in promoter (-500 bp to the Transcription Start Site), non-promoter CpG island, exon, intron and intergenic (everything else).

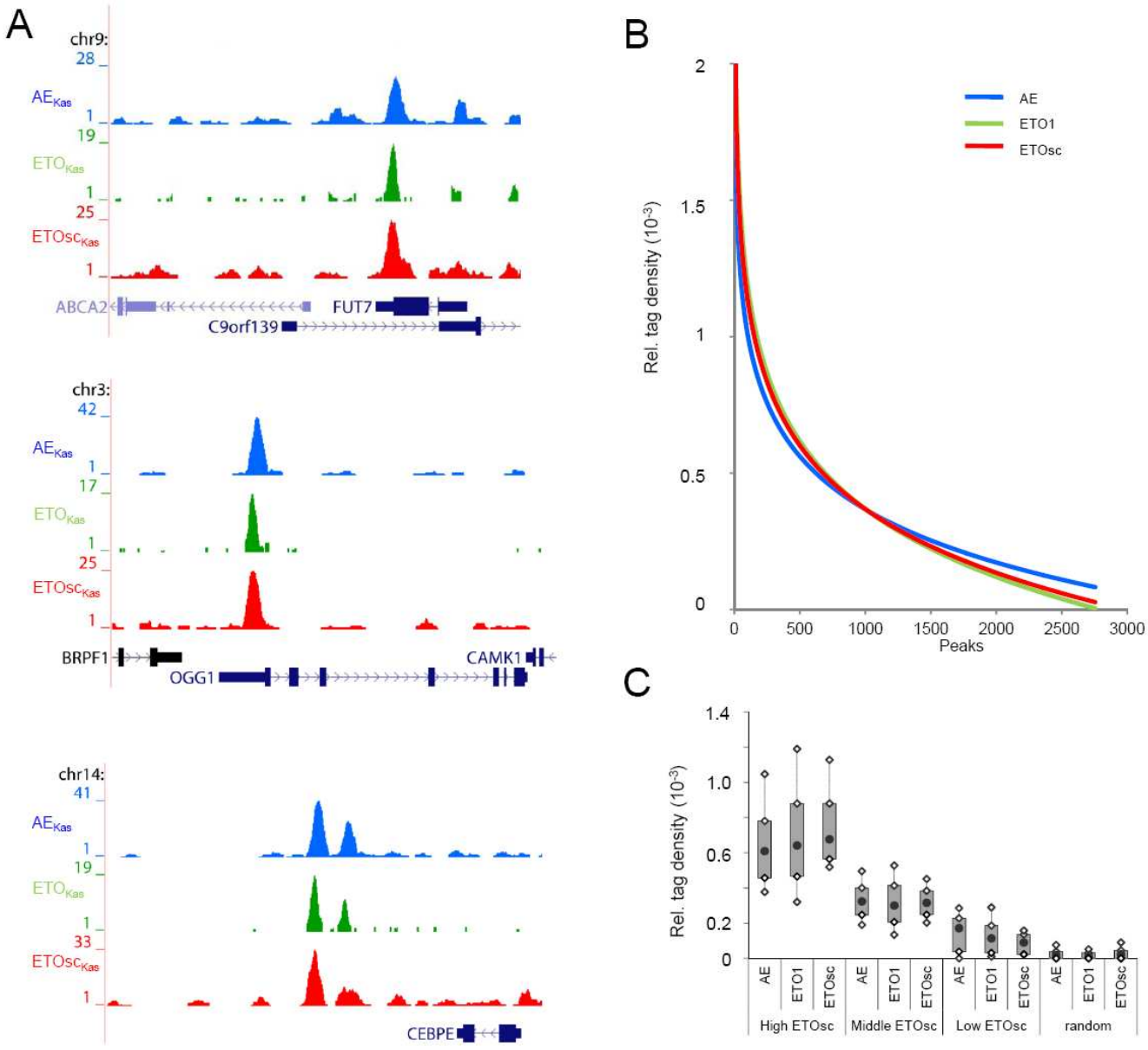

Figure 7. A. Analysis of AML1-ETO binding sites by two additional ETO antibodies, ETO1 and ETOsc. Overview of the *FUT7*, *OGG1* and *CEBPE* AML1-ETO binding sites in Kasumi-1 cells. In blue the AE ChIP-seq data is plotted, in green the ETO1 and in red the ETOsc data. **B**. Regression curve analysis of AE, ETO1 and ETOsc tags at the 2,754 AML1-ETO binding sites identified in SKNO-1 and Kasumi-1 cells. **C**. Boxplot showing the percentage of AE, ETO1 and ETOsc tags, within three groups of AML1-ETO binding sites that harbor different ETOsc densities or a set of random regions of similar size.

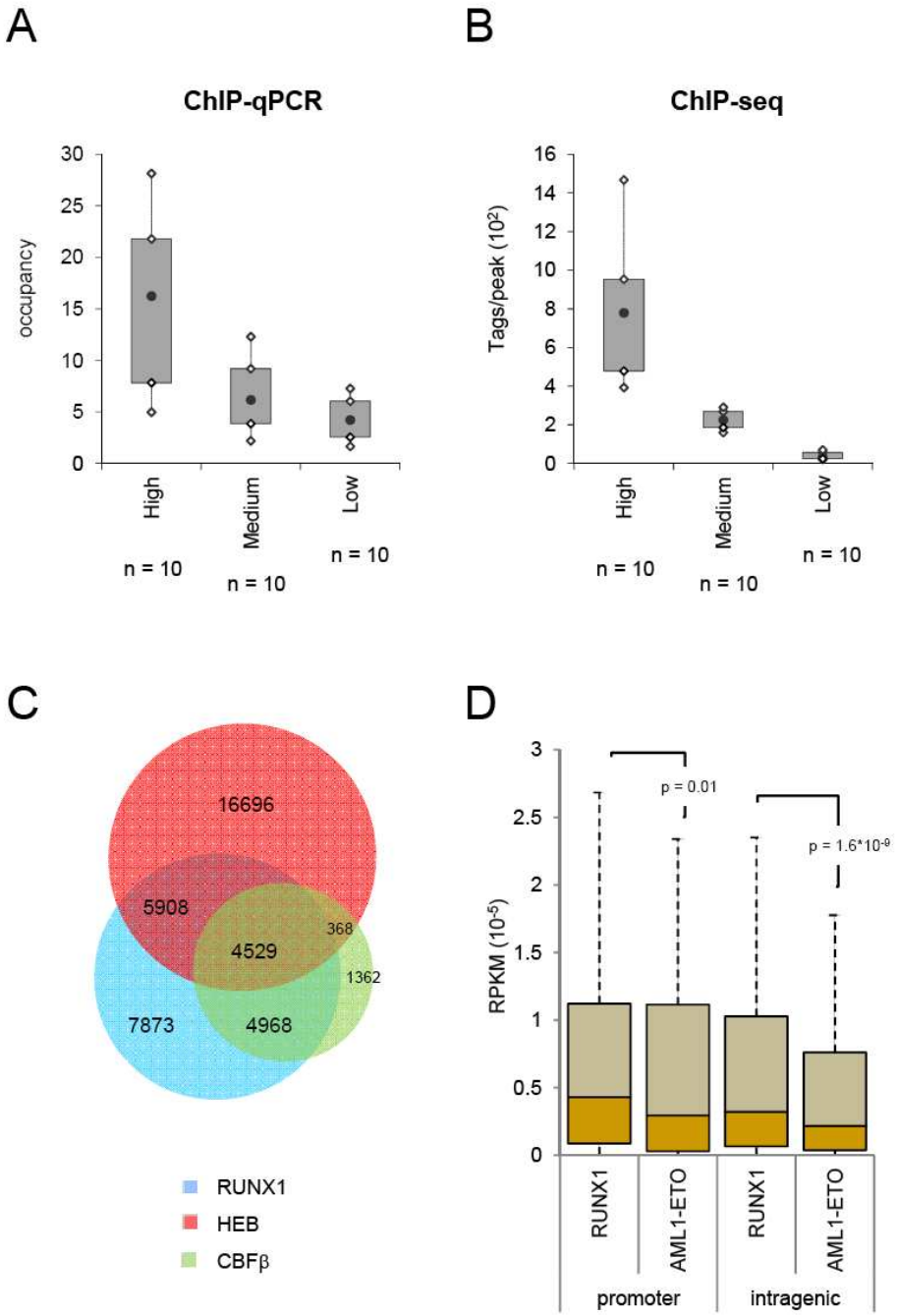

Figure 8. A. Validation of ChIP-sequencing data by qPCR. Randomly high, medium and low (n=10) AML1-ETO binding sites were selected and validated for AML1-ETO binding by ChIP-qPCR in SKNO-1 cells. Occupancy results for each class of binding sites (high, medium, low) are represented in a boxplot. **B**. SKNO-1 AML1-ETO ChIP-seq tag count for the selected high, medium and low binding sites. **C**. Venn diagram representing the overlap of RUNX1, CBFβ and HEB binding sites in t(8;21) cell lines. **D**. RPKM values as determined by RNA-seq of genes that have AML1-ETO or RUNX1 binding to its promoter (left) or to an intragenic (intron and exon) region (right).

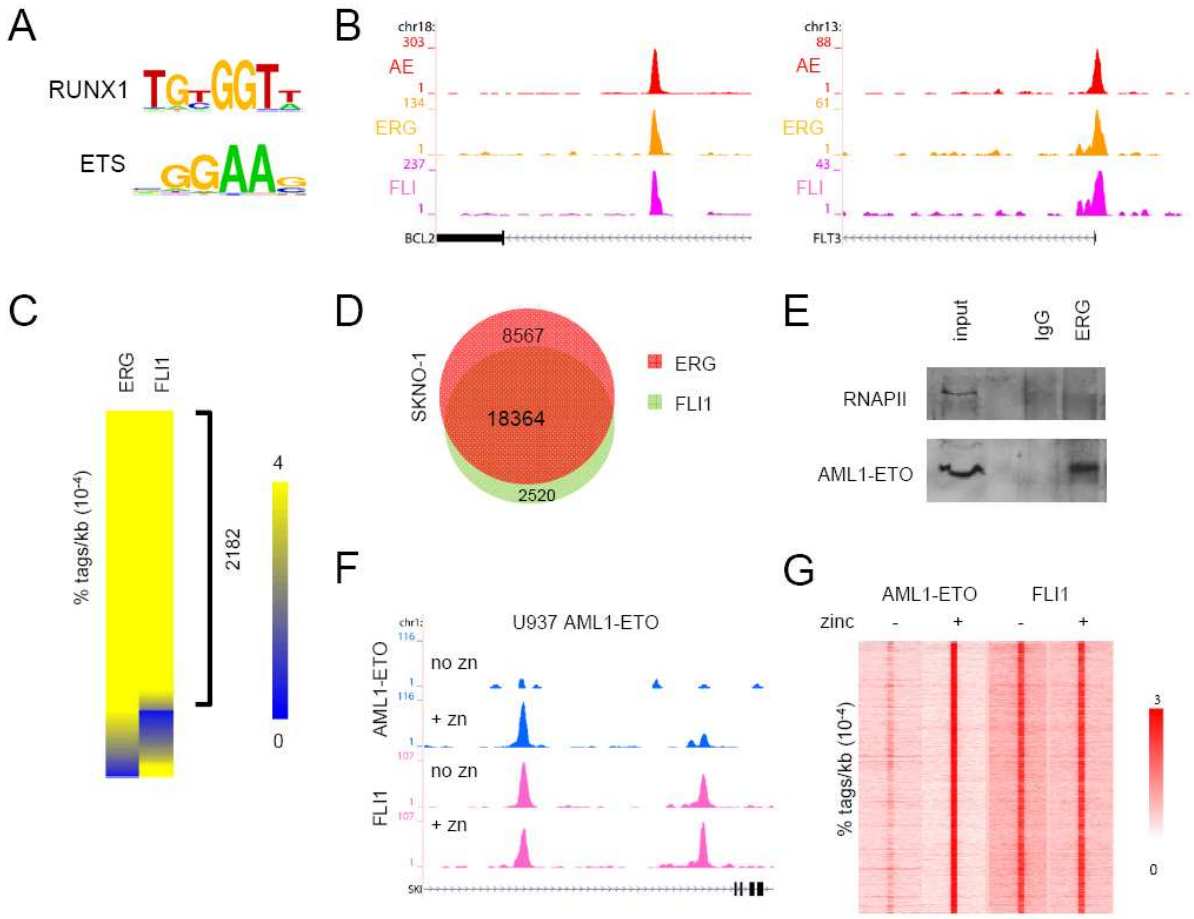

Figure 9. AML1-ETO is recruited to ETS factor binding sites. **A**. Overview of the RUNX1 and ETS core binding motif. **B**. Overview of the *BCL2* and *FLT3* AML1-ETO binding sites in SKNO-1 cells. In red the AML1-ETO (AE) ChIP-seq data is plotted, in orange the ERG and in pink the FLI1 data. **C**. Heat map displaying ERG and FLI1 tag densities at high confidence AML1-ETO binding sites. **D**. Venn diagram representing the overlap of ERG and FLI1 binding sites in SKNO-1 cells. **E**. Coimmunoprecipitation of AML1-ETO with ERG. Immunoprecipitations were performed in SKNO-1 cells using IgG and ERG antibodies and analyzed by Western using RNAPII and AML1-ETO antibodies. **F**. ChIP-seq using U937 cells expressing (+ zinc) or not expressing (no zinc) AML1-ETO. Overview of the *SKI* AML1-ETO binding site in U937 AML1-ETO cells. In blue the AE ChIP-seq data is plotted and in pink the FLI1 data. **G**. Intensity plot showing the tag density of AML1-ETO and FLI1 tags within a 10 kb window around AML1-ETO binding sites in U937 AML1-ETO cells treated or untreated with zinc.

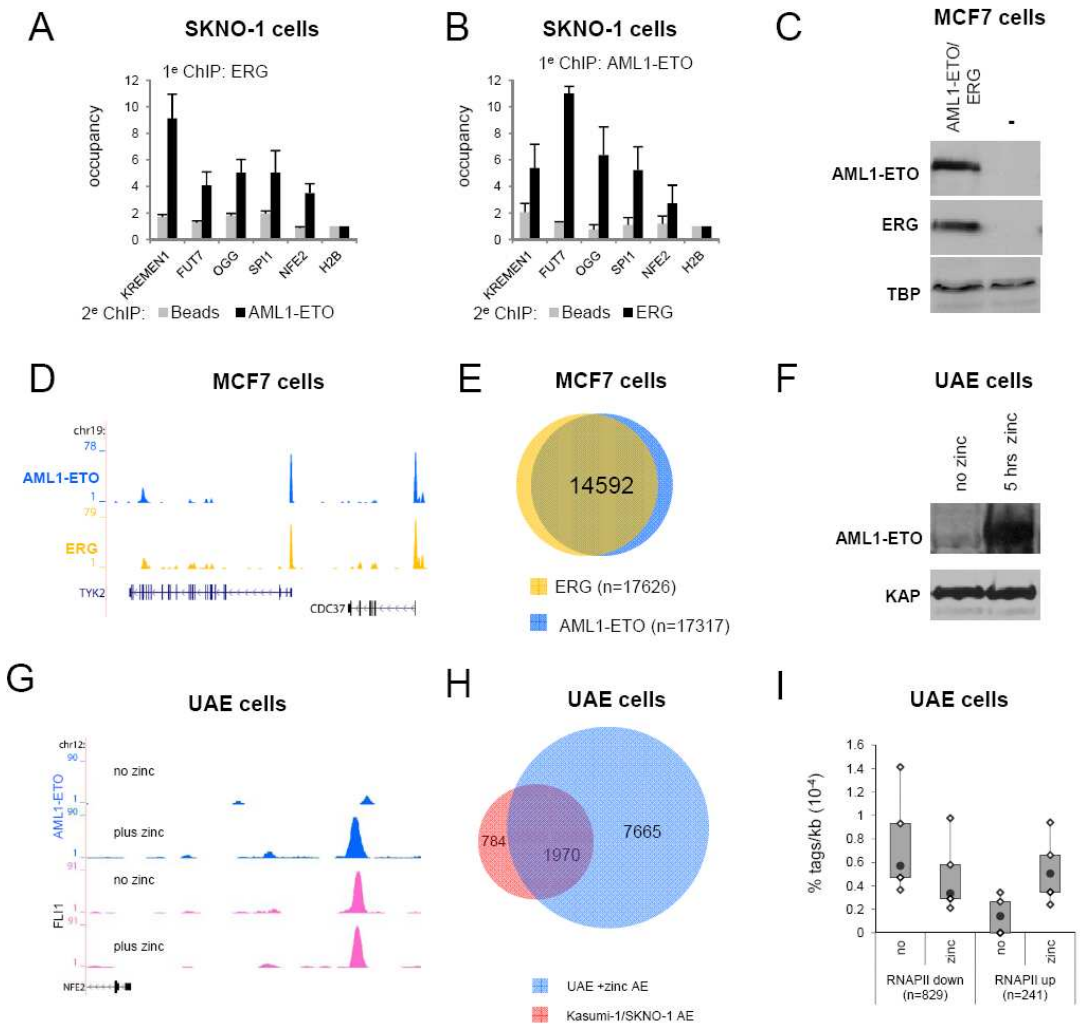

Figure 10. A, B. re-ChIP experiments using either ERG antibodies in the first round of ChIP followed by a second round using AML1-ETO and no antibodies **(A)** or vice versa **(B)**. **C**. MCF7 cells transfected with expression constructs for AML1-ETO and ERG or empty vectors. Resultant protein levels were detected by Western blot using antibodies recognizing AML1-ETO, ERG and TBP. **D**. Transfected AML1-ETO and ERG colocalize to the TYK2 genomic region in MCF7 cells. In blue the AML1-ETO ChIP-seq data is plotted, in yellow the ERG data. **E**. Venn diagram showing the overlap of AML1-ETO and ERG peaks after MACS peak calling for AML1-ETO and ERG in transfected MCF7 cells. **F**. UAE cells were treated with zinc to induce AML1-ETO expression. Protein levels were detected using Western blot analysis and antibodies recognizing AML1-ETO and KAP1. **G**. ChIP-seq using U937 cells expressing (plus zinc) or not expressing (no zinc) AML1-ETO. Overview of the *NFE2* AML1-ETO binding site in U937 AML1-ETO cells. In blue the AML1-ETO ChIP-seq data is plotted and in pink the FLI1 data. **H**. Venn diagram representing the overlap of AML1-ETO (AE) binding sites in cell lines (Kasumi-1 and SKNO-1) and zinc treated U937 AML1-ETO cells. **I**. RNAPII occupancy as determined by ChIP-seq of genes that have AML1-ETO binding upon zinc induction in U937 AML1-ETO cells and are up- or down regulated. RNAPII occupancy decreased for 829 genes upon AML1-ETO binding, while occupancy is increased for 241 genes upon AML1-ETO binding.

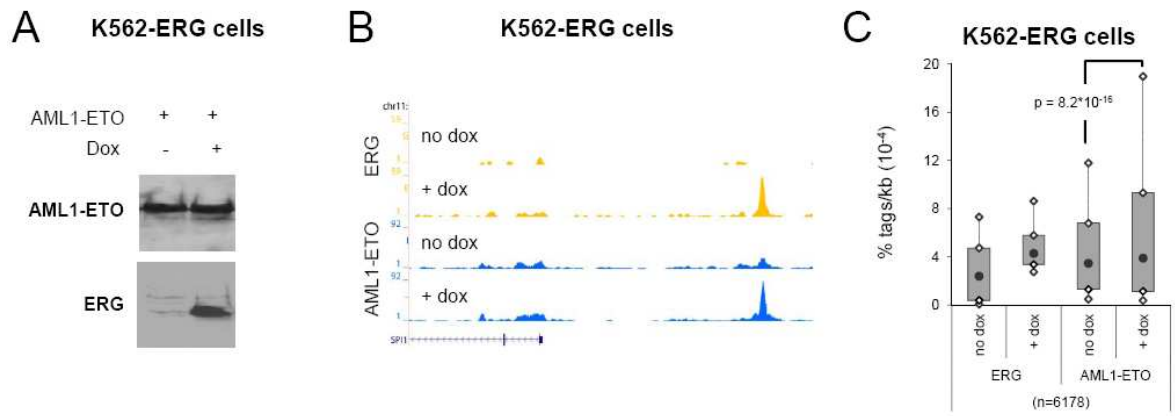

Figure 11. A. K562-ERG cells transfected with expression constructs for AML1-ETO or empty vectors and treated or not treated with dox for 72 hours. Resultant protein levels were detected using Western blot analysis and antibodies recognizing AML1-ETO and ERG. **B**. ChIP-seq using K562-ERG cells expressing high levels (plus dox) or low levels (no dox) ERG and transfected 24 hours before harvesting with AML1-ETO. Overview of the *SPI1* AML1-ETO/ERG binding site in K562-ERG cells. In blue the AML1-ETO (AE) ChIP-seq data is plotted and in yellow the ERG data. **C**. Boxplot showing the tag density of AML1-ETO and ERG tags in ERG binding sites in K562-ERG cells transfected with AML1-ETO and treated or untreated with dox.

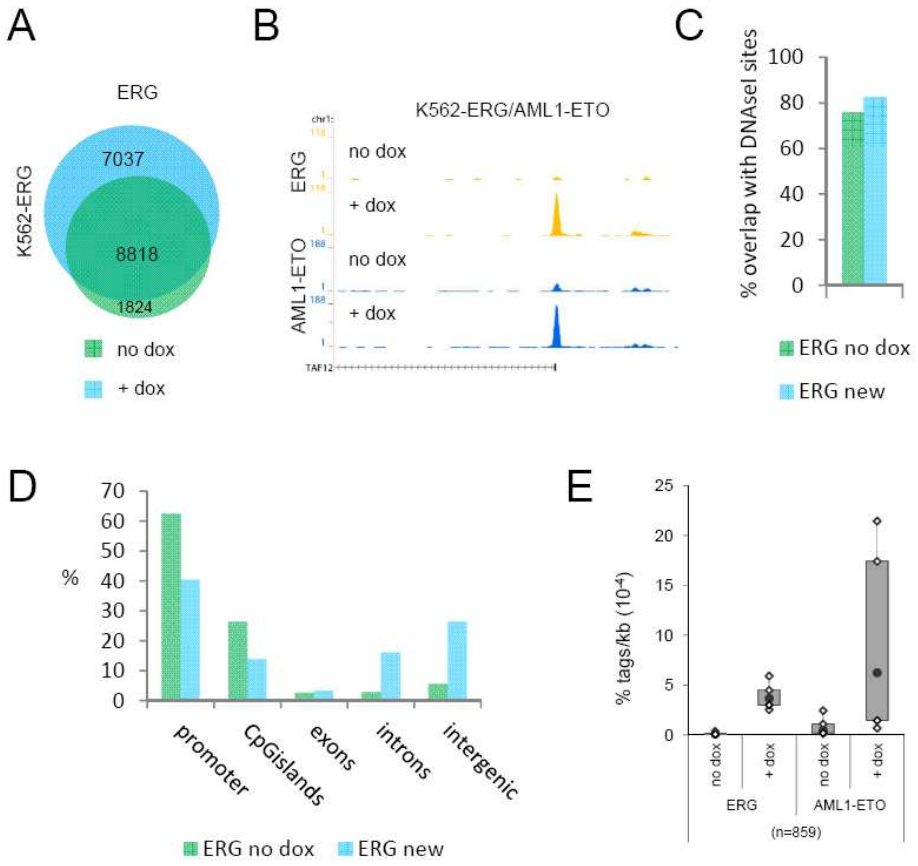

Figure 12. ETS factors facilitate AML1-ETO binding. **A**. Venn diagram representing the overlap of ERG binding sites in K562-ERG cells not treated, or treated for 72 hours with dox. **B**. ChIP-seq using K562-ERG cells expressing high levels (+ dox) or low levels (no dox) ERG. Overview of the *TAF12* AML1-ETO/ERG binding site in K562-ERG cells, transfected 24 hours before harvesting with AML1-ETO. In blue the AE ChIP-seq data is plotted and in yellow the ERG data. **C**. Overlap of DNAseI accessibility defined regions with ERG binding sites present before dox induction (ERG no dox) and ERG binding sites that appear after dox induction (ERG new). D. Distribution of the ERG 'no dox' and ERG 'new' binding site locations relative to RefSeq genes. **E**. Boxplot showing the tag density of AML1-ETO and ERG tags within ERG binding sites in K562-ERG cells transfected with AML1-ETO and treated or untreated with dox.

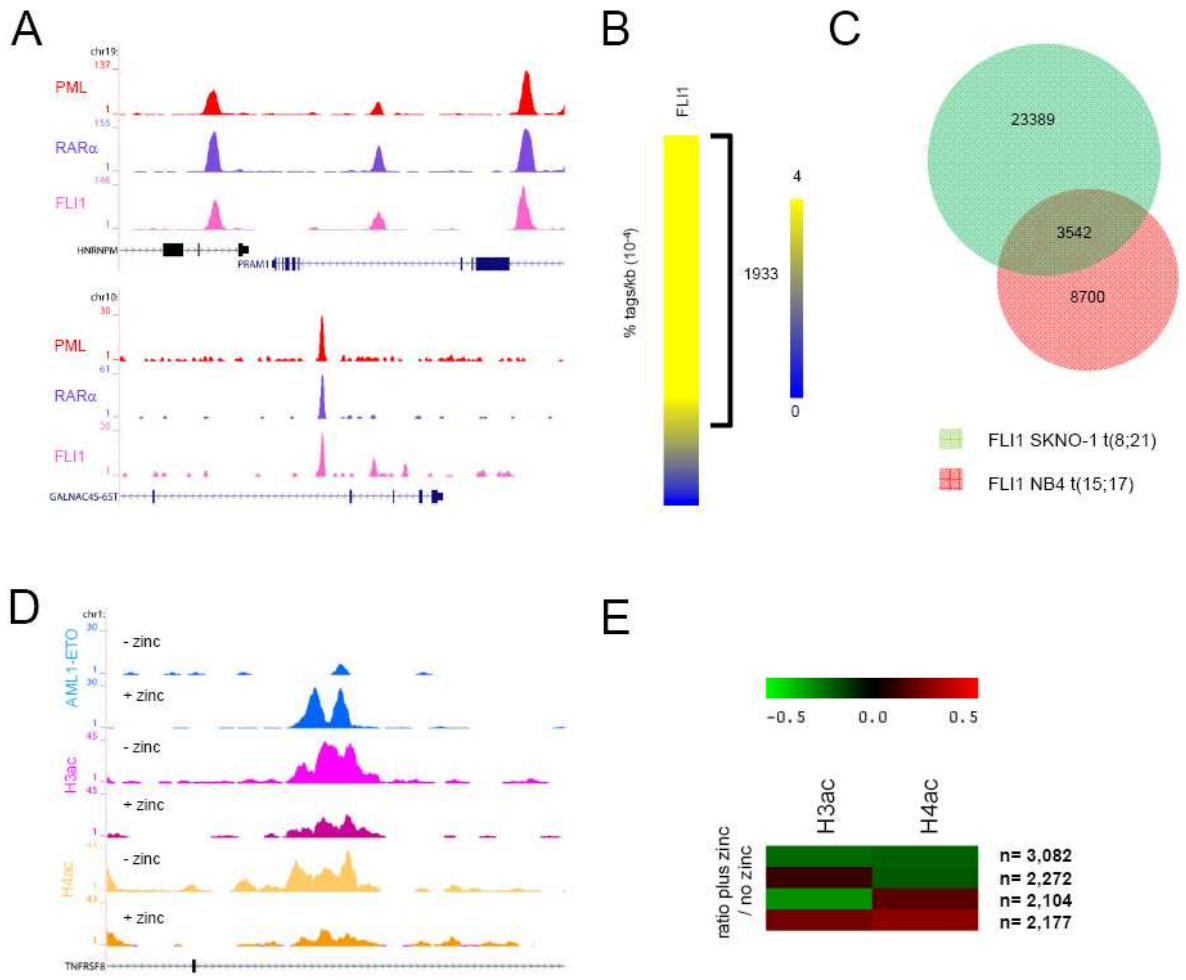

Figure 13. ETS factors colocalize with PML-RARα. **A**. Overview of the *PRAM1* and *GALNAC4S-6ST* genes in NB4 cells. In red the PML, in purple the RARα and in pink the FLI1 ChIP-seq data is plotted. **B**. Heat map displaying FLI1 tag densities at high confidence PML-RARα binding sites. **C**. Venn diagram representing the overlap of FLI1 binding sites in SKNO-1 and NB4 cells. **D**. Overview of the *TNFRSF8* gene in U937 AML1-ETO cells. In blue the AML1-ETO ChIP-seq data is plotted, in purple the H3ac and in yellow the H4ac data. **E**. Heatmap displaying the log2 ratio of H3ac or H4ac tags at AML1-ETO target regions in zinc treated cells versus untreated cells.

A

KEGG pathway	P-Value
Natural killer cell mediated cytotoxicity	8,3E-4
B cell receptor signaling pathway	1,5E-3
Neurotrophin signaling pathway	1,9E-3
Chemokine signaling pathway	3,3E-3
Acute myeloid leukemia	9,9E-3
NOD-like receptor signaling pathway	1,3E-2
Leukocyte transendothelial migration	1,8E-2

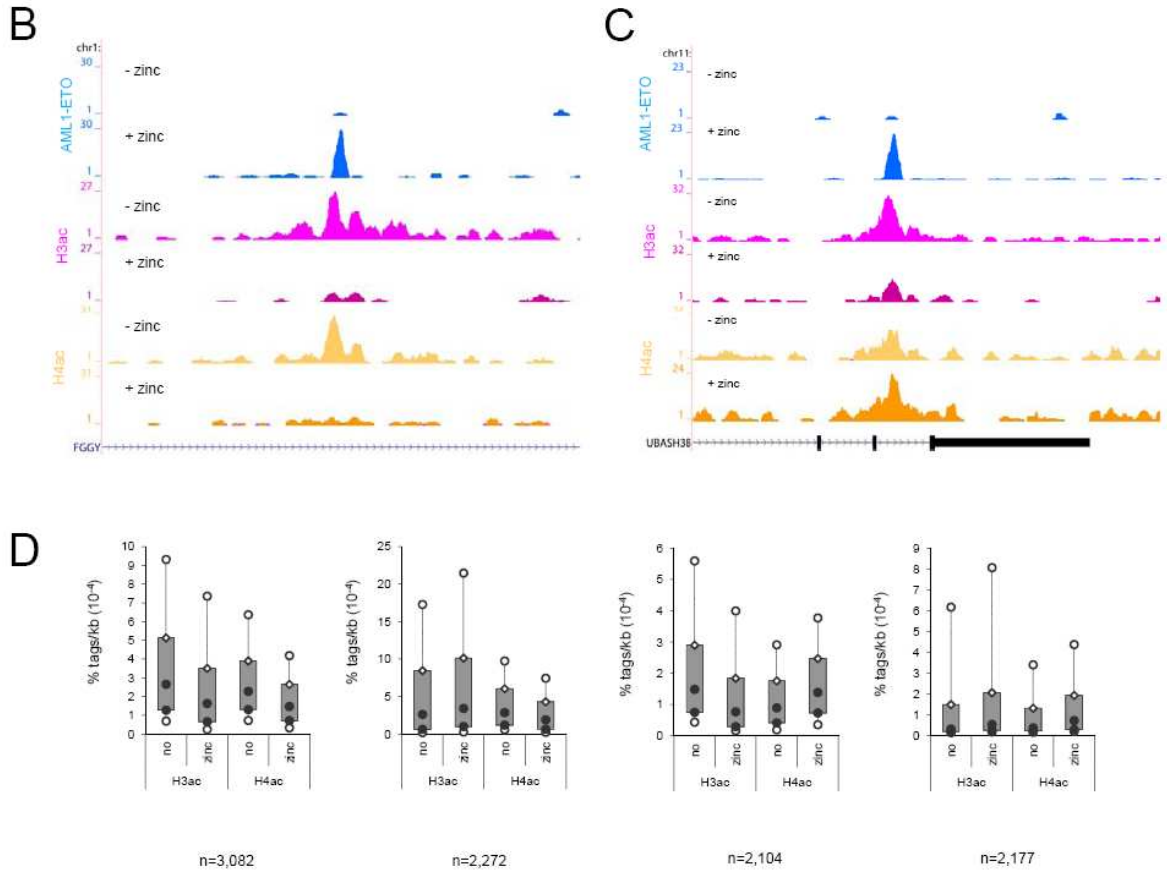

Figure 14. A. Functional annotation clustering to KEGG pathways of genes that are associated with AML1-ETO and PML-RARα common peaks. **B-C**. Overview of the *FGGY* (**B**) and *UBASH3B* (**C**) genes in U937 AML1-ETO cells. In blue the AML1-ETO ChIP-seq data is plotted, in purple the H3ac and in yellow the H4ac data. **D**. Boxplot displaying the H3ac or H4ac tag densities in zinc treated or untreated cells. From left to right: sites with decreased H3 and H4 acetylation upon AML1-ETO binding; sites with decreased H4 acetylation; sites with decreased H3 acetylation; sites with no changes in acetylation.

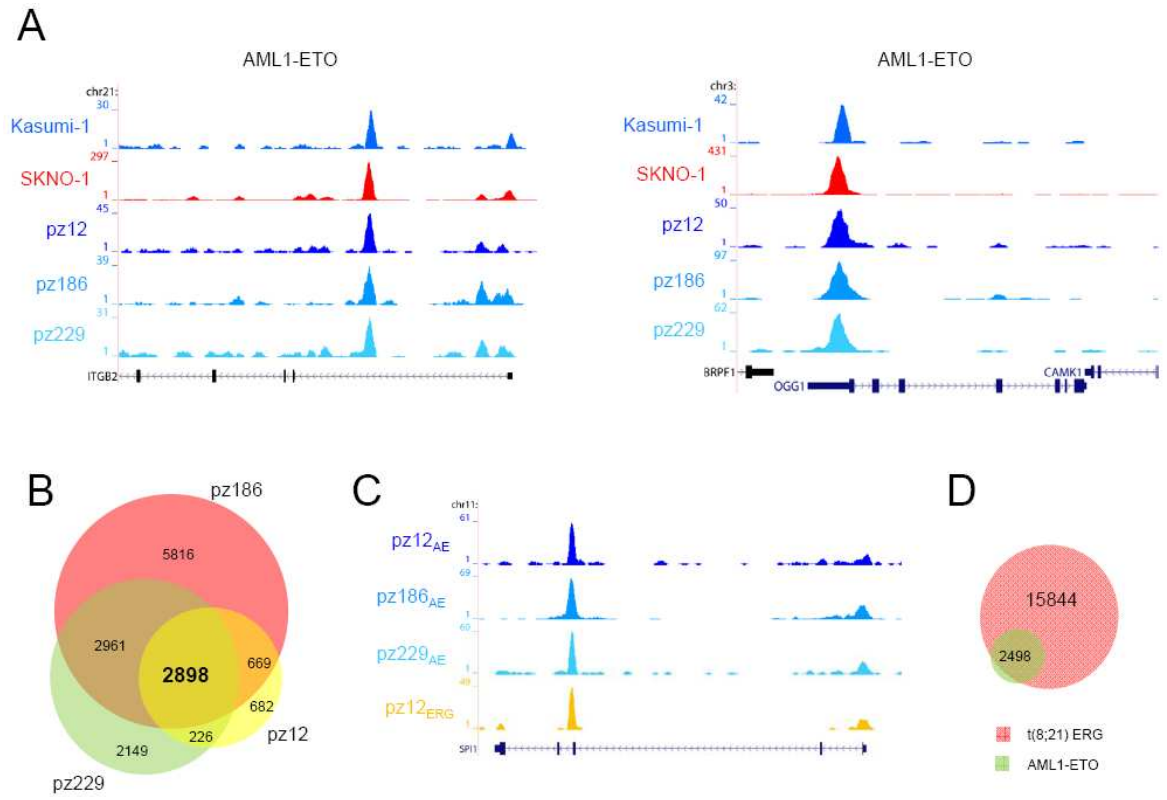

Figure 15. AML1-ETO binding sites in patient AML CD34^{+} cells with t(8;21). **A**. Overview of the *ITGB2* and *OGG1* AML1-ETO binding sites. Two cell lines (SKNO-1 and Kasumi-1) and blasts of three AML patients with t(8;21) were used in ChIP-seq experiments using a specific antibody that could recognize AML1-ETO (AE). **B**. Venn diagram representing the overlap of binding sites detected in patients AML cells with t(8; 21), n=3. **C**. Overview of the *SPI1* AML1-ETO binding site. A blast from one AML patient with t(8;21) was used in ChIP-seq experiments using a specific antibody that could recognize ERG and compared to the ChIP-seq results of AML1-ETO (AE) in three patient blasts with t(8;21). **D**. Venn diagram representing the overlap of the 2,898 common AML1-ETO binding sites detected in 3 patients with t(8;21) and ERG binding sites detected in one patient with t(8;21).

A

Enrichment Score: 4.88	P_Value
microtubule cytoskeleton	2.5E-7
cytoskeleton	1.2E-6
microtubule organizing center	2.9E-6
centrosome	8.4E-6
cytoskeleton	2.9E-4
Enrichment Score: 4.75	**P_Value**
Ras-association	3.8E-5
Enrichment Score: 4.59	**P_Value**
transcription (co)activator activity	1.6E-6
transcription factor binding	2.8E-6
Enrichment Score: 3.47	**P_Value**
regulation of cell death	7.6E-7
regulation of programmed cell death	1.0E-6
regulation of apoptosis	1.5E-6
Enrichment Score: 3.14	**P_Value**
leukocyte activation	5.2E-6
lymphocyte activation	1.9E-5
leukocyte differentiation	2.6E-4
T cell activation	2.9E-4
lymphocyte differentiation	6.7E-4
B cell activation	2.0E-3
hematopoiesis	3.7E-3
immune system development	6.1E-3

B

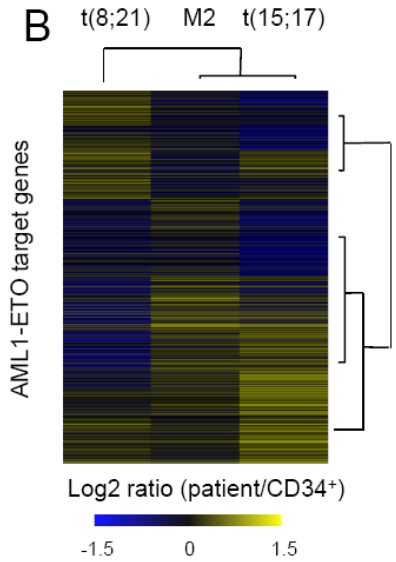

Figure 16. A. Functional annotation clustering (GO) of genes that are associated with AML1-ETO common peaks detected in patient blast cells. **B**. Clustering analysis of expression changes at the AML1-ETO target genes identified in AML patient blasts as compared to $CD34^+$cells. AML expression data from Valk et al. (2004) was evaluated for all AML1-ETO target genes in (i) t(8;21) cells as compared to normal $CD34^+$ cells as well as in (ii) FAB M2 non AML1-ETO AML cells as compared to normal $CD34^+$ cells and (iii) t(15;17) cells as compared to $CD34^+$ cells.

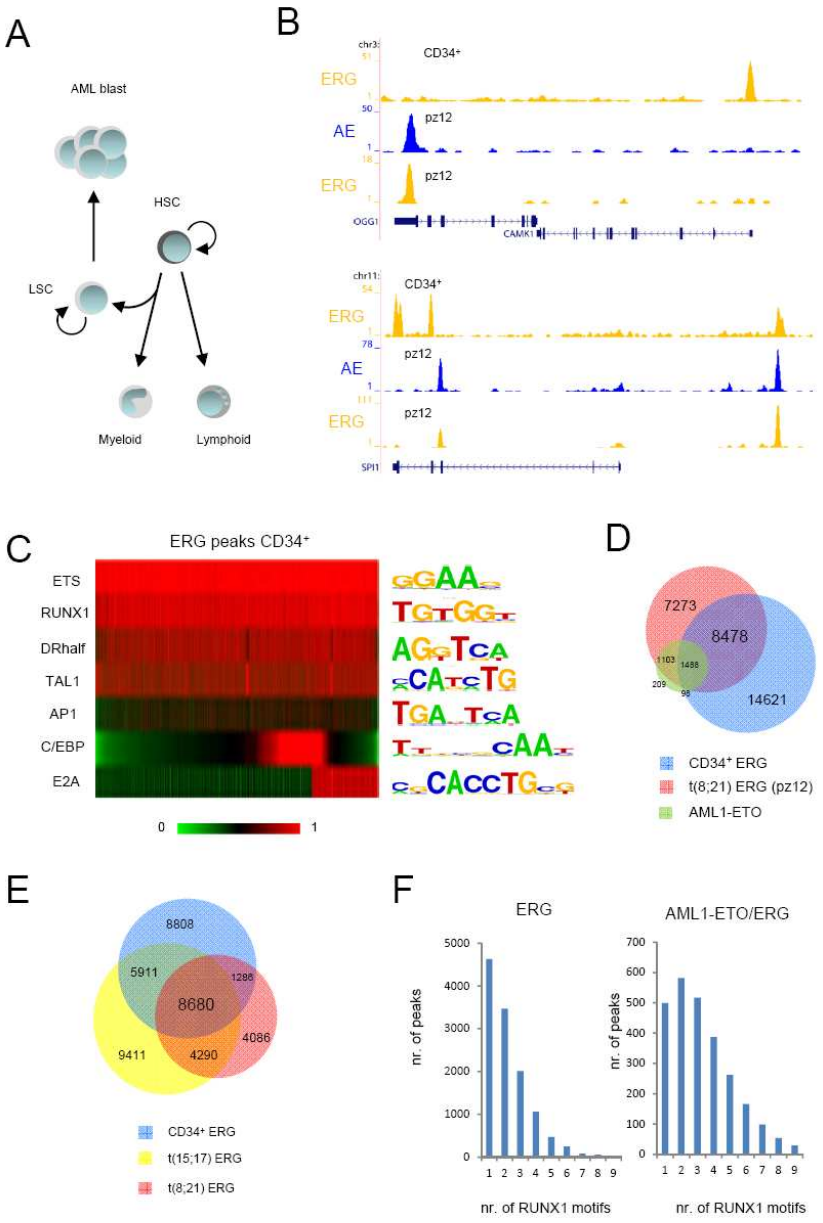

Figure 17. ERG identifies genomic regions important in hematopoietic development and has cell type specific binding profiles. **A**. Schematic representation of normal and aberrant hematopoietic differentiation. HSC, Hematopoietic Stem Cell; LSC, Leukemic Stem Cell. **B**. Overview of the *OGG1*, *CAMK1* and *SPI1* ERG binding sites in normal $CD34^+$ cells and ERG and AML1-ETO (AE) binding sites in blast cells from a patient with t(8;21). In yellow the ERG ChIP-seq data is plotted, in blue the AML1-ETO data. **C**. Heatmap display of motif scores of DNA sequences underlying ERG binding sites in $CD34^+$ cells. **D**. Venn diagram representing the overlap of ERG (pz12) and AML1-ETO binding sites in t(8;21) patient AML cells and ERG binding sites in normal $CD34^+$ cells. **E**. Venn diagram representing the overlap of ERG binding sites in normal $CD34^+$ cells and t(15;17) APL cells and t(8;21) AML patient cells. **F**. Number of RUNX1 motifs present in t(8;21) patient ERG binding sites not occupied by AML1-ETO (left), or present in AML1-ETO binding sites (right).

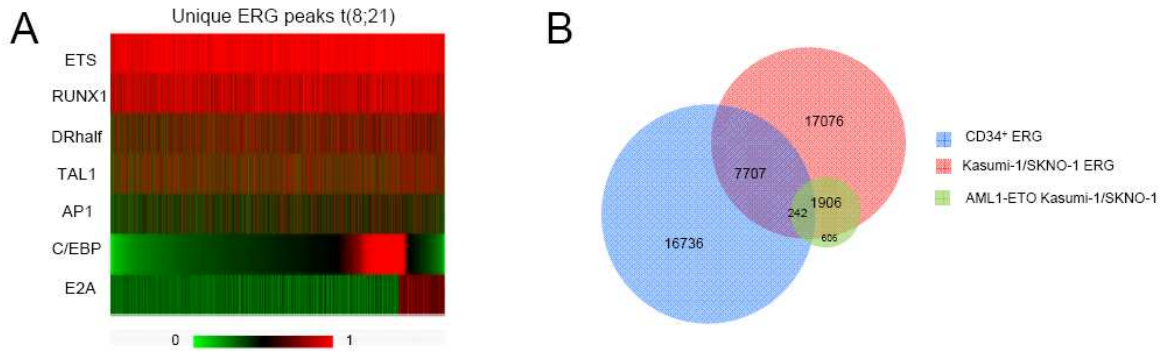

Figure 18. A. Heatmap display of enriched motifs present in DNA sequences underlying ERG binding sites that are present in t(8;21) cells but not in $CD34^+$ cells. **B**. Venn diagram representing the overlap of ERG and AML1-ETO binding sites in Kasumi-1/SKNO-1 cells and ERG binding sites in normal $CD34^+$ cells.

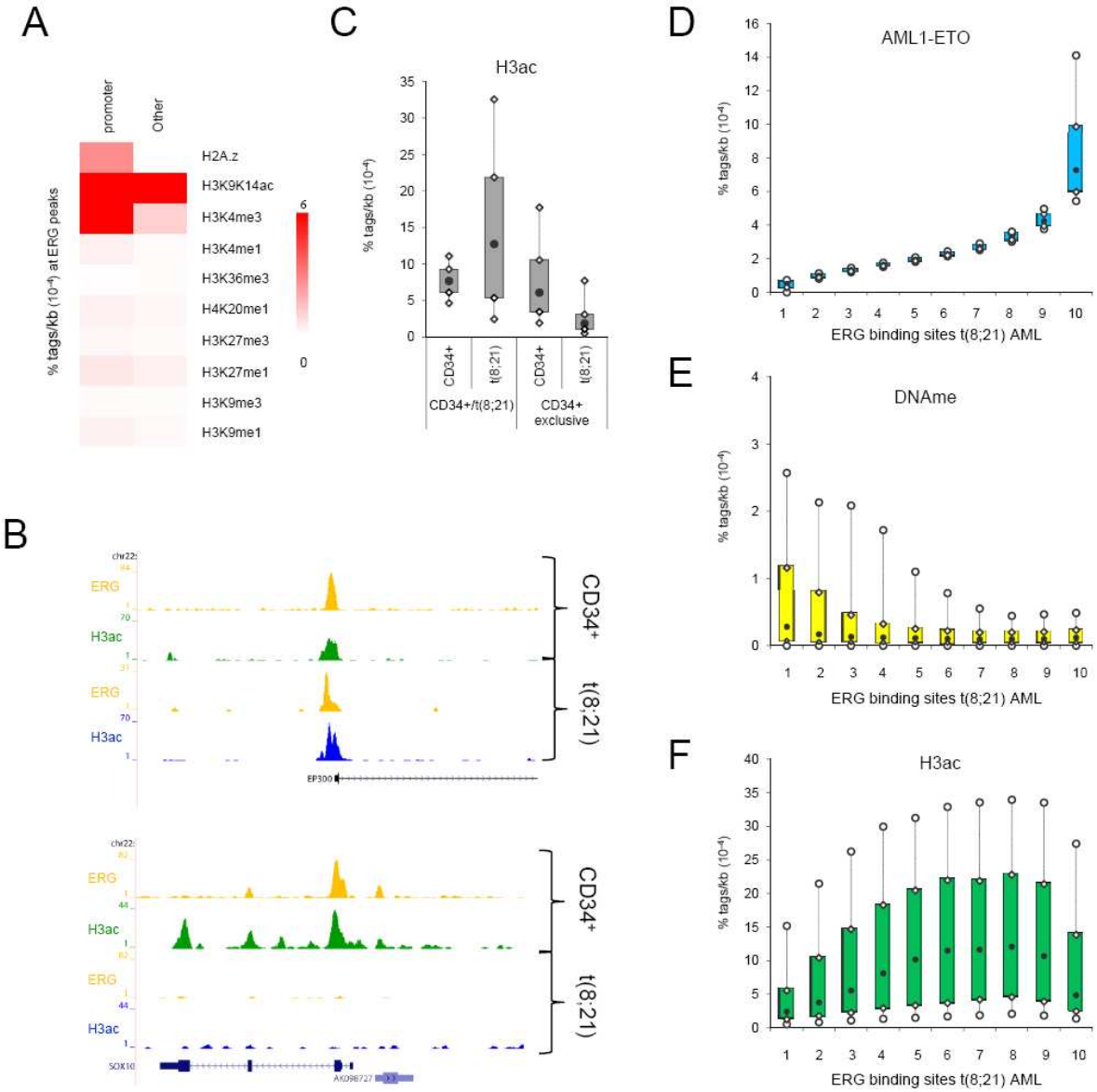

Figure 19. ERG defines H3 acetylation signatures in normal CD34$^+$ and t(8;21) blast cells. **A**. Heat map displaying median tag densities of a variety of chromatin modifications at ERG binding sites that are present in normal CD34$^+$ cells. **B**. Overview of the *SOX10* and *P300* genes in normal CD34$^+$ and AML cells with t(8;21). In yellow the ERG ChIP-seq data is plotted and in green the H3K9K14ac using normal CD34$^+$ cells and in blue the H3K9K14ac data using patient AML CD34$^+$ cells with t(8;21). **C**. Boxplot showing the percentage of H3K9K14ac tags in normal CD34$^+$ and patient t(8;21) AML cells in ERG peaks that are present in both normal CD34$^+$ and AML t(8;21) cells or ERG peaks that are unique for normal CD34$^+$ cells (CD34$^+$ exclusive). **D-F**. Boxplots showing the density of AML1-ETO (**D**), MethylCap-DNAme (**E**) and H3ac (**F**) tags in patient AML t(8;21) cells within 10 bins of ERG binding sites (pz12) that are ranked according to AML1-ETO tag density.

CHAPTER 4 DISCUSSION

Many breakpoints involved in specific chromosomal translocations have been cloned over the years. In most cases, however, the role of the chimeric oncofusion proteins in tumorigenesis has not been elucidated. In the case of AML our analysis of PML-RARα represented the first report of the genome-wide actions of an oncofusion protein (Martens et al., 2010). AML1-ETO has thus far only been studied using ChIP-chip in an inducible AML1-ETO cell line (Gardini et al., 2008), while here, we analyzed the genome-wide binding pattern of AML1-ETO, epigenomic features and its interplay with other regulators of hematopoiesis in cell lines and patient primary blasts.

To identify AML1-ETO binding we used antibodies specifically recognizing the AML1-ETO fusion point as well as two antibodies recognizing different parts of the ETO protein in ChIP-seq and identified 2,754 high confidence, mostly non-promoter, binding sites in Kasumi-1 and SKNO-1 cells. In addition we analyzed genome-wide RUNX1/AML1, HEB and CBFβ binding and could show enrichments of both RUNX1/AML1 and HEB at all high confidence AML1-ETO binding sites, while CBFβ enrichment was only detected at a subset.

Analysis of the high confidence AML1-ETO binding sites showed an abundance of ETS factor consensus motifs at nearly every position. ChIP-seq with FLI1 and ERG antibodies revealed the presence of these ETS factors at AML1-ETO binding sites in SKNO-1 cells, a finding that could be corroborated and extended to a primary AML blast with t(8;21). In addition to AML1-ETO, ETS factor colocalization could also be identified at sites bound by the oncofusion protein PML-RARα, substantiating in the APL-derived NB4 cells previous findings that identified co-occurrence of the ETS factor SPI1 with PML-RARα in U937-PR9 cells (Wang et al., 2010).

Interestingly, using an AML1-ETO inducible cell system revealed that AML1-ETO is recruited to sites pre-occupied by FLI1, uncovering ETS factors as proteins that facilitate binding of other proteins. Further analysis in an ERG inducible cell system showed that AML1-ETO can bind additional genomic regions when these are pre-marked or opened up by ERG binding. Together these data suggest that ETS factors have a pioneering function, demarcating genomic regions to which oncofusion proteins such as AML1-ETO can be recruited in a cell type specific fashion. The function of ERG in providing a docking platform for other hematopoietic regulators is further substantiated by the recent identification of a loss of function ERG mutant that still binds DNA but is suggested to have lost the potential to interact with other proteins (Loughran et al.,

2008) and from ChIP-seq studies in mice that suggest that ERG colocalizes with a variety of other hematopoiesis associated proteins (Wilson et al., 2010).

Increased expression of ERG in AMLs is associated with poor prognosis (Marcucci et al., 2005; Metzeler et al., 2009). The molecular mechanisms behind these findings are unclear. Our results suggest that binding of ERG is cell type specific and that it is associated with histone hyperacetylation. Increased levels of ERG expression might result in changes in global histone acetylation due to binding of ERG to more sites. In addition, our results reveal that overexpression of ERG results in localization of this protein to many previously unbound accessible genomic regions and thereby facilitate binding of secondary proteins. This function might be crucial in preventing normal hematopoietic differentiation in transformed cells and supporting leukemogenesis in high ERG expressing AMLs.

In addition to oncofusion protein expressing cells we assessed ERG binding in normal hematopoietic $CD34^+$ cells. Normal $CD34^+$ cells have the potential to differentiate along the lymphoid and myeloid lineages dependent on the culture conditions used, while the t(8;21) and APL cells are transformed and likely blocked at a certain stage of the myeloid differentiation program. Analysis and comparison of ERG binding sites in these cell types revealed that ERG binding sites are marked with 'active' H3 acetylation. Extending these results to cells that express oncofusion proteins revealed that a main molecular strategy of AML1-ETO involves targeting of histone deacetylation activities to ERG and FLI1 bound hematopoietic regulatory sites. Interestingly our study shows that PML-RARα also colocalizes with ETS factors and previously we reported that PML-RARα has similar epigenetic effects (Martens et al., 2010), suggesting that AML1-ETO and PML-RARα utilize similar molecular mechanisms to block differentiation. Indeed, recruitment of histone deacetylation activities to hyperacetylated ETS factor regulatory sites can be expected to have a significant impact on transcription and epigenetic organization and likely represents a crucial event in the transformation process. Moreover, these observations also highlight the potential of using specific HDAC inhibitors or other epigenetic-based drugs in AML treatment. Specific targeting of the epigenetic modifications that underlie 'normal' ETS factor binding sites or targeting the acetylase/deacetylase containing complexes (Bantscheff et al., 2011) might provide an attractive approach to therapeutically eradicate leukemic cells.

Comparing our PML-RARα and AML1-ETO binding profiles revealed many common genomic targets, amongst which the hematopoietic master regulators *SPI1* and *RUNX1*. Apart from this

several other molecular similarities could be uncovered. First, both oncofusion proteins form oligomeric complexes as an effect of the multimerization properties of the fusion partners PML and ETO, respectively. Consequently, the oligomeric complex can target DNA binding templates that contain multiple consensus sequences and thereby deviate from parental protein binding, although the DNA binding domain and hence cis-acting sequence recognition of the RARα and AML1 moiety is not changed. Secondly, both oncofusion proteins have a protein partner, HEB and CBFβ that bind to the ETO and AML1 moiety of AML1-ETO, respectively, and RXR that binds the RARα moiety of PML-RARα. Third, our study showed almost exclusive binding of AML1-ETO and PML-RARα to regions occupied by ERG and/or FLI1. As also the ETS factor SPI1 has previously been reported to interact with PML-RARα (Wang et al., 2010), these results indicate that both oncofusion proteins are targeted to and could potentially interfere with ETS factors. Finally, our previous observation that PML-RARα recruits histone deacetylase activities (Martens et al., 2010) could in this study be extended to AML1-ETO, revealing that both oncofusion proteins recruit histone deacetylase activities to their binding sites. It is tempting to speculate that other oncofusion proteins might also share many of these features or, vice versa, that any protein that is altered such that it confers these four properties has the potential to transform cells. Still, many targets of AML1-ETO and PML-RARα are not shared and our results suggest that ETS factors might be important determinants for guiding this AML subtype specific oncofusion protein binding. The differences in ETS factor binding regions between AML subtypes might account for the ‘cell stage’ specific block of differentiation and features of the diseases. Future analysis of both these common and specific aspects of various AML subtypes are expected to yield further insights on how to therapeutically eradicate these cancer cells.

4.1 CONCLUSION

Acute myeloid leukemia (AML) associated oncofusion proteins play a critical role in development and progression of the disease. Here, we identified high confidence binding sites of the oncofusion protein AML1-ETO in two t(8;21) cell lines and three patients AML blasts and found colocalization of AML1-ETO with subsets of ERG and FLI1 occupied regulatory regions, a finding that could be extended to PML-RARα in Acute Promyelocytic Leukemia (APL). ERG, which is generally associated with H3 hyperacetylation, is shown to recruit AML1-ETO in a cell type specific manner, resulting in local decreases in histone acetylation. Together our results suggest that ERG/FLI1 demarcate hematopoietic regulatory sites and promote leukemogenesis by providing target sites for aberrant epigenetic regulation by oncofusion proteins.

APPENDIX

Primers used in this study

ChIP:

SPI1	Forward	GGGTAAGAGCCTGTGTCAGC
	Reverse	CAGATGCACGTCCTCGATAC
FUT7	Forward	TGAAACCAACCCTCAAGGTC
	Reverse	TCACTGGCATGAATGAGAGC
NFE2	Forward	GGTTAGCAGCATACGTGGAG
	Reverse	ACGATACGGAGAAAACCACG
OGG1	Forward	CCACCCTGATTTCTCATTGG
	Reverse	CAACCACCGCTCATTTCAC
VEGF	Forward	GGTTTGGATCCTCCCATTTC
	Reverse	CAGTCAGTGGTGGGGAGAG
ITGAM	Forward	GCTTCCTTGTGGTTCCTCAG
	Reverse	AGGAGCCAGAACCTGGAAG
CD344	Forward	AGTTTGGCTTGTGGGAACTG
	Reverse	GACAAGGCCACTGAGAAAGC
KREMEN1	Forward	CGAGAGTGACATCCAGTTGC
	Reverse	TTCACAACCGTTCCAGATGA
H2B	Forward	TTGCATAAGCGATTCTATATAAAAGCG
	Reverse	ATAAAGCGCCAACGAAAAGG
MYOG	Forward	AAGTTTGACAAGTTCAAGCACCTG
	Reverse	TGGCACCATGCTTCTTTAAGTC

Cloning GST fusion proteins AML1-ETO:

GST-1	forward	ACTGCGGATCCCGTATCCCCGTAG
	reverse	CAGTGAATTCTCAGTGCTTCTCAG
GST-2	forward	ACTGCGGATCCGGGCCCCGAGAACCTC
	reverse	CAGTGAATTCTCAGAGTTGCCTGGC
GST-3	forward	ACTGCGGATCCCTGGCTAATCAACAG
	reverse	CAGTGAATTCTCATCTGTCTGGAGTTC
GST-4	forward	ACTGCGGATCCACCAAAGAAAATGGC
	reverse	CAGTGAATTCTCAATGCAACCCCATAG
GST-5	forward	ACTGCGGATCCAGCCACAGGGAC
	reverse	CAGTGAATTCTCATTCCCGATGCGC
GST-6	forward	ACTGCGGATCCAGTCCCGTCAACC
	reverse	CAGTGAATTCTCAACTCTCGCTTGAATC
GST-7	forward	ACTGCGGATCCTGCTGGAATTGTG
	reverse	CAGTGAATTCTCACTAGCGAGGGGTTG

qPCR validation of high confidence AML1-ETO SKNO-1/Kasumi-1 binding sites

High regions		
1	forward	AAGGGAGGGGAGCTAACTGA
	reverse	GGCTAATCCCACAGAGCAAG
2	forward	CACGCTGGCTACATTTCTCA
	reverse	GTGTCCCCTCTTGCTGACAT
3	forward	CTTCAGTGGCAAACCCAGTT
	reverse	GCAAGGAAGCTGAGGATGAG
4	forward	TGTGTTGGTTGGAAGCTGAA
	reverse	AAGACCTGTTGCCAGCATCT
5	forward	TTGTTGGGGAACACTTCACA
	reverse	AAGGCTGAGAAAAGGGAAGC
6	forward	CTGGACTGGGGAAGGATTTT
	reverse	ACCCCACACACACTCCCTTA
7	forward	AAATGGCAACTGGACCAAAG
	reverse	GTCGACATCTCCTCCAGCTC
8	forward	TCCACAGAAGCCTCCTTGTT
	reverse	TTGTTTCACCACCAGACTGC
9	forward	AATTGCTGTGCACTGTGTCC
	reverse	GACCACAGCATCCCATTCTT
10	forward	CCAAGTTTGCGCAATAGGAC
	reverse	CCATGTGCCTTGCACAATAA
Middle regions		
1	forward	GGCCACACTTCATTTCACCT
	reverse	TAGCGGGAGAGGCAGAGATA
2	forward	TGACGCTTAAGAGCCCAGAT
	reverse	AGCAAGACCACTGCTGGAAT
3	forward	CAGCTTGTTTGCACTTTGGA
	reverse	AGCAGCCTGACTTGAAAAGC
4	forward	GGGTCACATCTCCTCCTTCA
	reverse	GCCACTCAAGCTCACTCTCC
5	forward	GCATTTGGAGGCTACTGCTC
	reverse	TCGGAGGTGAGAATGCTCTT
6	forward	TCTGCTGACAACCTGAATGC
	reverse	GGCTTAGGATGGGGGAGTAG
7	forward	AGAGCTCAGGTGTCGTCCAT
	reverse	GCAAACTGAGCTGTGGCATA
8	forward	ACAGGCATCTCCCAGCTCTA
	reverse	CTTGTGTGCTGGAGGTTGTG
9	forward	TCTCCAAGCAGCTGATGATG
	reverse	AGATGAATGGGAGGGAGCTT
10	forward	GGGAAAGGTCCAGAGAGAGG
	reverse	TGTCTGGAAGGGGAATTCAG
Low regions		
1	forward	GCTGGCAGTTAAGGGATGAG
	reverse	CTCTAGCTGCTGCCCTGTCT
2	forward	AAGCTGGAGAACAAGGCTCA
	reverse	GTCAGGGGGTGACACAGACT

3	forward	TCCTACGTTCTGCCCATTGT
	reverse	CTCCCAAAGAGTTGCCAGAC
4	forward	GAGAGACTGCTGCGGGTAAC
	reverse	GCTTCTGCAAAGCCTGACTC
5	forward	CACCAGCCTGAACAGATGAA
	reverse	TCCAAACAGCAAAGGAGCTT
6	forward	GAATCTGGGTGTTGCAAGGT
	reverse	GGTGATCCTAGGGGGAGAAG
7	forward	CTGGGACGTGAAGAGGAGAC
	reverse	AGAGCCTTACAATGCCTGGA
8	forward	TTCCTATGGACTCCCACAGC
	reverse	AGTCCATGGGGCAGTAGATG
9	forward	GGACTTCCAGGCCATGACTA
	reverse	TCCTTCTCTTTGGGGTCCTT
10	forward	GCAGAGCTTGTGGGAGTTTC
	reverse	CAGAGAGACACGCCTGTACG

Profiles analyzed in this study

Cells	ChIP antibody/technique	Treatment	Mapped reads	reference
Kasumi-1	AE (A706)	no	6716821	
Kasumi-1	HEB (sc-357)	no	5885202	
Kasumi-1	ETO1 (A710)	no	6738375	
Kasumi-1	ETOsc (sc-9737)	no	5193085	
SKNO-1	AE (A706)	no	9474494	
SKNO-1	CBF (A1329)	no	2084211	
SKNO-1	ERG (sc-353)	no	13373986	
SKNO-1	FLI1 (sc-356)	no	1609327	
SKNO-1	RUNX1 (ab-23980)	no	2084211	
SKNO-1	RNA-seq	no	16178852	
AML pz12	AE (A706)	no	11324391	
AML pz12	ERG (sc-353)	no	16659875	
AML pz1 6	AE (A7 6)	no	83 29 2	
AML pz186	H3K9K14ac (Diagenode)	no	10175724	
AML pz186	MethylCap	no	34716102	
AML pz229	AE (A706)	no	8882375	
AML pz229	H3K9K14ac (Diagenode)	no	15944616	
AML pz229	MethylCap	no	21305015	
CD34+ nr29	ERG (sc-353)	no	16965117	
CD34+ nr30	H3K9K14ac (Diagenode)	no	16201598	
CD34+ nr30	FLI1 (sc-356)	no	16191803	
NB4	PML (H238)	no		Martens et al., 2010
NB4	RARa (Diagenode)	no		Martens et al., 2010
NB4	FLI1 (ab-15289)	no	8935568	
APL pz74	ERG	no	17758130	
MCF7	ERG	AML1-ETO/ERG	3544120	

		transfected		
MCF7	AML1-ETO	AML1-ETO/ERG transfected	3648588	
K562-ERG	ERG	AML1-ETO transfected, no dox	23220874	
K562-ERG	ERG	AML1-ETO transfected,72 hrs dox	18572309	
K562-ERG	AML1-ETO	AML1-ETO transfected, no dox	13700478	
K562-ERG	AML1-ETO	AML1-ETO transfected,72 hrs dox	12259664	
UAE	AE (A706)	no	8277859	
UAE	AE (A706)	5 hrs zinc	7670219	
UAE	FLI1 (ab-15289)	no	17661457	
UAE	FLI1 (ab-15289)	5 hrs zinc	19010064	
UAE	H3K9K14ac (Diagenode)	no	14723129	
UAE	H3K9K14ac (Diagenode)	5 hrs zinc	15057351	
UAE	H4panac (Upstate)	no	13195517	
UAE	H4panac (Upstate)	5 hrs zinc	11996351	
UAE	RNAPII (Diagenode)	no	6648533	
UAE	RNAPII (Diagenode)	5 hrs zinc	9130135	
CD133+	H3K4me3	no		Cui et al., 2009
CD133+	H3K9me1	no		Cui et al., 2009
CD133+	H3K9me3	no		Cui et al., 2009
CD133+	H3K27me1	no		Cui et al., 2009
CD133+	H3K27me3	no		Cui et al., 2009
CD133+	H4K20me1	no		Cui et al., 2009
CD133+	H3K4me1	no		Cui et al., 2009
CD133+	H3K36me3	no		Cui et al., 2009

Scripts used in this study

Task	Name script	Used to generate figures
Peak calling	MACS	2B; 5D; 8A; 9C; 11B, D; 13D, E; 3B, 4C; 6E, H; 14B
Tag counting	peakstats.py	2B, C; 5C, G; 8E, 9B, E; 15A, C-F; 3F, G; 4B, D; 6I; 7C; 10D
Motif discovery	gimme_motifs.py	5A
Motif counting	pwmscan.py	13C,F; 14A
Motif scoring	pwm_scores.py	13C; 14A
Peak annotation	genomic_distribution.sh	2D, 8D
Intensity plot	makeColorProfiles.pl	5G

For clustering and heatmap generation TMEV (http://www.tm4.org/mev/) was used and for functional annotation DAVID (http://david.abcc.ncifcrf.gov/).

REFERENCES

Akashi K, Traver D, Kondo M, Weissman IL. Lymphoid development from hematopoietic stem cells. Int J Hematol 1999; 69: 217-26.

Akashi K, Traver D, Miyamoto T, Weissman IL. A clonogenic common myeloid progenitor that gives rise to all myeloid lineages. Nature 2000; 404:193-7.

Alcalay M, Meani N, Gelmetti V, Fantozzi A, Fagioli M, Orleth A, Riganelli D, Sebastiani C, Cappelli E, Casciari C, et al. Acute myeloid leukemia fusion proteins deregulate genes involved in stem cell maintenance and DNA repair. The Journal of clinical investigation 2003; 112: 1751-1761.

Al-Hajj M, Wicha MS, Benito-Hernandez A, Morrison SJ, Clarke MF. Prospective identification of tumorigenic breast cancer cells. Proc Natl Acad Sci U S A 2003; 100: 3983-3988.

Amann JM, Nip J, Strom DK, Lutterbach B, Harada H, Lenny N, Downing JR, Meyers S, Hiebert SW. ETO, a target of t(8;21) in acute leukemia, makes distinct contacts with multiple histone deacetylases and binds mSin3A through its oligomerization domain. Molecular and cellular biology 2001; 21:6470-6483.

Anderson MK, Hernandez-Hoyos G, Diamond RA, Rothenberg EV. Precise developmental regulation of Ets family transcription factors during specification and commitment to the T cell lineage. Development 1999; 126:3131-48.

Antonchuk J, Sauvageau G, Humphries RK. HOXB4-induced expansion of adult hematopoietic stem cells ex vivo.Cell 2002; 109: 39-45.

Asou H, Tashiro S, Hamamoto K, Otsuji A, Kita K, Kamada N. Establishment of a human acute myeloid leukemia cell line (Kasumi-1) with 8;21 chromosome translocation. Blood 1991; 77:2031-2036.

Baldus CD, Thiede C, Soucek S, Bloomfield CD, Thiel E, Ehninger G. BAALC expression and FLT3 internal tandem duplication mutations in acute myeloid leukemia patients with normal cytogenetics: prognostic implications. J Clin Oncol 2006; 24:790-797.

Bantscheff M, Hopf C, Savitski MM, Dittmann A, Grandi P, Michon AM, Schlegl J, Abraham Y, Becher I, Bergamini G, et al. Chemoproteomics profiling of HDAC inhibitors reveals selective targeting of HDAC complexes. Nat Biotechnol 2011; 29: 255-265.

Barjesteh van Waalwijk van Doorn-Khosrovani S, Erpelinck C, Meijer J, van Oosterhoud S, van Putten WL, Valk PJ, Berna Beverloo H, Tenen DG, Löwenberg B,Delwel R. Biallelic mutations in the CEBPA gene and low CEBPA expression levels as prognostic markers in intermediate-risk AML. Hematol J 2003; 4:31-40.

Bergsagel DE, Valeriote FA. Growth characteristics of a mouse plasma cell tumor. Cancer Res 1968; 28:2187-2196.

Bhardwaj G, Murdoch B, Wu D, Baker DP, Williams KP, Chadwick K, Ling LE, Karanu FN, Bhatia M. Sonic hedgehog induces the proliferation of primitive human hematopoietic cells via BMP regulation. Nat Immunol 2001 ;2:172-80.

Birdsey GM, Dryden NH, Amsellem V, Gebhardt F, Sahnan K, Haskard DO, Dejana E, Mason JC, Randi AM. Transcriptionfactor Erg regulates angiogenesis and endothelial apoptosis through VE-cadherin. Blood 2008; 111:3498-506.

Bonnet D, Dick JE. Human acute myeloid leukemia is organized as a hierarchy that originates from a primitive hematopoietic cell. Nat. Med 1997; 3:730-737.

Brinkman AB, Simmer F, Ma K, Kaan A, Zhu J, Stunnenberg, H. G. Whole-genome DNA methylation profiling using MethylCap-seq. Methods 2010; 52:232-6.

Buick RN, Pollak MN. Perspectives on clonogenic tumor cells, stem cells, and oncogenes. Cancer Res 1984; 44:4909-4918.

Burda P, Laslo P, Stopka T. The role of PU.1 and GATA-1 transcription factors during normal and leukemogenic hematopoiesis. Leukemia 2010; 24:1249-57.

Cairoli R, Beghini A, Grillo G, Nadali G, Elice F, Ripamonti CB, Colapietro P, Nichelatti M, Pezzetti L, Lunghi M, et al. Prognostic impact of c-KIT mutations in core binding factor leukemias: an Italian retrospective study. Blood 2006; 107:3463-3468.

Cameron ER, Neil JC. The Runx genes: lineage-specific oncogenes and tumor suppressors. Oncogene 2004;23: 4308-4314.

Cammenga J, Horn S, Bergholz U, Sommer G, Besmer P, Fiedler W, Stocking C. Extracellular KIT receptor mutants, commonly found in core binding factor AML, are constitutively active and respond to imatinib mesylate. Blood 2005; 106:3958-3961.

Care RS, Valk PJ, Goodeve AC, Abu-Duhier FM, Geertsma-Kleinekoort WM, Wilson GA, Gari MA, Peake IR, Löwenberg B, Reilly JT. Incidence and prognosis of c-KIT and FLT3 mutations in core-binding factor (CBF) acute myeloid leukaemias. Br J Haematol 2003; 121:775-777.

Cobaleda C, Gutierrez-Cianca N, Perez-Losada J, Flores T, Garcia-Sanz R, Gonzalez M, Sanchez-Garcia I. A primitive hematopoietic cell is the target for the leukemic transformation in human Philadelphia-positive acute lymphoblastic leukemia. Blood 2000; 95:1007-1013.

Cozzio A, Passegue E, Ayton PM, Karsunky H, Cleary ML, Weissman IL. Similar MLL-associated leukemias arising from self-renewing stem cells and short-lived myeloid progenitors. Genes Dev 2003; 17:3029-3035.

Cui K, Zang C, Roh TY, Schones DE, Childs RW, Peng W, Zhao K. Chromatin signatures in multipotent human hematopoietic stem cells indicate the fate of bivalent genes during differentiation. Cell Stem Cell 2009; 4: 80-93.

Dash A, Gilliland DG. Molecular genetics of acute myeloid leukaemia. Best Pract Res Clin Haematol 2001; 14:49-64.

Davis JN, McGhee L, Meyers S. The ETO (MTG8) gene family. Gene 2003; 303:1–10.

de Bruijn MF, Speck NA. Core-binding factors in hematopoiesis and immune function. Oncogene 2004; 23: 4238-4248.

de Guzman CG, Warren AJ, Zhang Z, Gartland L, Erickson P, Drabkin H, Hiebert SW, Klug CA. Hematopoietic stem cell expansion and distinct myeloid developmental abnormalities in a murine model of the AML1-ETO translocation. Mol Cell Biol 2002; 22:5506-5517.

de The, H, Chomienne C, Lanotte M, Degos L, Dejean A. The t(15;17) translocation of acute promyelocytic leukaemia fuses the retinoic acid receptor alpha gene to a novel transcribed locus. Nature 1990; 347:558-561.

Delattre O, Zucman J, Plougastel B, Desmaze C, Melot T, Peter M, Kovar H, Joubert I, de Jong P, Rouleau G, Aurias A, Thomas G. Gene fusion with an ETS DNA-binding domain caused by chromosome translocation in human tumours. Nature 1992; 359:162-5.

Denissov S, van Driel M, Voit R, Hekkelman M, Hulsen T, Hernandez N, Grummt I, Wehrens R, Stunnenberg, H. Identification of novel functional TBP-binding sites and general factor repertoires. The EMBO journal 2007; 26:944-954.

Deschler, B, Lubbert, M. Acute myeloid leukemia: epidemiology and etiology. Cancer 2006; 107:2099–2107.

Deshpande AJ, Cusan M, Rawat VP, Reuter H, Krause A, Pott C, Quintanilla-Martinez L, Kakadia P, Kuchenbauer F, Ahmed F, et al. Acute myeloid leukemia is propagated by a leukemic stem cell with lymphoid characteristics in a mouse model of CALM/AF10-positive leukemia. Cancer Cell 2006; 10:363-374.

Domen J, Cheshier SH, Weissman IL. The role of apoptosis in the regulation of hematopoietic stem cells: Overexpression of Bcl-2 increases both their number and repopulation potential. J.Exp.Med. 2000; 191:253-264.

Domen J, Weissman IL. Self-renewal, differentiation or death: regulation and manipulation of hematopoietic stem cell fate. Mol.Med.Today 1999; 5:201-208.

Downing JR, Head DR, Curcio-Brint AM, Hulshof MG, Motroni T. A, Raimondi SC, Carroll AJ, Drabkin HA, Willman C, Theil KS, et al. An AML1/ETO fusion transcript is consistently detected by RNA-based polymerase chain reaction in acute myelogenous leukemia containing the (8;21)(q22;q22) translocation. Blood 1993; 81:2860-2865.

Downing JR. The core-binding factor leukemias: lessons learned from murine models. Curr Opin Genet Dev 2003; 13:48-54.

Egger G, Liang G, Aparicio A, Jones PA. Epigenetics in human disease and prospects for epigenetic therapy. Nature 2004; 429:457-463.

Erickson P, Gao J, Chang K.S, Look T, Whisenant E, Raimondi S, Lasher R, Trujillo J, Rowley J, Drabkin H. Identification of breakpoints in t(8;21) acute myelogenous leukemia and isolation of a fusion transcript, AML1/ETO, with similarity to Drosophila segmentation gene, runt. Blood 1992;80: 1825-1831.

Erickson PF, Robinson M, Owens G, Drabkin HA. The ETO portion of acute myeloid leukemia t(8;21) fusion transcript encodes a highly evolutionarily conserved, putative transcription factor. Cancer Res 1994; 54, 1782-1786.

Espey DK, Wu XC, Swan J, Wiggins C, Jim MA, Ward E, Wingo PA, Howe HL, Ries LA, Miller BA, et al. Annual report to the nation on the status of cancer, 1975-2004, featuring cancer in American Indians and Alaska Natives. Cancer 2007; 110:2119-2152.

Estey E, Döhner H. Acute myeloid leukaemia. Lancet 2006; 368:1894-1907.

Follows GA, Tagoh H, Lefevre P, Hodge D, Morgan GJ, Bonifer, C. Epigenetic consequences of AML1-ETO action at the human c-FMS locus. The EMBO journal 2003; 22:2798-2809.

Frank R, Zhang J, Uchida H, Meyers S, Hiebert SW, Nimer SD. The AML1/ETO fusion protein blocks transactivation of the GM-CSF promoter by AML1B. Oncogene 1995; 11: 2667-2674.

Fröhling S, Scholl C, Gilliland DG, Levine RL. Genetics of myeloid malignancies: pathogenetic and clinical implications. J Clin Oncol 2005; 23:6285-6295.

Garcia M, Jemal A, Ward EM, Center MM, Hao Y, Siegel RL, Thun MJ. Global Cancer Facts & Figures 2007. American Cancer Society: Atlanta 2007.

Gardini A, Cesaroni M, Luzi L, Okumura, AJ, Biggs JR, Minardi SP, Venturini E, Zhang DE, Pelicci PG, Alcalay M. AML1/ETO oncoprotein is directed to AML1 binding regions and co-localizes with AML1 and HEB on its targets. PLoS genetics 2008; 4, e1000275.

Gelmetti V, Zhang J, Fanelli M, Minucci S, Pelicci PG, Lazar MA. Aberrant recruitment of the nuclear receptor corepressor-histone deacetylase complex by the acute myeloid leukemia fusion partner ETO. Mol Cell Biol 1998; 18:7185-7191.

Göttgens B, Nastos A, Kinston S, Piltz S, Delabesse EC, Stanley M, Sanchez MJ, Ciau-Uitz A, Patient R, Green AR. Establishing the transcriptional programme for blood: the SCL stem cell enhancer is regulated by a multiprotein complex containing Ets and GATA factors. EMBO J. 2002; 21:3039-50.

Grignani F, De Matteis S, Nervi C, Tomassoni L, Gelmetti V, Cioce M, Fanelli M, Ruthardt M, Ferrara FF, Zamir I, et al. Fusion proteins of the retinoic acid receptor-alpha recruit histone deacetylase in promyelocytic leukaemia. Nature 1998; 391:815-818.

Grimwade D, Walker H, Oliver F, Wheatley K, Harrison C, Harrison G, Rees J, Hann I, Stevens R, Burnett A, et al. The importance of diagnostic cytogenetics on outcome in AML: analysis of 1,612 patients entered into the MRC AML 10 trial. The Medical Research Council Adult and Children's Leukaemia Working Parties. Blood 1998; 92:2322-2333.

Grisolano JL, O'Neal J, Cain J, Tomasson MH. An activated receptor tyrosine kinase, TEL/PDGFbetaR, cooperates with AML1/ETO to induce acute myeloid leukemia in mice. Proc Natl Acad Sci U S A 2003; 100;9506-9511.

Gross CT, McGinnis W. DEAF-1, a novel protein that binds an essential region in a Deformed response element. EMBO J 1996 ;15:1961-1970.

Hao QL, Thiemann FT, Petersen D, Smogorzewska EM, Crooks GM. Extended long-term culture reveals a highly quiescent and primitive human hematopoietic progenitor population. Blood 1996; 88:3306-3313.

Harris NL, Jaffe ES, Diebold J, Flandrin G, Muller-Hermelink HK, Vardiman J, Lister TA, Bloomfield CD. The World Health Organization classification of neoplastic diseases of the hematopoietic and lymphoid tissues. Report of the Clinical Advisory Committee meeting, Airlie House, Virginia, November, 1997. Ann Oncol 1999; 10:1419-1432.

Hart A, Melet F, Grossfeld P, Chien K, Jones C, Tunnacliffe A, Favier R, Bernstein A. Fli-1 is required for murine vascular and megakaryocytic development and is hemizygously deleted in patients with thrombocytopenia. Immunity 2000; 13:167-77.

Higuchi M, O'Brien D, Kumaravelu P, Lenny N, Yeoh E.J, Downing J.R. Expression of a conditional AML1-ETO oncogene bypasses embryonic lethality and establishes a murine model of human t(8;21) acute myeloid leukemia. Cancer Cell 2002; 1:63-74.

Holyoake TL, Jiang X, Jorgensen HG, Graham S, Alcorn MJ, Laird C, Eaves AC, Eaves CJ. Primitive quiescent leukemic cells from patients with chronic myeloid leukemia spontaneously initiate factor- independent growth in vitro in association with up-regulation of expression of interleukin-3. Blood 2001; 97:720-728.

Huntly BJ, Shigematsu H, Deguchi K, Lee BH, Mizuno S, Duclos N, Rowan R, Amaral S, Curley D, Williams IR, Akashi K, Gilliland DG. MOZ-TIF2, but not BCR-ABL, confers properties of leukemic stem cells to committed murine hematopoietic progenitors. Cancer Cell 2004; 6:587-596.

Jemal A, Siegel R, Ward E, Hao Y, Xu J, Murray T, Thun MJ. Cancer statistics, 2008. CA Cancer J Clin 2008; 58:71-96.

Kakizuka A, Miller WH Jr, Umesono K, Warrell RP Jr, Frankel SR, Murty VV, Dmitrovsky E, Evans RM. Chromosomal translocation t(15;17) in human acute promyelocytic leukemia fuses RAR alpha with a novel putative transcription factor, PML. Cell 1991; 66: 663-674.

Kaushansky K. Lineage-specific hematopoietic growth factors, N Engl J Med 2006; 19:2034-45.

Kelly LM, Gilliland DG. Genetics of myeloid leukemias. Annu Rev Genomics Hum Genet 2002; 3:179-198.

Kelly LM, Liu Q, Kutok JL, Williams IR, Boulton CL, Gilliland DG. FLT3 internal tandem duplication mutations associated with human acute myeloid leukemias induce myeloproliferative disease in a murine bone marrow transplant model. Blood 2002; 99:310-318.

Kleinsmith LJ, Pierce GB ,Jr. Multipotentiality of Single Embryonal Carcinoma Cells. Cancer Res 1964; 24:1544-1551.

Kondo M, Weissman IL, Akashi K. Identification of clonogenic common lymphoid progenitors in mouse bone marrow. Cell 1997; 91:661-72.

Kosmider O, Moreau-Gachelin F. From mice to human: the "two-hit model" of leukemogenesis. Cell Cycle 2006; 5:569-570.

Krivtsov AV, Twomey D, Feng Z, Stubbs MC, Wang Y, Faber J, Levine JE, Wang J, Hahn WC, Gilliland DG, Golub TR, Armstrong SA. Transformation from committed progenitor to leukaemia stem cell initiated by MLL-AF9. Nature 2006; 442:818-822.

Kruse EA, Loughran SJ, Baldwin TM, Josefsson EC, Ellis S, Watson DK, Nurden P, Metcalf D, Hilton DJ, Alexander W.S, et al. Dual requirement for the ETS transcription factors Fli-1 and Erg in hematopoietic stem cells and the megakaryocyte lineage. Proc Natl Acad Sci U S A. 2009; 106: 13814-13819.

Kuriyama, K. FAB amd WHO classification of leukemia. Nippon Naika Gakkai Zasshi 2003; 92: 934-41.

Kwok C, Zeisig BB, Qiu J, Dong S, So CW. Transforming activity of AML1-ETO is independent of CBFbeta and ETO interaction but requires formation of homo-oligomeric complexes. Proc Natl Acad Sci U S A 2009;106: 2853-2858.

Lane SW, Scadden DT, Gilliland DG. The leukemic stem cell niche: current concepts and therapeutic opportunities. Blood 2009; 114:1150-1157.

Larochelle A, Vormoor J, Hanenberg H, Wang JC, Bhatia M, Lapidot T, Moritz T, Murdoch B, Xiao XL, Kato I, Williams DA, Dick JE. Identification of primitive human hematopoietic cells capable of repopulating NOD/SCID mouse bone marrow: implication for gene therapy. Nat Med 1996; 2:1329-1337.

Lavau C, Luo RT, Du C, Thirman MJ. Retrovirus-mediated gene transfer of MLL-ELL transforms primary myeloid progenitors and causes acute myeloid leukemias in mice. Proc Natl Acad Sci U S A 2000; 97:10984-10989.

Lefebvre JM, Haks MC, Carleton MO, Rhodes M, Sinnathamby G, Simon MC, Eisenlohr LC, Garrett-Sinha LA, Wiest DL. Enforced expression of Spi-B reverses T lineage commitment and blocks betaselection. J Immunol 2005; 174:6184-94.

Lessick SL, Ladanyi M. Molecular Pathogenesis of Ewing Sarcoma: New Therapeutic and Transcriptional Targets. Annu Rev Pathol. 2011; Jan 25.

Lin RJ, Nagy L, Inoue S, Shao W, Miller WH Jr, Evans RM. Role of the histone deacetylase complex in acute promyelocytic leukaemia. Nature 1998; 391: 811-814.

Liu P, Tarle SA, Hajra A, Claxton DF, Marlton P, Freedman M, Siciliano MJ, Collins FS. Fusion between transcription factor CBF beta/PEBP2 beta and a myosin heavy chain in acute myeloid leukemia. Science 1993; 261:1041-1044.

Liu XS, Brutlag DL, Liu JS. An algorithm for finding protein-DNA binding sites with applications to chromatin-immunoprecipitation microarray experiments. Nat Biotechnology 2002; 20:835-839.

Lo-Coco F, Ammatuna E, Montesinos P, Sanz MA. Acute promyelocytic leukemia: recent advances in diagnosis and management. Semin Oncol 2008; 35:401-409.

Loughran SJ, Kruse EA, Hacking DF, de Graaf CA, Hyland CD, Willson TA, Henley KJ, Ellis S, Voss AK, Metcalf D, et al. The transcription factor Erg is essential for definitive hematopoiesis and the function of adult hematopoietic stem cells. Nature immunology 2008; 9: 810-819.

Lowenberg B, Downing JR, Burnett A. Acute myeloid leukemia. N Engl J Med 1999; 341:1051-62.

Lutterbach B, Westendorf JJ, Linggi B, Patten A, Moniwa M, Davie JR, Huynh KD, Bardwell VJ, Lavinsky RM, Rosenfeld MG, et al. ETO, a target of t(8;21) in acute leukemia, interacts with the N-CoR and mSin3 corepressors. Mol Cell Biol 1998; 18:7176-7184.

Mackillop WJ, Ciampi A, Till JE, Buick RN. A stem cell model of human tumor growth: implications for tumor cell clonogenic assays. J Natl Cancer Inst 1983; 70: 9-16.

Marcucci G, Baldus CD, Ruppert AS, Radmacher MD, Mrozek K, Whitman SP, Kolitz JE, Edwards CG, Vardiman JW, Powell BL, et al. Overexpression of the ETS-related gene, ERG, predicts a worse outcome in acute myeloid leukemia with normal karyotype: a Cancer and Leukemia Group B study. J Clin Oncol 2005; 23:9234-9242.

Martens JH, Brinkman AB, Simmer F, Francoijs KJ, Nebbioso A, Ferrara F, Altucci L, Stunnenberg HG. PML-RARalpha/RXR Alters the Epigenetic Landscape in Acute Promyelocytic Leukemia. Cancer cell 2010; 17:173-185.

Martens JH, Verlaan M, Kalkhoven E, Dorsman JC, Zantema A. Scaffold/matrix attachment region elements interact with a p300-scaffold attachment factor A complex and are bound by acetylated nucleosomes. Mol Cell Biol 2002; 22: 2598-2606.

Martens JH. Acute myeloid leukemia: a central role for the ETS factor ERG. Int J Biochem Cell Biol. 2011; 43:1413-1416.

Matozaki S, Nakagawa T, Kawaguchi R, Aozaki R, Tsutsumi M, Murayama T, Koizumi T, Nishimura R, Isobe T, Chihara K. Establishment of a myeloid leukaemic cell line (SKNO-1) from a patient with t(8;21) who acquired monosomy 17 during disease progression. British journal of haematology 1995; 89:805-811.

McCulloch EA, Till JE. Perspectives on the properties of stem cells. Nat. Med 2005; 11: 1026-1028.

Mendelsohn ML. Chronic infusion of tritiated thymidine into mice with tumors. Science 1962; 135:213-215

Metzeler KH, Dufour A, Benthaus T, Hummel M, Sauerland MC, Heinecke A, Berdel WE, Buchner T, Wormann B, Mansmann U, et al. ERG expression is an independent prognostic factor and allows refined risk stratification in cytogenetically normal acute myeloid leukemia: a comprehensive analysis of ERG, MN1, and BAALC transcript levels using oligonucleotide microarrays. J Clin Oncol 2009; 27:5031-5038.

Meyer C, Kowarz E, Hofmann J, Renneville A, Zuna J, Trka J, Ben Abdelali R, Macintyre E, De Braekeleer E, De Braekeleer M, et al. New insights to the MLL recombinome of acute leukemias. Leukemia 2009; 23:1490-1499.

Meyers S, Lenny N, Hiebert SW. The t(8;21) fusion protein interferes with AML-1B-dependent transcriptional activation. Mol Cell Biol 1995; 15:1974-1982.

Minucci S, Maccarana M, Cioce M, De Luca P, Gelmetti V, Segalla S, Di Croce L, Giavara S, Matteucci C, Gobbi A, et al. Oligomerization of RAR and AML1 transcription factors as a novel mechanism of oncogenic activation. Molecular cell 2000; 5:811-820.

Mitelman F, Johansson B, Mertens F. The impact of translocations and gene fusions on cancer causation. Nat Rev Cancer 2007; 7:233-245.

Mitelman F, Johansson B, Mertens F. Mitelman Database of Chromosome Aberrations in Cancer 2009. <http://cgap.nci.nih.gov/Chromosomes/ Mitelman>.

Miyoshi H, Ohira M, Shimizu K, Mitani K , Hirai H , Imai T , Yokoyama K, Soeda E, Ohki M. Alternative splicing and genomic structure of the AML1 gene involved in acute myeloid leukemia. Nucleic Acids Res 1995; 23:2762-2769.

Miyoshi H, Shimizu K, Kozu T, Maseki N, Kaneko Y, Ohki M. t(8;21) breakpoints on chromosome 21 in acute myeloid leukemia are clustered within a limited region of a single gene, AML1. Proc Natl Acad Sci U S A 1991; 88:10431-10434.

Mochmann LH, Bock J, Ortiz-Tanchez J, Schlee C, Bohne A, Neumann K, Hofmann WK, Thiel E, Baldus CD. Genome-wide screen reveals WNT11, a non-canonical WNT gene, as a direct target of ETS transcription factor ERG. Oncogene 2011; 30:2044-56.

Moreau-Gachelin F. Lessons from models of murine erythroleukemia to acute myeloid leukemia (AML): proof-of-principle of co-operativity in AML. Haematologica 2006; 91:1644-1652.

Morris SW, Kirstein MN, Valentine MB, Dittmer KG, Shapiro DN, Saltman DL, Look AT. Fusion of a kinase gene, ALK, to a nucleolar protein gene, NPM, in non-Hodgkin's lymphoma. Science 1994; 263:1281-1284.

Morrison SJ, Uchida N, Weissman IL. The biology of hematopoietic stem cells. Annual review of cell and developmental biology 1995; 11: 35-71.

Morrison SJ, Wandycz AM, Hemmati HD, Wright DE, Weissman I L. Identification of a lineage of multipotent hematopoietic progenitors. Development 1997; 124:1929-39.

Mortazavi A, Williams BA, McCue K, Schaeffer L, Wold B. Mapping and quantifying mammalian transcriptomes by RNA-Seq. Nat Methods 2008; 5:621-628.

Mrózek K, Marcucci G, Paschka P, Bloomfield CD. Advances in molecular genetics and treatment of core-binding factor acute myeloid leukemia. Curr Opin Oncol 2008; 20:711-718.

Mrózek K, Marcucci G, Paschka P, Whitman SP, Bloomfield CD. Clinical relevance of mutations and gene-expression changes in adult acute myeloid leukemia with normal cytogenetics: are we ready for a prognostically prioritized molecular classification? Blood 2007; 109:431-448.

Mukouyama Y, Chiba N, Hara T, Okada H, Ito Y, Kanamaru R, Miyajima A, Satake M, Watanabe T. The AML1 transcription factor functions to develop and maintain hematogenic precursor cells in the embryonic aorta-gonad-mesonephros region. Dev Biol 2000; 220, 27-36.

Muller-Tidow C, Steffen B, Cauvet T, Tickenbrock L, Ji P, Diederichs S, Sargin B, Kohler G, Stelljes M, Puccetti E, et al. Translocation products in acute myeloid leukemia activate the Wnt signaling pathway in hematopoietic cells. Mol Cell Biol 2004; 24:2890-2904.

Nielsen R, Pedersen TA, Hagenbeek D, Moulos P, Siersbaek R, Megens E, Denissov S, Borgesen M, Francoijs KJ, Mandrup S, Stunnenberg HG. Genome-wide profiling of PPARg:RXR and RNA polymerase II occupancy reveals temporal activation of distinct metabolic pathways and changes in RXR dimer composition during adipogenesis. Genes Dev 2008; 22:2953-2967.

Nikolova-Krstevski V, Yuan L, Le Bras A, Vijayaraj P, Kondo M, Gebauer I, Bhasin M, Carman CV, Oettgen P. ERG is required for the differentiation of embryonic stem cells along the endothelial lineage. BMC Dev Biol 2009; 9:72.

Nilsson L, Astrand-Grundstrom I, Anderson K, Arvidsson I, Hokland P, Bryder D, Kjeldsen L, Johansson B, Hellstrom-Lindberg E, Hast R, Jacobsen SE. Involvement and functional impairment of the CD34(+)CD38(-)Thy-1(+) hematopoietic stem cell pool in myelodysplastic syndromes with trisomy 8. Blood 2002; 100:259-267.

Nimer SD, Moore M. A. Effects of the leukemia-associated AML1-ETO protein on hematopoietic stem and progenitor cells. Oncogene 2004; 23: 4249-4254.

Nishida S, Hosen N, Shirakata T, Kanato K, Yanagihara M, Nakatsuka S, Hoshida Y, Nakazawa T, Harada Y, Tatsumi N, et al. AML1-ETO rapidly induces acute myeloblastic leukemia in cooperation with the Wilms tumor gene, WT1. Blood 2006; 107:3303-3312.

Nucifora G, Larson R.A, Rowley JD. Persistence of the 8;21 translocation in patients with acute myeloid leukemia type M2 in long-term remission. Blood 1993; 82:712-715.

Ogawa M. Differentiation and proliferation of hematopoietic stem cells, Blood 1993; 11:2844-53.

Okuda T, Cai Z, Yang S, Lenny N, Lyu CJ, van Deursen JM, Harada H, Downing JR. Expression of a knocked-in AML1-ETO leukemia gene inhibits the establishment of normal definitive hematopoiesis and directly generates dysplastic hematopoietic progenitors. Blood 1998; 91: 3134-3143.

O'Reilly LA, Harris AW, Tarlinton DM, Corcoran LM, Strasser A. Expression of a bcl-2 transgene reduces proliferation and slows turnover of developing B lymphocytes in vivo. J Immunol 1997; 159:2301-2311.

Orkin SH, Zon LI. Hematopoiesis and stem cells: plasticity versus developmental heterogeneity. Nat.Immunol. 2002; 3:323-328.

Park CH, Bergsagel DE, McCulloch EA. Mouse myeloma tumor stem cells: a primary cell culture assay. J. Natl. Cancer Inst 1971; 46:411-422.

Passegue E, Jamieson CH, Ailles LE, Weissman IL. Normal and leukemic hematopoiesis: are leukemias a stem cell disorder or a reacquisition of stem cell characteristics? Proc Natl Acad Sci U S A 2003; 100:11842-11849.

Pavesi G, Mereghetti P, Mauri G, Pesole G. Weeder Web: discovery of transcription factor binding sites in a set of sequences from co-regulated genes. Nucleic Acids Res. 2004; 32:199-203.

Peterson LF, Zhang DE. The 8;21 translocation in leukemogenesis. Oncogene 2004; 23:4255-4262.

Pierce GB, Wallace C. Differentiation of malignant to benign cells. Cancer Res 1971; 31:127-134
.
Pimanda JE, Ottersbach K, Knezevic K, Kinston S, Chan WY, Wilson NK, Landry JR, Wood AD, Kolb-Kokocinski A, Green AR, et al. Gata2, Fli1, and Scl form a recursively wired gene-regulatory circuit during early hematopoietic development. Proc Natl Acad Sci U S A. 2007; 104:17692-7.

Preudhomme C, Sagot C, Boissel N, Cayuela JM, Tigaud I, de Botton S, Thomas X, Raffoux E, Lamandin C, Castaigne S, et al. Favorable prognostic significance of CEBPA mutations in patients with de novo acute myeloid leukemia: a study from the Acute Leukemia French Association (ALFA). Blood 2002; 100:2717-2723.

Raslova H, Komura E, Le Couédic JP, Larbret F, Debili N, Feunteun J, Danos O, Albagli O, Vainchenker W, Favier R. FLI1 monoallelic expression combined with its hemizygous loss underlies Paris-Trousseau/Jacobsen thrombopenia. J Clin Invest 2004; 114:77-84.

Redner RL, Rush EA, Faas S, Rudert WA, Corey SJ. The t(5;17) variant of acute promyelocytic leukaemia expresses a nucleophosmin-retinoic acid receptor fusion. Blood 1996; 87:882-886.

Reilly, JT. Class III receptor tyrosine kinases: role in leukaemogenesis. Br J Haematol 2002; 116:744-757.

Renneville A, Roumier C, Biggio V, Nibourel O, Boissel N, Fenaux P, Preudhomme C. Cooperating gene mutations in acute myeloid leukemia: a review of the literature. Leukemia 2008; 22:915-931.

Reya T, Clevers H. Wnt signalling in stem cells and cancer. Nature 2005; 434: 843-50.

Reya T, Morrison SJ, Clarke MF, Weissman IL. Stem cells, cancer, and cancer stem cells. Nature 2001; 414:105-111.

Romana SP, Mauchauffe M, Le Coniat M, Chumakov I, Le Paslier D, Berger R, Bernard OA. The t(12;21) of acute lymphoblastic leukemia results in a tel-AML1 gene fusion. Blood 1995; 85:3662-3670.

Roudaia L, Cheney MD, Manuylova E, Chen W, Morrow M, Park S, Lee CT, Kaur P, Williams O, Bushweller JH, et al. CBFbeta is critical for AML1-ETO and TEL-AML1 activity. Blood 2009; 113:3070-3079.

Sahin FI, Kizilkilic E, Bulakbasi T, Yilmaz Z, Boga C, Ozalp O, Karakus S, Ozdogu H. Cytogenetic findings and clinical outcomes of adult acute myeloid leukaemia patients. Clin Exp Med 2007; 7:102-10.

Schepers H, van Gosliga D, Wierenga AT, Eggen BJ, Schuringa JJ, Vellenga E. STAT5 is required for long-term maintenance of normal and leukemic human stem/progenitor cells. Blood 2007; 110: 2880-2888.

Schessl C, Rawat VP, Cusan M, Deshpande A, Kohl TM, Rosten PM, Spiekermann K, Humphries RK, Schnittger S, Kern W, et al. The AML1-ETO fusion gene and the FLT3 length mutation collaborate in inducing acute leukemia in mice. J Clin Invest 2005; 115:2159-2168.

Schnittger S, Kohl TM, Haferlach T, Kern W, Hiddemann W, Spiekermann K, Schoch C. KIT-D816 mutations in AML1-ETO positive AML are associated with impaired event-free and overall survival.Blood 2006; 107:1791-1799.

Schuringa JJ, Chung KY, Morrone G, Moore MA. Constitutive activation of STAT5A promotes human hematopoietic stem cell self-renewal and erythroid differentiation. J.Exp.Med. 2004; 200:623-635.

Schwarz-Cruz-y-Celis, A, Melendez-Zajgla, J. Cancer stem cells. Rev. Invest. Clin. 2011; 63:179 -186 (2011).

Sharrocks AD, Brown AL, Ling Y, Yates PR. The ETS-domain transcription factor family. The international journal of biochemistry & cell biology 1997; 29:1371-1387.

Singh SK, Clarke ID, Terasaki M, Bonn VE, Hawkins C, Squire J, Dirks PB. Identification of a cancer stem cell in human brain tumors. Cancer Res 2003; 63:5821-5828.

Soltysova A, Altanerova V, Altaner C. Cancer stem cells. Neoplasma 2005; 52:435-440.

Speck NA, Gilliland DG. Core-binding factors in haematopoiesis and leukaemia. Nat Rev Cancer 2002; 2:502-513.

Spyropoulos DD, Pharr PN, Lavenburg KR, Jackers P, Papas TS, Ogawa M, Watson DK. Hemorrhage, impaired hematopoiesis, and lethality in mouse embryos carrying a targeted disruption of the Fli1 transcription factor. Mol Cell Biol 2000; 20:5643-52.

Stankiewicz MJ, Crispino JD. ETS2 and ERG promote megakaryopoiesis and synergize with alterations in GATA-1 to immortalize hematopoietic progenitor cells. Blood 2009; 113:3337-47.

Taoudi S, Bee T, Hilton A, Knezevic K, Scott J, Willson TA, Collin C, Thomas T, Voss AK, Kile BT, et al. ERG dependence distinguishes developmental control of hematopoietic stem cell maintenance from hematopoietic specification. Genes Dev 2011; 25:251-262.

Taussig DC, Miraki-Moud F, Anjos-Afonso F, Pearce DJ, Allen K, Ridler C, Lillington D, Oakervee H, Cavenagh J, Agrawal SG, et al. Anti-CD38 antibody-mediated clearance of human repopulating cells masks the heterogeneity of leukemia-initiating cells. Blood 2008; 112:568-575.

Thijs G, Lescot M, Marchal K, Rombauts S, De Moor B, Rouzé P, Moreau Y. A higher-order background model improves the detection of promoter regulatory elements by Gibbs sampling. Bioinformatics 2001; 17:1113-1122.

Till JE, McCulloch EA, Siminovitch L. A Stochastic Model of Stem Cell Proliferation, Based on the Growth of Spleen Colony-Forming Cells. Proc Natl Acad Sci U S A 1964; 51:29-36.

Toyota M, Kopecky KJ, Toyota MO, Jair KW, Willman CL, Issa JP. Methylation profiling and acute myeloid leukemia. Blood 2001; 97:2823-2829.

Tsuzuki S, Taguchi O, Seto M. Promotion and maintenance of leukemia by ERG. Blood 2011; 117: 3858-3868.

Uchida H, Zhang J, Nimer SD. AML1A and AML1B can transactivate the human IL-3 promoter. J. Immunol 1997; 158:2251-2258.

Valk PJ, Bowen DT, Frew ME, Goodeve AC, Lowenberg B, Reilly JT. Second hit mutations in the RTK/RAS signaling pathway in acute myeloid leukemia with inv(16). Haematologica 2004;89:106.

Valk PJ, Verhaak RG, Beijen MA, Erpelinck CA, Barjesteh van Waalwijk van Doorn-Khosrovani S, Boer JM, Beverloo HB, Moorhouse MJ, van der Spek PJ, Lowenberg B, et al. Prognostically useful gene-expression profiles in acute myeloid leukemia. The New England journal of medicine 2004; 350:1617-1628.

Van Den Berg DJ, Sharma AK, Bruno E, Hoffman R. Role of members of the Wnt gene family in human hematopoiesis. Blood 1998; 92:3189-202

van Heeringen SJ, Veenstra GJ. GimmeMotifs: a de novo motif prediction pipeline for ChIP-sequencing experiments. Bioinformatics 2011; 27:270-271.

Wang J, Hoshino T, Redner RL, Kajigaya S, Liu JM. ETO, fusion partner in t(8;21) acute myeloid leukemia, represses transcription by interaction with the human NCoR/ mSin3/HDAC1 complex. Proc Natl Acad Sci U S A 1998; 95:10860-10865.

Wang JC, Dick JE. Cancer stem cells: lessons from leukemia. Trends Cell Biol 2005; 15:494-501.

Wang K, Wang P, Shi J, Zhu X, He M, Jia X, Yang X, Qiu F, Jin W, Qian M, et al. PML/RARalpha targets promoter regions containing PU.1 consensus and RARE half sites in acute promyelocytic leukemia. Cancer cell 2010; 17:186-197.

Wang L, Gural A, Sun XJ, Zhao X, Perna F, Huang G, Hatlen MA, Vu L, Liu F, Xu H, et al. The leukemogenicity of AML1-ETO is dependent on site-specific lysine acetylation. Science 2011; 333:765-759.

Wantzin, GL, Killmann SA. Nuclear labelling of leukaemic blast cells with tritiated thymidine triphosphate after daunomycin. Eur J Cancer 1977; 13:647-655.

Warner JK, Wang JC, Hope KJ, Jin L, Dick JE. Concepts of human leukemic development. Oncogene 2004; 23: 7164-7177.

Weissman, IL. Stem cells: units of development, units of regeneration, and units in evolution. Cell; 100:157-68.

Welboren WJ, van Driel MA, Janssen-Megens EM, van Heeringen SJ, Sweep FC, Span PN, Stunnenberg HG. ChIP-Seq of ERa and RNA polymerase II defines genes differentially responding to ligands. Embo J. 2009; 28:1418-28.

Swerdlow SH, Campo E, Harris NL, Jaffe ES, Pileri SA, Stein H, Thiele J, Vardiman JW. WHO classification of tumours of haematopoietic and lymphoid tissues. IARC Press: Lyon 2008.

Wichmann C, Becker Y, Chen-Wichmann L, Vogel V, Vojtkova A, Herglotz J, Moore S, Koch J, Lausen J, Mantele W, et al. Dimer-tetramer transition controls RUNX1/ETO leukemogenic activity. Blood 2010; 116:603-613.

Wierenga AT, Schepers H, Moore MA, Vellenga E, Schuringa JJ. STAT5-induced self-renewal and impaired myelopoiesis of human hematopoietic stem/progenitor cells involves down-modulation of C/EBPalpha. Blood 2006; 107:4326-4333.

Wilson NK, Foster SD, Wang X, Knezevic K, Schutte J, Kaimakis P, Chilarska PM, Kinston S, Ouwehand WH, Dzierzak E, et al. Combinatorial transcriptional control in blood stem/progenitor cells: genome-wide analysis of ten major transcriptional regulators. Cell Stem Cell 2010; 7:532-544.

Wuchter C, Karawajew L, Ruppert V, Buchner T, Schoch C, Haferlach T, Ratei R, Dorken B, Ludwig WD. Clinical significance of CD95, Bcl-2 and Bax expression and CD95 function in adult de novo acute myeloid leukemia in context of Pglycoprotein function, maturation stage, and cytogenetics. Leukemia 1999; 13:1943-1953.

Yergeau DA, Hetherington CJ, Wang Q, Zhang P, Sharpe AH, Binder M, Marin-Padilla M, Tenen DG, Speck NA, Zhang DE. Embryonic lethality and impairment of haematopoiesis in mice heterozygous for an AML1-ETO fusion gene. Nature genetics 1997; 15: 303-306.

Yoneda-Kato N, Look AT, Kirstein MN, Valentine MB, Raimondi SC, Cohen KJ, Carroll AJ, Morris SW. The t(3;5)(q25.1;q34) of myelodysplastic syndrome and acute myeloid leukemia produces a novel fusion gene, NPM-MLF1. Oncogene 1996; 12:265-275.

Yuan Y, Zhou L, Miyamoto T, Iwasaki H, Harakawa N, Hetherington C.J, Burel SA, Lagasse, E, Weissman, IL, Akashi K, et al. AML1-ETO expression is directly involved in the development of acute myeloid leukemia in the presence of additional mutations. Proc Natl Acad Sci USA 2001; 98:10398-10403.

Zeng C, McNeil S, Pockwinse S, Nickerson J, Shopland L, Lawrence JB, Penman S, Hiebert S, Lian JB, van Wijnen AJ, et al. Intranuclear targeting of AML/CBFalpha regulatory factors to nuclear matrix-associated transcriptional domains. Proc Natl Acad Sci U S A 1998; 95:1585-1589.

Zhang J, Kalkum M, Yamamura S, Chait BT, Roeder RG. E protein silencing by the leukemogenic AML1-ETO fusion protein. Science 2004; 305:1286-1289.

Zhang Y, Liu T, Meyer CA, Eeckhoute J, Johnson DS, Bernstein BE, Nussbaum C, Myers RM, Brown M, Li W, et al. Model-based analysis of ChIP-Seq (MACS). Genome biology 2008; 9:R137.

Zhang XK, Watson DK. The FLI-1 transcription factor is a short-lived phosphoprotein in T cells. J Biochem 2005; 137:297-302.

Zou GM. Cancer stem cells in leukemia, recent advances. J. Cell. Physiol 2007; 213:440-444.

PART II: Tissue-engineered esophagus: an *in vitro* study.

CHAPTER 1 INTRODUCTION

1.1 Diseases causing esophageal loss or dysfunction

There are several conditions where esophageal replacement and substitution is required but esophageal reconstruction still remains a challenging issue for pediatric and adult general surgeons. Although this organ looks “simple” from the anatomical point of view, replacing the native esophagus is the most compelling part of an esophagectomy because of the difficulties in reproducing the essential properties and functions of the original structure.

1.1.1 Esophageal cancer. Nowadays esophageal cancer is the ninth most represented neoplasia in the world and the fifth most frequent cancer in the developed countries. Because of considerable delay in diagnosis and comorbdity, definitive surgical resection is possible in only ~20% of cases (Mariette et al., 2007). Actually, the incidence of esophageal cancer is approximately 3-6 cases/100.000/year, and the three principal histological types are: i) small cell carcinoma, ii) squamous cell carcinoma, and iii) adenocarcinoma. However, the incidence of adenocarcinoma of the cardias and lower esophagus has raised dramatically in the West countries during the last three decades, while the squamous cell type remains the most frequent type in Asia (Kato et al., 2007). Among the causes of esophageal cancer several factors that can damage DNA have been founded in the past decade, including heavy alcohol consumption, tobacco use, chronic acid reflux, Barrett's esophagus, diet (low in fruits and vegetables), and obesity. Sometimes it is also associated with certain rare medical conditions like achalasia, esophageal webs, and tylosis.

1.1.2 Caustic ingestion. Esophageal injury can occur from ingestion of bases, acids, and bleaches, but ingestion of substances containing bases produces the most significant injury. Since then the Poison Prevention Packaging Act in 1970 and the Federal Hazardous Substances Act in 1972 have toughened regulations, and now proper labeling including antidote instructions, concentration restrictions (10%), and child-resistant packaging is required. Despite these precautions, it is still estimated that 5,000 accidental lye ingestions occur yearly by children less

than 5 years of age. These ingestions are accidental in the pediatric population, mostly at home and in the kitchen, and almost invariably intentional in the adult population (suicide attempts).

1.1.3 Esophageal atresia. Esophageal atresia incidence is known to be around 1:3000. It is suitable of colon or gastric interposition only in a few cases referable to its "long-gap" first type, that represent not more than 5% of all these patients with four or more vertebral bodies interposed between the two esophageal stumps. In a part of them a few months delay in the definitive attempt to perform the anastomosis gives reason of the malformation, even if paying the cost of an increased risk of stenosis due to the traction between the stumps (Bagolan et al., 2004). So, only a few parts of these patients really need an esophageal substitution. Apart of them, a small number of patients with recurrent tracheo-esophageal fistula (less of 5% of esophageal atresia patients) need esophageal substitution because of the fair amount of free esophageal wall to close the fistula. Moreover, rare long type of congenital esophageal stenosis is even prone to colon or gastric interposition. Finally, complicated attempts to resolve this malformation with repeated operations easily lead to a severe esophageal stenosis because of the consequent poor vascular supply.

1.1.4 Benign end stage esophageal pathologies. Miscellaneous includes different patients lacking good esophageal tissue for reconstruction and needing substitution, like benign tumors, long term naso-gastric intubation, previous unsatisfactory surgery or dilatations, end-stage achalasia, perforations.

1.2 Surgical strategies for esophageal reconstruction

Typically, the esophagus has little redundancy, so autologous tissue for reconstruction is not available. Even small segmental defects often require complex tubular interpositions. Autologous graft tissue derived from stomach, skin, small or large intestine, has been used for segmental esophageal defects repair, but complication rates are high, ranging from 30% to 40% (Gawad et al., 1999; Alcantara et al., 1997; Ellis., 1999).

In the adult patients esophageal cancer and suicidal caustic ingestion are the most frequent conditions requiring a long tract esophageal replacement. Surgery is still the recommended standard treatment for operable patients with localized tumors (Tis – T1a – N0), for squamous cell carcinoma as well as for adenocarcinoma. The operative approach for malignant cancer

varies from conventional transthoracic esophagectomy chiefly for palliation, to limited esophagectomy without thoracotomy, to en-bloc esophagectomy, and to extended esophagectomy with 3-field lymph node dissection for curative purposes. (Logan, 1963; Law et al., 2001; Altorki et al., 2001)

Transhiatal esophagectomy gives lower morbidity to the patients affected by esophageal carcinoma, but the trans thoracic approach with simultaneous linfadenectomy offers better survival prognosis. Among the ancillary therapies the preoperative chemoradiotherapy seems to give the best survival addiction to these patients.

Wide surgical resection for malignancies needs either a reattachment of the shortened esophagus to stomach or replacement of the excised portion with some form of intestinal substitute. The colon is considered a well-functioning and durable esophageal substitute. For esophageal reconstruction, an isoperistaltic colon graft should be used because an antiperistaltic reconstruction may be associated with significant spasms. The left colon enables the most extensive mobilization of the graft (Khan et al., 2008).

The best approach for esophagectomy and esophageal substitution is still unidentified, but, since surgery states as the main step in the esophageal cancer treatment options, actually it does exist in four main therapeutic combinations:

i) esophagectomy with chemo- or chemoradiotherapy;

ii) primary definitive chemoradiotherapy with or without salvage esophagectomy;

iii) preoperative chemoradiotherapy and subsequent planned esophagectomy; and

iv) minimally invasive transthoracic esophagectomy as an alternative technical approach.

Intractable benign stenosis actually are more rare to encounter since the endoscopic therapeutic options have become affordable, increasing the use of dilatations and stents.

Esophageal dilatations, usually performed in an antegrade way with guidewire directed balloons or Savary dilators, but sometimes aborally through a gastrostomy too, are the most frequently performed therapies in the treatment of different kinds of esophageal stenosis. Recently esophageal stenting have been reported to produce good results thanks to the use of polytetrafluoroetylene stents, hypothesizing larger indications in the attempt of saving the native esophagus (Atabek et al., 2007).

Preservation of the native esophagus is desirable and can be achieved in most cases. As a first management, esophageal dilatations of the resulting stricture can be used. If dilatation is

considered to have failed or if the esophagus cannot be salvaged, esophageal bypass or substitution is indicated. Operations currently used are colonic interposition, gastric tube esophagoplasty, jejunal interposition, and gastric advancement (Cywes et al., 1993; Othersen et al., 1988; Spitz et al., 1984; Stone et al., 1986; Ring et al., 1982).

Esophageal substitution is barely performed in the pediatric age. It represents the definitive attempt to resolve an intractable disease like a "long-gap" esophageal atresia or major disruptions like caustic ingestion, as previously described. But the colon interposition, gastric pull-up or other different techniques still have lot of negative consequences on the esophageal physiology due to the different composition and motility.

Alternatives for esophageal replacement in infants and children in the past have included a right or left colon interposition (running the large intestine from the back of the throat to the stomach), formation of gastric tube (creating a tube from part of the stomach and swinging it up to the backing of the throat), and a jejunal interposition (running small intestine from the back of the throat to the stomach). All of these have advantages and disvantages related to short and long term complications.

1.3 Tissue engineering and organ replacement

Artificial transplantation or transplanted organs is a successful therapy for otherwise incurable end-stage diseases or tissue loss. However, such interventions are challenged by organ shortage, the necessity of lifelong immunosuppression and its potential for serious complications. Tissue engineering has emerged as a rapidly expanding approach to address these problems and is a major component of regenerative medicine. Tissue engineering is an interdisciplinary field that applies the principles and methods of bioengineering, material science, and life sciences toward the assembly of biologic substitutes that will restore, maintain, and improve tissue functions following damage either by disease or traumatic processes (Knight et al., 2004; Shieh et al., 2005).

The general principle of tissue engineering involve combining naturally or artificially derived scaffolds, cells and signalling molecules which may be bounded to the scaffold or infused onto it to build a threedimensional living construct that is functionally, structurally and mechanically equal to or better than the tissue that is to be replaced.

1.3.1 Scaffold. Scaffold materials are three-dimensional tissue structures that guide the organization, growth and differentiation of cells. An ideal scaffolds must be biocompatible and should be able to

i) naturally providing cell attachment and support
ii) dispose of sufficient area to allow cell proliferation
iii) develop the ability of shaping specific structures
iv) *in vivo* degrade without release of toxic materials
v) allow tissue remodelling and resorption avoiding foreign body reaction
vi) allow the ingrowth of host cells.

It is well-known that cell-extracellular matrix (ECM) interaction plays a basic role in the regulation of cell migration, proliferation, differentiation and survival (Rosso et al., 2004). So, various ECM-derived scaffolds, such as collagen, alginate, Matrigel and hyaluronic acid, have been used for cell culture and tissue engineering purposes (Freyman et al., 2001; Marijnissen et al., 2002). However, synthetic scaffolds present the some advantages in comparison with natural scaffolds: tightly control of physical properties, such as mechanical strength, degradation rate and pore size, and production with fewer batch-to-batch variations. Moreover, scaffolds can be designed to incorporate ECM molecules that affect cell regulation, function and reorganization. Nevertheless, the surface of synthetic polymers often needs to be modify to get an optimum substrate for tissue engineering. So, adhesion molecules can be adsorbed or covalently bound to the surface of scaffolds. ECM adhesion proteins, such as fibronectin, collagen and laminin, present some disvantages in the view of medical applications (Langer et al., 2004). They can elicit immune response, since they are isolated from other organisms and need to be purified. They also need to be refreshed continuously, because they are object of proteolytic degradation. On the contrary, small peptides, containing only the sequence responsible for cell adhesion, are characterized by higher stability, easier characterization, and possibility to be packed with an higher density on surfaces (Cook et al., 1997). Thus, their use can overcome most of problems connected to ECM proteins. For example, small peptides can be design to contain RGD sequence (Arg-Gly-Asp) which mediates cell-adhesion via cell membrane integrin receptors, or heparin binding sequences able to interact with cell membrane heparin sulphate proteoglycans.

At present, the *in vivo* quick capillary ingrowth into tissue substitutes is thought to be a basic step for the survival of the implanted cells and the related *in vivo* successful implant (Mooney et al.,

1999). To improve new capillary ingrowth from the host vascular network, several approaches have been proposed, including the delivery of angiogenic factors and prevascularization using co-cultures with endothelial cells or by implantation in the mesentery (Holder et al., 1997).

1.3.2 Cell source. Another basic step in tissue engineering is the choice of the cell type and source. The cell type that could be used should be able to generate sufficient numbers of cells that maintain the appropriate phenotype and perform the required biological functions. For example, cells must produce extracellular matrix in the correct organization, secrete cytokines and other signaling molecules, and interact with neighboring cells/tissues. The transplanted cells can be primary cells (mature cells), or stem cells (either adult or embryonic).

Primary cells are mature cells specific to tissue type that can be harvested directly from the recipient, so avoiding immunological rejection. Moreover, autologous cells contained in the tissue-engineered devices play an important role to improve the *in vivo* integration of the implants because they could represent a signal for the recruitment of the host cells and the lowering of inflammatory response (Marzaro et al., 2002; Conconi et al., 2005). Although mature cells are still used in tissue engineering, but these cells may not be the best source of cells for tissue regeneration, primarily because these adult cells have already differentiated and committed to a specific cell type and proliferation rates tend to be low and for some phenotypes, e.g., spinal cord neurons, harvesting from a patient or donor is not an option. These limitations have stimulated studies to find and develop alternative cell sources for tissue engineering strategies and stem cells are already providing solutions to some of the problems encountered using mature cells.

Stem cells can be defined as undifferentiated cells that can proliferate and have the capacity both to self-renew and to differentiate to one or more types of specialized cells under appropriate conditions. There are two main types of stem cells, embryonic and adult. Embryonic stem cells (ESCs) are totipotent and, accordingly, they can differentiate into all three embryonic germ layers. On the other hand adult stem cells are just multipotent; their potential to differentiate into different cell types seems to be more limited.

Embryonic stem cells (ES cells) are stem cells derived from the inner cell mass of an early stage embryo known as a blastocyst (4-5 days post fertilization). ES cells are pluripotent, therefore they are able to differentiate into all cell types found in adult human body (Edwards, 2004; Gardner, 2007). Pluripotency distinguishes ES cells from multipotent progenitor cells found in the adult;

these only form a limited number of cell types. When no stimuli is given for differentiation, (i.e. when grown *in vitro*), ES cells maintain pluripotency through multiple cell divisions. Because of their plasticity and potentially unlimited capacity for self-renewal, ES cell therapies have been proposed for regenerative medicine and tissue engineering but ES cells use is restricted due to teratoma formation and ethical concerns.

Adult stem cells are undifferentiated cells found among differentiated cells in a tissue or organ where they act as reservoirs to maintain and repair the tissue when required. Both their potency and proliferative potential are typically narrower than those of their embryonic counterparts. For a long time, adult stem cells have been considered to be a safer option for clinical applications than ESC because they have not been shown to form teratomas. They have thus far been the only stem cells used to successfully used in tissue engineering applications. The range of cell sources for adult stem cells continues to increase but among them bone marrow adult stem cell populations has been most thoroughly characterized. Bone marrow contains two major types of stem cells, (1) hematopoietic stem cells which forms all the types of blood cells in the body and discussed in other portion of the thesis and (2) marrow stromal cells also known as MSCs.

Bone marrow stromal cells were first described in 1976 by Alexander Friedenstein. He and his colleagues showed that bone marrow stroma contains cells that adhere to tissue culture plastic. He determined that these cells (1) belong to a rare population in the bone marrow, (2) did not enter "S" phase until up to 60 hours after initial plating, (3) showed a high replicative capacity *in vitro*, (4) were clonogenic, and (5) formed colonies of irregular shape and density (Phinney, 2002). Moreover, he showed these cells were capable of forming bone even after multiple passages.

These stromal cells can be expanded in vitro over several passages and can differentiate into cells of some mesenchymal tissues, such as osteoblasts, chondrocytes, adipocytes, myocytes, tenocytes, and haematopoiesis supporting stromal cells (Caplan et al., 1998) (Figure 1). Based on this multilineage differentiation capacity, Caplan coined the term mesenchymal stem cells (MSCs). MSCs represent a minor fraction in bone marrow about 0.001-0.01% of all nucleated cells in the marrow (Pittenger et al., 1999). Furthermore the prevalence of MSC decline over age. MSC (Stromal cells) play an important role as a microenvironment (stroma) for the developing hematopoietic stem and progenitor cells in the bone marrow (Baksh et al., 2004). In addition to

bone marrow MSC-like cells also have been isolated from adipose tissue, synovium, placenta, amniotic fluid, lung and human umbilical cord blood (Zuk et al., 2001; In 't Anker et al., 2003).

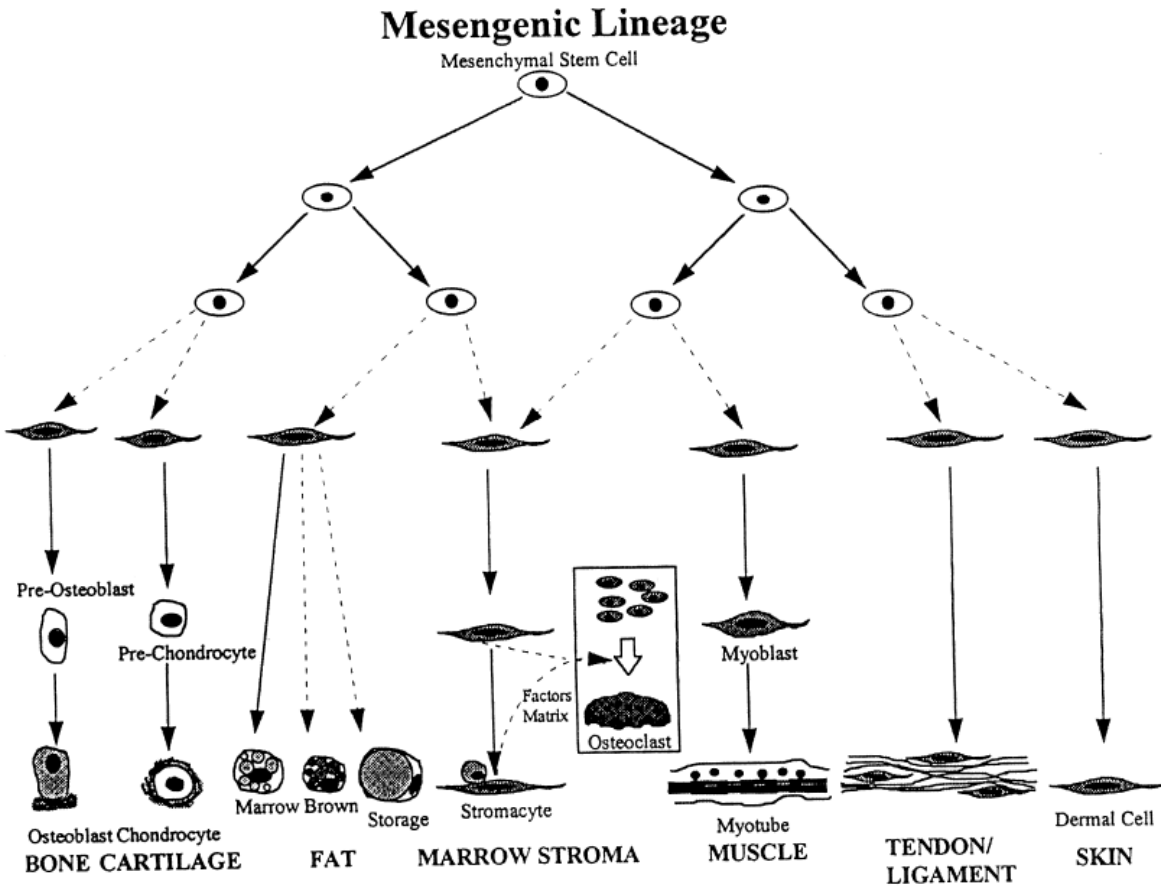

Figure 1. Mesengenic lineage pathway. The process of mesengenesis involves the generation of multiple mesenchymal end-stage phenotypes from the differentiation of a multipotent mesenchymal stem cell (MSC) through a multistep series of developmental changes in response to microenvironmental stimuli. The lineages are illustrated from left to right in the order of most to least characterized (adapted from Caplan et al., 1998).

Isolation of MSCs from BM involve culture of bone marrow mononuclear cells in selective media on a plastic substrate, which allow fibroblast-like cells (later named MSCs) to adhere while others, such as hematopoietic cells, do not. However, studies have shown that MSC cultures based solely on adherence to plastic are highly heterogeneous (Prockop et al., 2001; Simmons et al., 1991). Other protocols have also been developed to isolate MSCs, including flow cytometry and cell sorting with antibodies to cell surface markers such as STRO-1 (Simmons and Torok-Storb., 1991), SSEA-1/CD15 (Anjos-Afonso and Bonnet, 2007). The STRO-1 surface

marker is found on ~10% of bone marrow mononuclear cells. Fibroblast-like colony forming units (CFU-F) are exclusively STRO-1pos and have shown adipogenic, myogenic, and fibroblastic potential, yet the vast majority of these cells are erythroid precursors (Simmons and Torok-Storb., 1991). Anjos-Afonso and Bonnet demonstrated that single cell-derived populations of murine BM derived MSCs characterized by Stage Specific Embryonic Antigen-1 (SSEA-1) expression, were capable of differentiation in-vivo, thus showing their true stem cell properties (Anjos-Afonso and Bonnet, 2007).

The capacity to differentiate into multiple mesenchymal lineages, including bone, fat and cartilage, is being used as a functional criterion to define human MSCs. Cells from MSC culture are known to be positive for the surface peptides CD 105 (SH2), CD73, and the surface receptors CD29, CD71, CD90, CD123, and CD166 and negative for hematopoietic and endothelial markers, such as, CD11b, CD14, CD31 and CD45. Other cell types also express these markers, thus it would be preferable if there were truly a unique marker to identify the most immature and therefore the most highly potent MSCs. Till now a unique marker has not been found on MSCs to distinguish them from all other cell types and still all current selection protocols produce heterogeneous cultures with respect to surface markers (Alhadlaq and Mao, 2004).

Beside many issues remain to be solved regarding their characteristics, phenotype and behavior in culture; however MSCs have already demonstrated their efficacy in preliminary tissue engineering application (Macchiarini et al., 2008).

1.4 Tissue engineered esophageal substitutes

In the last years, several tissue engineering-based approaches using artificial and natural scaffolds have been proposed for the repair of experimental created defects in the esophagus. However, the obtained results are very difficult to compare because of the large variability about the animal model (rat, dog and rabbit), the time-points (from few weeks to several months), the dimension and the location of the oesophageal defects. In this section we will review about the findings related to the use of tissue engineered devices composed of artificial or natural scaffolds.

1.4.1 Artificial scaffolds. Polytetrafluoroethylene (PTFE) oval patches (3x2 mm) were used to repair full-thichkness defects in the abdominal esophagus of Wistar rats (n=10) but unsatisfactory results have been obtained. Indeed, after 28 days from surgery, the implants were replaced by

fibrous tissue (Gonzalez et al, 2003). Despite the low number (n=10) of rabbits enclosed in another study, it was suggested that polyvinylidene fluoride (PVDF) may represent a promising material for esophageal replacement. In this study semicircular esophageal defect (0.5x1 cm) 2 cm proximal to the cardia was closed with PVDF mesh. At 3 month, no stricture or perforation was revealed. A complete regeneration of the mucosal layer was well visible and immunostaining showed an initial organization of the muscle layer. On the contrary, the same authors showed that implants composed of polyglactin 910 mesh were accompanied by high and early rate of anastomotic leakage (Lynen Jansen P et al, 2004).

Most of artificial materials can be extruded and develop leakage and stenosis. Thus, to avoid these effects and maintain the mechanical properties of synthetic scaffolds, many researchers have tried to improve artificial esophageal substitutes using also cells and extracellular matrix components.

Sato and co-workers developed a polyglycolyc acid (PGA) mesh-collagen tube whose inner side was covered *in vitro* by cultured human esophageal epithelial cells. Tubes were wrapped in the latissimus dorsi muscle flaps of athymic rats. After 28 days from grafting, neovascularization appeared in the collagen layer and the grafted epithelium grew to 15 cell layer, mimicking human esophageal one (Sato M et al, 1994). In similar work *in vitro* tubes composed of PGA and collagen layers covered or containing human esophageal epithelial cells and fibroblasts, respectively were used. No stenosis was observed 14 days after grafting of the constructs into muscle flaps of athimic rats (n=2). The Authors noted that fibroblasts improved proliferation and differentiation of epithelial cells, that *in vivo* formed 20 layers of stratification (Miki et al, 1999).

Very interesting findings were obtained using collagen-coated vicryl mesh to patch partial (3x2.5 cm) and total segmental (6x2.5 cm) full thickness defects in the cervical esophagus of 24 dogs. At 2 weeks, the patches were covered by epithelial cells. After 6 months from reconstructive surgery, the implants reached almost the thickness of normal esophagus and contained glands. Moreover, an initial regeneration of muscle layer was visible (Shinhar D et al, 1998).

Esophagus organoid units obtained from neonatal or adult Lewis rats were seeded onto biodegradable polymer tubes composed of PGA and poly-L-lactic acid (PLLA) to generate engineered constructs. These constructs were implanted in syngeneic hosts (n=11) to repair both 2-cm long circumferential and 2.5x1 cm partial defects of the abdominal esophagus. At day 42,

histological analysis revealed that implants were remodelled into a complete esophageal wall, including mucosa, submucosa and muscolaris propria (Grikscheit).

1.4.2 Natural scaffolds. ECM is composed of a complex mixture of structural and functional proteins, among which collagen is the most abundant and perhaps the most commonly used for therapeutic application (Badylak, 2004)

Takimoto and co-workers used two-layered tubes consisting of a collagen sponge matrix (types I and III) and an inner silicon stent to repair 5-cm cervical esophageal defects in 43 dogs. When the stent was removed after 2 or 3 weeks, dogs were unable to swallow and constriction of patches was visible. On the contrary, stenosis did not occur in any dogs in which the stents remained in place for 4 weeks. In these animals oral feeding was possible. The implants were covered by stratified epithelium, contained glands and showed striated muscle tissue organized into an inner circular and an outer longitudinal layer (Takimoto et al., 1998*)*. The same research group implanted the collagen tubes described above to replace a 5 cm thoracic defect in 9 dogs. The mucosa was fully regenerated within 3 months and the glands at 12 months. Although the skeletal muscle regenerated close to the anastomoses, it did not extend into the middle of regenerated esophagus even after 24 months. It was suggested that these disappointing results could be due to an insufficient blood supply (Yamamoto et al., 1999). So, in another work they evaluated in 14 dogs whether omental pedicle wrapping of the prosthesis could promote tissue regeneration and prolonged retention of the silicone stent could prevent stenosis. Not only did most dogs die, but only a thin epithelial and submucosal layer regenerated indicating that other approaches to improve neo-vascularization must be designed (Yamamoto et al, 2000).

Type I collagen-based scaffold with human cells also have been suggested for esophagus substitution. In attempt fibroblasts was embedded in collagen superimposed on another collagen layer containing smooth muscle cells. Next, esophageal epithelial cells were cultured on the collagen layer containing fibroblasts. After 1 week of *in vitro* culture, the collagen sheets were transplanted in the latissimus dorsi muscle of two athymic rats. At 2 weeks, microscopic examination revealed that epithelial, submucosal and muscle layers were reconstructed (Hayashi et al., 2004). Although collagen represents one of the most widely used ECM molecule for tissue engineering purposes, its mechanical properties appear not fully suitable to reconstruct structures, like esophagus, that need tensile strength.

In the last years, biologic scaffolds derived from decellularized tissues and organs have been successfully used in both pre-clinical animal studies and in human clinical applications. Acellular matrices (AMs) are obtained by treating tissues with various reagents (Gilbert et al., 2006) that remove the cellular part leaving almost intact the ECM network. It has been demonstrated that they can support *in vitro* adhesion, growth and function of several cell types (Burra et al., 2004; Dettin et al., 2005; Conconi et al., 2005). Moreover, *in vivo* AMs can act as a template allowing the ingrowth of the host cells and can be remodeled in a living tissue (Parnigotto et al., 2000; Marzaro et al., 2006; Conconi et al., 2000). Moreover, they represent preformed structures whose length and gauges can be choice according to the dimension of the defect to be repaired. Another advantage is the possibility to have easy and unlimited availability of inexpensive grafts containing tissue-specific proteins. Both xenogeneic and homologous AMs have been used to engineer esophageal substitutes.

AlloDerm®, an acellular donor derived human dermal matrix, is mainly used to improve the healing of burns and chronic ulcers. This xenogenic AM was checked to repair a 2x1 cm cervical esophageal defect in twelve dogs. After 3 months from reconstructive surgery, no anastomotic leak, stricture or diverticular formation occurred. At the same time an intact epithelium covered the luminal side of patches and numerous blood vessels were observed (Isch et al., 2001).

Small intestinal submucosa (SIS) also has been used to repair esophagus defects. This AM is obtained from the jejunum by mechanically removing the mucosa, muscularis externa and serosa. Thus, the remaining SIS tissue represents submucosa and basal layers of mucosa. SIS was used to repair either large defects (about 5 cm in length) encompassing 40% to 50% of the circumference of esophagus (n=11) or complete circumferential segmental defects (n=4). Biomaterial was inserted in the cervical tract of esophagus of female dogs. The use of SIS as tube grafts resulted in early stricture. On the contrary, semicircunmferential patches were progressively remodeled showing abundant vascularization. During the first 50 days morphological analysis revealed the deposition of neo-matrix consisting of amorphous collagenous connective tissue inside which spindle-shape cells positive to anti-actin antibody were present. By 5 months post-surgery, only small amount of collagenous connective tissue remained into the patches that were replaced by organized bundles of skeletal muscle cells (Badylak et al, 2000). SIS was also employed by Lopes and colleagues (Lopes et al., 2006) for the repair of either semicircunferential (10 mm in length) or segmental (5 mm in lenght) defects performed at the cervical esophagus of adult

female Lewis rats. In accordance with the previous observations (Badylak et al., 2000), unsatisfactory results were obtained with tube-shape grafts. Indeed, all animals (n=24) died within the first post-operative month due to esophageal dysfunction. On the contrary, rats (n=34) receiving semicircumferential patches resumed a solid diet within few days after surgery and were sacrificed until 5 months. The results showed that SIS was able to induce esophageal regrowth. Initially the authors observed the formation of new collagen tissue that, after detachment into the esophageal lumen, was progressively replaced by adjacent esophageal tissue. At 5 months, both epithelial and muscle regeneration was complete and patches were also immunoreactive against anti- protein S-100 antibody.

In another study urinary bladder matrix (UCM), obtained from porcine bladders and composed of the basement membrane of the tunica mucosa and the subjacent tunica propria, was used to repair full circumferential esophageal defects (about 5 cm) in the mid-cervical region of 22 adult female mongrel dogs. Scar tissue formation and severe stricture occurred within 21 days when UBM tube scaffold replaced full thickness segments. On the contrary, animals, repaired with UBM plus either a partial (30%) or complete (100%) covering with native muscle tissue, survived until 230 days with minimal stricture and normal clinical outcome. Patches were completely remodeled with the formation of well organized esophageal tissue layers. Moreover, the mechanical properties of remodeled esophagus tissue were very similar to those of native tissue (Badylak et al., 2005). Taken together, these results pointed out the important role of normal host skeletal muscle cells to obtain a constructive remodeling response.

AM derived from porcine aorta was used by a research group who created a 2 cm circular defect on half the circumference of the distal esophagus in 10 pigs (Kajitani et al., 2001). After 6 weeks from surgery, endoscopy showed that mucosal coverage was complete and minimal to no stenosis was observed. At 7 weeks, the regeneration of mucosal and submucosal, but not muscular layers was achieved. In the center of patches nerves and fragments of elastin fibers were identified.

In view of human applications, homologous AMs can present some advantages in comparison with xenogeneic AMs, because they may evoke lower inflammatory responses and their use is not connected with the risk of zoonosis. Today, xenotransplation can be hindered by the presence of natural antibodies to the terminal galactose alpha 1,3 galactose epitope, that is expressed on the cell membranes of all mammals except those of human and old world primates (Badylak, 2004) These antibodies can mediate hyperacute or delayed rejection of xenogeneic AMs. Starting from

this basis, other research groups have investigated the possibility to obtain esophageal substitutes starting from homologous tissues.

Gastric AM was used to repair semicircular defects (about 3-4 mm in width and 5 mm in length) in the abdominal esophagus of 27 F344 female rats (Urita et al, 2007). No stenosis or dilatation was observed at the implant site. At 2 weeks the patches were fully covered by stratified squamous epithelium. They were progressively remodeled in a non-inflammatory connective tissue containing fibroblasts and blood vessels. Nevertheless, muscle regeneration was not achieved even 18 months after implantation.

Our research group has proposed the use of homologous esophageal acellular matrix (HEAM), because it presents thickness and structure close to the native tissue. (Marzaro et al., 2006) The detergent-enzymatic method (Meezan et al., 1975) employed to produce the AMs preserved matrix integrity and completely removed the major histocompatibility complex markers. However, the expression of bFGF as protein was maintained and HEAM showed strong angiogenic activity on chorioallontoic membrane. Using 3-4 month old pigs, 2-cm diameter defects in the tonaca muscolaris of thoracic esophagus wall were covered with patches composed of either HEAM alone (n=3) and repopulated *in vitro* with autologous smooth muscle cells (SMCs) (n=3), isolated from a cervical esophagus biopsy in newborn pigs. At 3 week from surgery, the patches composed of only acellular matrices showed a more severe inflammatory response and were negative for α-smooth muscle actin immunostaining. On the contrary, the cell-matrix implants presented ingrowth of SMCs, showing an early organization into small fascicules. Collectively, these results confirm the positive contribution of implanted autologous cells to the regeneration process.

1.5 Aim of the study

- To isolation and culture of rabbit bone marrow MSC
- To Characterize MSC in regard to their differentiation potential
- To characterize esophageal acellular matrix
- To characterize acellular matrix seeded with mesenchymal stem cells(MSCs)

CHAPTER 2 MATERIALS AND METHODS

2.1 Acellular matrices. Esophagus, obtained from rabbits, were stripped of overlying tissue, rinsed four times in phosphate buffered saline (PBS) containing 1% antibiotic and antimicotic solution (AF, Sigma Chemical Company, St Louis, MO, USA), and then treated according Marzaro et al., 2006. The esophagus was treated with distilled water for 72 h at 4°C, then with 4% sodium deoxycholate (Sigma) for 4 h, and finally with 50 kU DNase-I/ml (Sigma) in 1M NaCl (Sigma) for 3 h. Acellular matrices were stored in PBS at 4 °C until use. The presence of cellular elements was verified histologically (hematoxylin–eosin and DAPI staining) after each cycle. Samples were fixed in 4% formalin, embedded in paraffin, cut into 5 μm slices, and stained with hematoxylin-eosin or DAPI. Furthermore, the treated esophagus was examined by SEM. Five micrometer frozen sections were cut, air dried and fixed with methanol. Endogenous peroxidase activity was quenched by incubating in 30 % H_2O_2 for 1 h. The slides were blocked in 10% normal horse serum for 45 min at room temperature. Samples were then incubated overnight at 4^{o}C with monoclonal anti-MHC class I, anti-MHC class II antibodies diluted in 3% HS, then incubated in secondary antibody (Vectastain ABC kit, Vector Laboratories) for 30 minutes at RT. Slides were developed using peroxidase substrate kit (DAB, Vector Laboratories) and counterstained with hematoxylin. For negative controls, the primary antibody was omitted.

2.2 Cell culture. Femur and tibiae were isolated from rabbit ^{in} sterile conditions. The tip of each bone was removed and the marrow was harvested by inserting a syringe needle (27-gauge) into one end of the bone and flushed with Dulbecco's Modified Eagle's Medium (DMEM; Gibco) supplemented with penicillin-streptomycin. Mononuclear cell (MNCs) fraction was then isolated by density gradient centrifugation using Ficoll. Cells were cultured in αMEM containing 15% fetal bovine serum (FBS), 2mm L-glutamine (Gibco, USA), 1% antibiotic solution (Sigma) at 37ºC in a humidified atmosphere containing 95% air and 5% CO_2. The medium was changed to remove non adherent cells 48 h after seeding and every 3 days thereafter. Each primary culture was replated to 2 new flasks when the Mesenchymal stem cells (MSCs) grew to approximately 70%-80% confluence.

2.3 Adipogenic, osteogenic, and myogenic differentiation of MSCs. P3 cells were seeded in 24 well plate and treated with adipogenic medium (low glucose DMEM supplemented with 10% fetal bovine serum, 1% antibiotic solution, 1 μM dexamethasone, 0.5 mM 3-isobutyl-1-methyl

xanthine, 10 μg/mL insulin and 60 μM indomethacin). Media were changed twice a week. At 3 weeks from induction, adipogenic differentiation was confirmed by the formation of lipid vacuoles stainable with Oil-Red-O.

For osteogenic differentiation P3 cells were seeded in 24 well plate and cultured with osteogenic medium (MEM supplemented with 10% fetal bovine serum, 1% antibiotic and antimicotic solution, 100 nM dexamethasone, 10 mM β-glycerophosphate, 0.05mM 2-phosphate ascorbic acid). Osteogenic mineral deposits were confirmed by Von Kossa staining.

P3 MSCs were used for myogenic differentiation. Smooth muscle cell differentiation was induced in αMEM medium containing 10 % FCS, 1% antibiotic and ascorbic acid for 14 days with media chance in every 3 days (Marzaro et al 2006). Differentiated cells were culture in chamber slides (BD Falcon) and fixed by methanol and acetic acid (1:1) at –20 °C. After washing, fixed cells were incubated for 20 min at room temperature with PBS containing 10% HS. Samples were then incubated at RT for 1 h with a rabbit anti-mouse actin (Abcam) and myosin (Abcam) followed by incubation with biotinylated Pan-Specific secondary antibody (Vector lab). The samples were detected by Texas Red® Avidin D (Vector lab) and examined under a fluorescence microscope.

2.4 Cell cultures on acellular matrices. P3 MSCs ($4x10^6$ cells/mL) were seeded on external side of the decellularized matrix in 24 well culture plates. The culture surface was about 3 cm^2. The cells were maintained in respective culture media as mentioned above. To evaluate cell adhesion at 24 and 72 h and 7 days after seeding, matrices were fixed with 3% gluteraldehyde (Merck, Darmstadt, Germany) in 0.1M cacodylate buffer (pH 7.2). After critical point drying and gold sputtering, cultures were examined by a scanning electron microscope. Matrices without cells were used as control. Cell adhesion was also confirmed by hematoxylin-eosin and DAPI stainings.

2.5 Cell cultures in bioreactor. Tubular esophageal acellular matrices were seeded with MSCs at passage 3. MSCs were detached from culture flasks, diluted with medium (1×10^7cells per mL), and applied them longitudinally to the external surface of the matrix with 200uL pipette. After every 15 min, we rotated the matrix 90 degrees until all surfaces had been completely exposed to cells. Matrix was then mounted onto a shaft of the bioreactor. Cell medium was added to totally submerge the seeded matrix and bioreactor was placed in static position for 24 hour to promote cell adhesion. After 24 hour media volume were reduced so that nearly half of the matrix

was exposed to media and rotation was started at 2 revolutions per min (37°C, 5% CO_2) for the next 48 hour. The total period of bioreactor culture was 72 h. Seeded matrix was evaluated at 24 h and 72 h by hematoxylin–eosin and DAPI stainings, and SEM.

CHAPTER 3 RESULTS

3.1 Acellular matrices

Four cycles of the detergent-enzymatic treatment were sufficient to completely decellularize esophagus specimens as determined by hematoxylin- eosin and DAPI stainings (Figure 2). SEM observation showed that the external side of esophagus matrix was characterized by bundles of irregularly arranged fibers (Figure 3). Treated tissues were free from MHC I and II antigen expression (Figure 4).

3.2 Cell cultures

BMSCs were isolated from bone marrow aspirate by their ability to adhere to tissue culture plastic. Cultured rabbit bone marrow mesenchymal stem cells displayed typical fibroblastic morphology (Figure 5). The cells were allowed to proliferate until a sufficient number were obtained for seeding onto the acellular matrices. The multi-lineage differentiation potential of the BMSCs was assessed by examining their osteogenic and adipogenic capacities. The BMSC population was successfully differentiated into both osteoblasts and adipocytes, as shown by the presence minerals accumulation by Von Kossa staining and fat vacuoles stained with oil red-O (Figure 6A and B). Smooth muscle cells differentiated from MSC showed more intense alpha actin immunostaning (Figure 7).

3.3 *In vitro* cultures of MSCs on acellular matrices in 24 well plate

SEM images at 24 h showed that many round cells attached to matrix obtained by the detergent-enzymatic method (Figure 8A). At 72 h, cells were more flattened and almost completely covered the matrix surface (Figure 8B) and at 7 days (Figure 8C) cells formed the completely monolayer over the matrix. The surface of not reseeded acellular matrices, used as control, did not present cells. Histological staining confirmed the presence of cells on all over the matrix (Figure 9).

3.4 Cell seeding on acellular matrix in bioreactor

The procedure applied to seed BMSCs on tubular esophageal acellular matrix allowed easy and highly efficient cell seeding. The bioreactor worked properly and no contamination was observed during the whole culture period. MSCs were seeded on the matrix (Figure 10A), then kept in the bioreactor (Figure 10B) and completely immersed in media in static condition for 24 h. The cells

attached to matrix and formed a monolayer but showed unsystematic pattern of alignment as shown by the SEM images (Figure 10C and 10D).

After 24 h from seeding the motor of bioreactor was started for another 48 hour for the rotation of the seeded matrix. SEM images at 72 h (Figure 10E and 10F) showed that the MSCs formed a complete monolayer all over the matrix and aligned in the direction of rotation. Moreover, the appearance of cells changed from a fibroblast like appearance to a more fusiform shape and cells were elongated. Histological staining after 72 h further confirmed that MSCs covered the matrix (Figure 11).

3.5 FIGURES

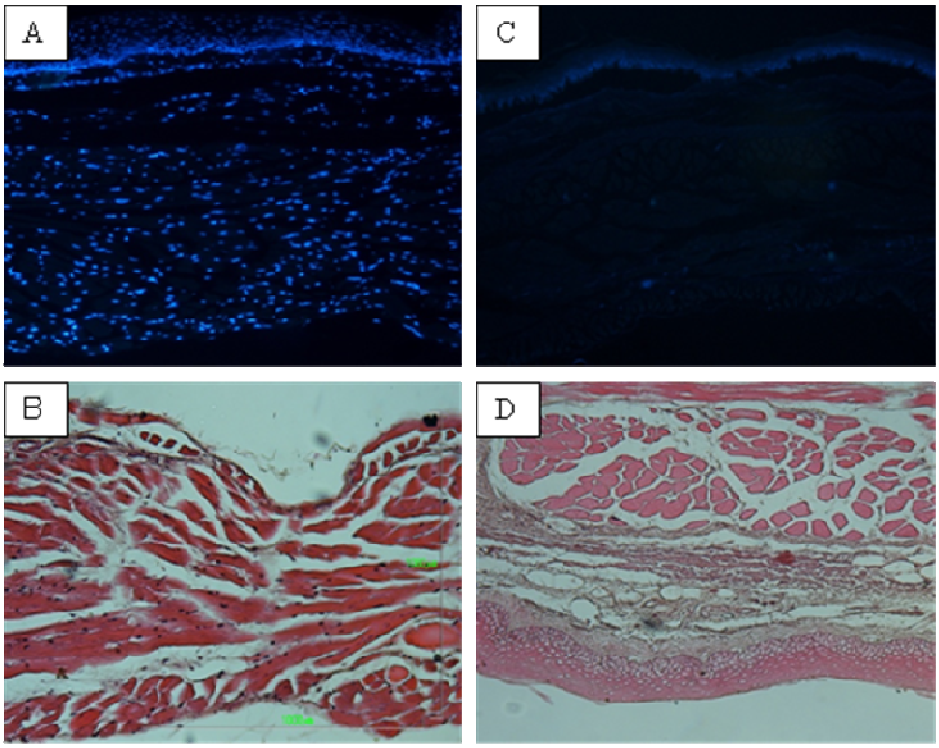

Figure 2. A and **C** are DAPI staining of non treated rabbit esophagus and after 4 cycles of the detergent-enzymatic treatment. **B** and **D** are hematoxylin–eosin staining of non treated rabbit esophagus and after 4 cycles of the detergent-enzymatic treatment.

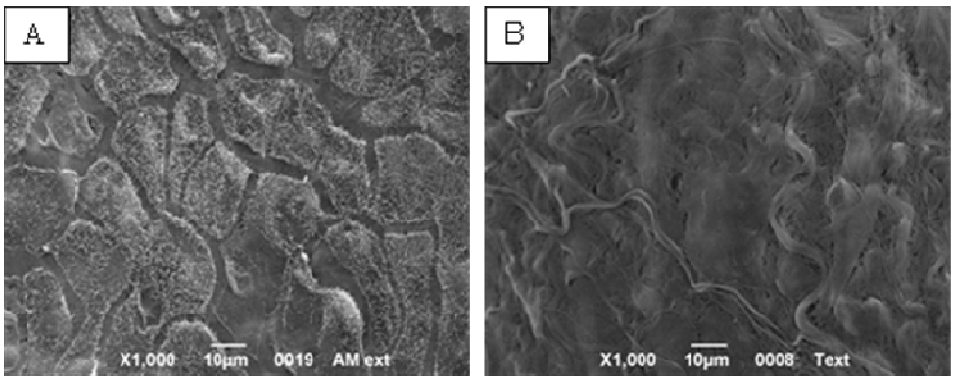

Figure 3. A. Scanning electron microscopy of non treated esophagus. **B**. After 4 cycles of the detergent-enzymatic treatment**.**

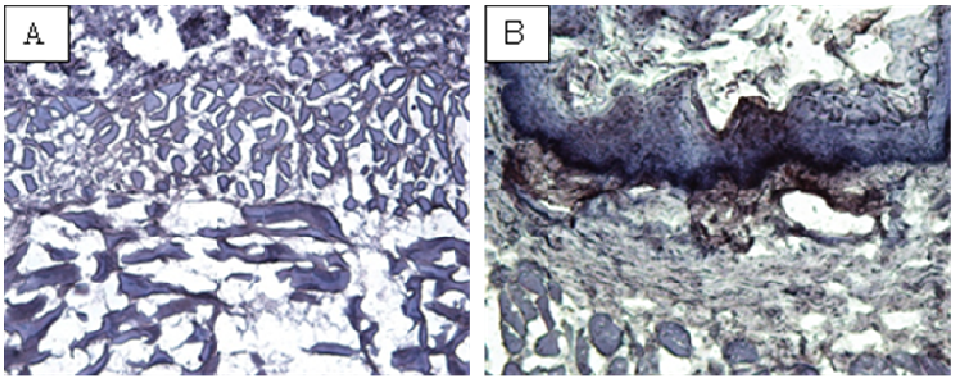

Figure 4. A. Treated esophagus after 4 cycles of detergent-enzymatic treatment and and immunostainined with monoclonal anti-MHC class I antibody. **B**. Nontreated stained with anti-MHC class I antibody**.**

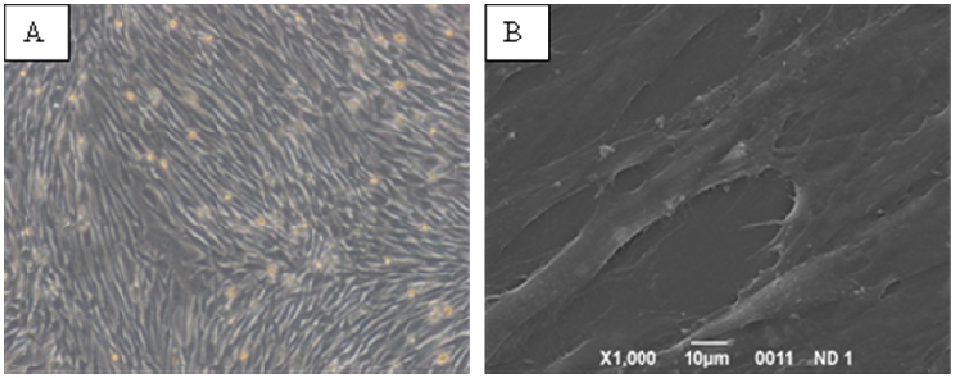

Figure 5. A. Light microscopy (magnification x100) P2 MSC cultures. **B**. Scanning electron microscopy of P2 MSCs.

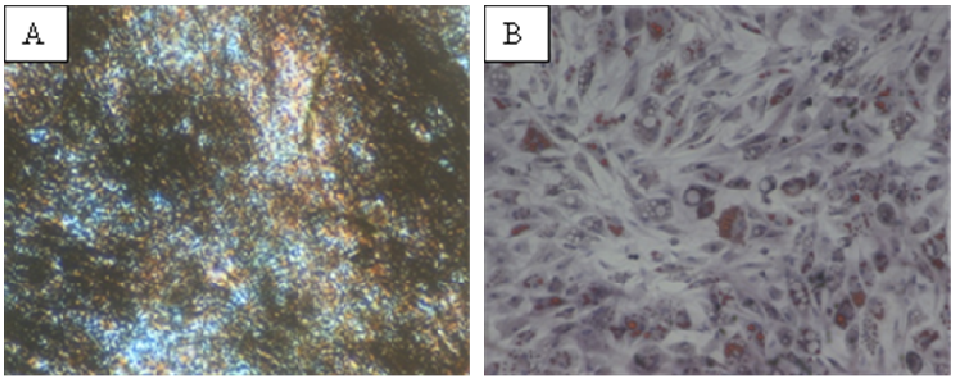

Figure 6. Multi-lineage differentiation potential of BMSCs. Expanded BMSCs from passage 3 were incubated in osteogenic or adipogenic differentiation medium for 3 weeks. **A**. Minerals characteristic of osteogenic differentiation were stained with von Kossa staining. **B**. Fat vacuoles characteristic of adipocytes were stained with oil red-O. Magnification x100.

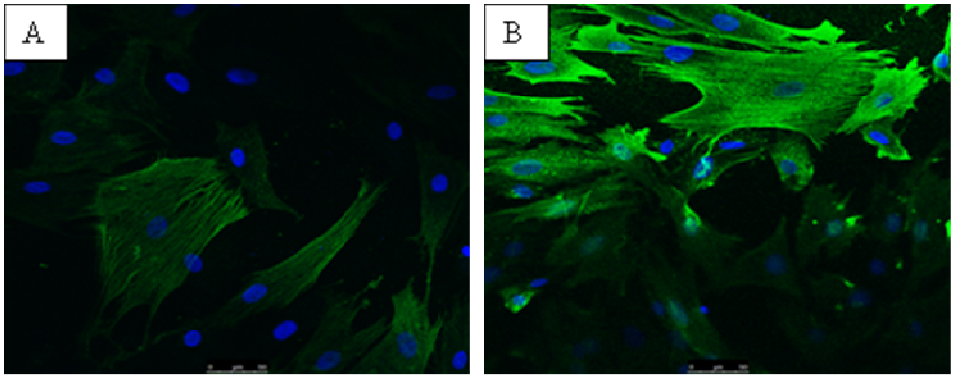

Figure 7. Immunofluorescence of MSC for α-SMA (green) counterstained with DAPI (blue). **A.** Control MSCs after 14 days**. B.** MSCs exposed to BME and AA for 14 days are more confluent and are marked by the appearance of pronounced actin stress fibers**.** Magnification x100.

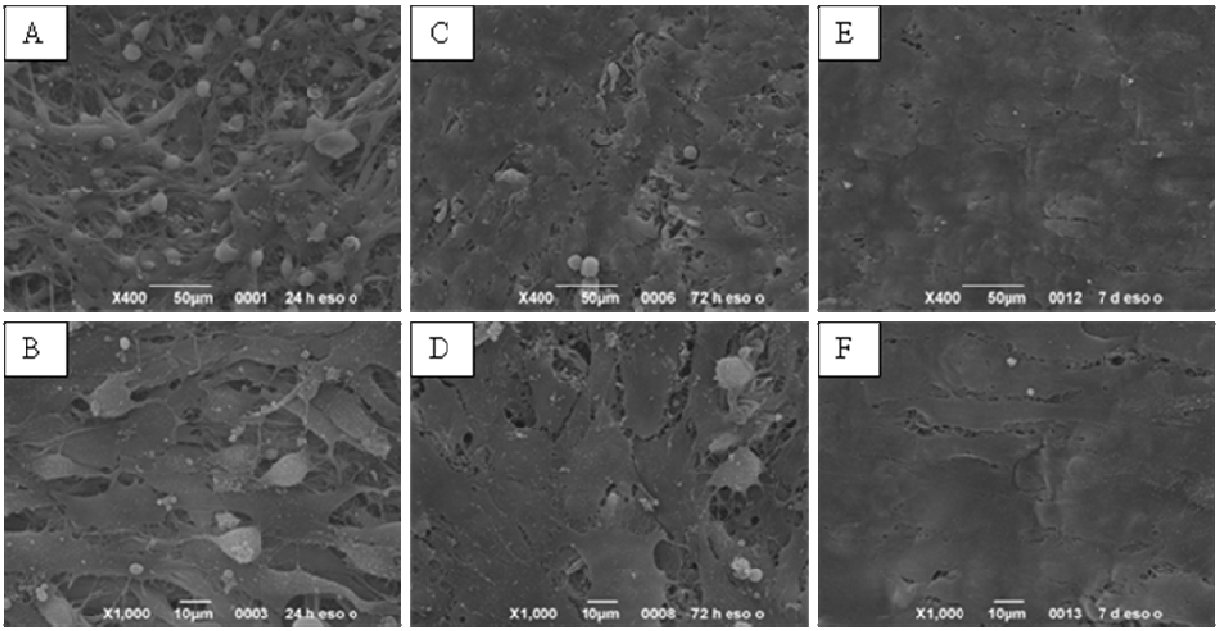

Figure 8. A and B. Scanning electron microscopy of acellular esophageal matrices after 24 from MSC seeding. **C** and **D.** After 72. **E** and **F.** After 7 days.

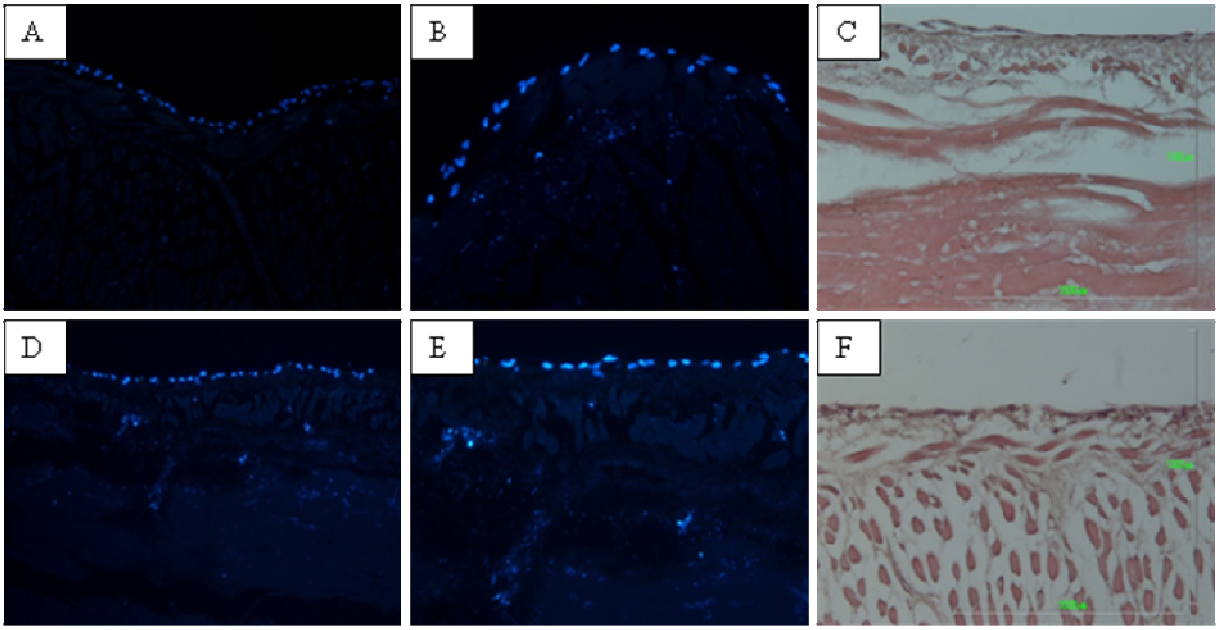

Figure 9. A and B. treated matrix seeded with MSCs and stained with DAPI after 72h. **C**. Haematoxylin–eosin staining after 72h. **D and E** DAPI stained matrix after 7 days from seeding. **F**. Haematoxylin–eosin staining after 7 days.

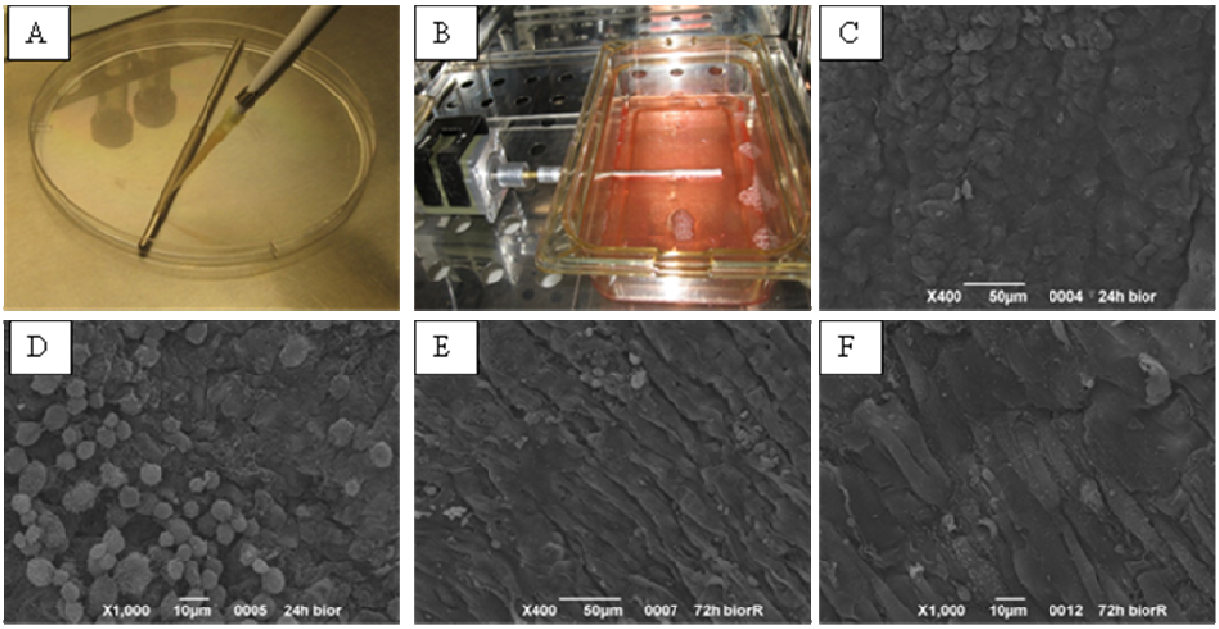

Figure 10. Seeding of the cells on acellular matrix and culture in bioreactor. **A**. Cell seeding on acellular esophageal matrix. **B**. Bioreactor used in this study. **C** and **D**. Scanning electron microscopy of MSCs seeded esophagus matrices after 24h. **E** and **F.** After 72 h from cell seeding.

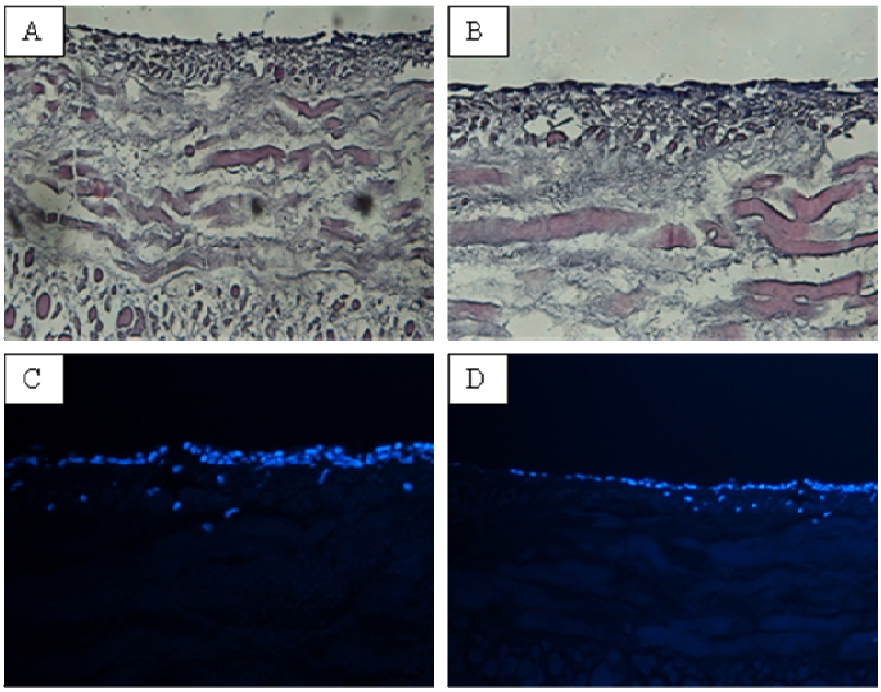

Figure 11. A and B. Haematoxylin–eosin stained matrix after 72h from cell seeding using bioreactor. **C and D**. DAPI staining after 72h of the same matrix.

CHAPTER 4 DISCUSSION

Recent technological progress in the field of tissue engineering has provided some possible alternative approaches for reconstruction of the esophagus. There is a need for tissue engineering of esophageal tissue as it has widespread application for the pediatric and adult patients. Long gap atresia, cancer, Barrett's esophagus, and esophagus strictures and stenosis (corrosive esophagitis after alkaline ingestions) are some pathologic states that may necessitate esophagus replacement (Patrick et al., 1998; American cancer Society., 2007). However, attempts to replace the esophagus with natural, synthetic, and experimental substitutes have been futile because of problems such as leakage, infections, or stenosis being associated with them (Takimoto et al., 1995; Chen and Badylak, 2001; Lindberg and Badylak, 2001). Furthermore, none of the tissue-engineered approaches guarantees a full reconstruction of muscle layer and nervous fiber network that allow the formation of a functional new esophagus.

In the present work we have demonstrated that esophagus matrices obtained by a detergent-enzymatic method can support in vitro adhesion of MSCs both in static condition and bioreactor thereby suggesting an alternative tissue-engineered approach to the repair or replacement of esophagus defects.

In the last few years, evidences has been accumulated that acellular matrices could be successfully employed to repair skin (Takami et al., 1996) intestinal (Parnigotto et al., 2000) urethral (Parnigotto et al., 2000) and skeletal muscle (Marzaro et al., 2002; Conconi et al, 2005) defects in experimental animals. Moreover, tissue-engineered constructs, populated with autologous cells, are showing promising results in early clinical trials (Atala et al., 2006; Macchiarini et al., 2008; Priya et al., 2008).

These biocompatible scaffolds function as templates that provide a structural support during tissue development. Moreover, decellularized matrices obtained from human skin (Isch et al., 2001) or porcine aorta (Kajitani et al., 2001) has been already used for esophageal replacement. We proposed the use of homologous esophageal acellular matrix, because it presents thickness and structure close to the native tissue. The detergent-enzymatic method employed to obtain the acellular matrices preserves matrix integrity (Livesey et al., 1995) which represents an important factor to avoid their *in vivo* destruction ensuing from the obvious inflammatory response (Burge et al, 1990). Additionally, the decellularization process abolishes the risk of rejection (Allman et

al, 2001) since it completely removes the major histocompatibility complex markers (the MHC class I and MHC class II antigens). We demonstrated that 4 cycles of the detergent-enzymatic treatment was sufficient to reduce the expression of MHC antigens in rabbit esophagus matrix.

An ideal cell source for tissue engineering should have the capacity to first proliferate and then differentiate *in vitro*, via medium supplementation in a manner that can be reproducibly controlled. MSC are non hematopoietic multipotent stem cells that exist in bone marrows for the whole lifespan of mammals. MSCs are one of the most promising candidates for tissue engineering, as these cells have the potential for multilineage differentiation (Pittenger et al, 1999). Studies revealed that MSCs can also differentiate into SMCs using different factors (Wen-Chi et al., 2006). Further autologous MSCs offer functional restoration without the need for immunosuppression.Taken together, the robust capacity of MSCs for proliferation and differentiation establish them as a suitable cell source for tissue engineering.

Adequate amount of cells and cell attachment on 3D matrices is a prerequisite to the production of clinically relevant engineered tissue. Hence we obtained an *in vitro* esophageal substitute composed of autologous MSCs seeded on homologous esophageal acellular matrix. Our findings demonstrate that esophageal acellular matrix was able to support cell adhesion, and in as much as just after 24 h from seeding, the scaffold appeared completely covered by MSC both in static culture and bioreactor.

The alignment of cells perpendicular to the direction of strain has been reported in a number of previous studies (Cha et al., 2006; Haga et al., 2007; Hayakawa et al., 2000; Hayakawa et al., 2001; Nerem, 2001) using sheet membranes and a monolayer of smooth muscle cells of vascular or esophageal origin. Cyclic stress also promotes the expression of smooth muscle-like properties also reported in number of studies (Kobayashi et al., 2004; Park et al., 2004; Engelmayr et al., 2006*)*. The current study also demonstrated that direction of the rotation changed the morphology and alignment of MSCs. MSCs changed their morphology in response to rotation: they were elongated and oriented in the direction of rotation after exposure to rotation for 48 hours.

4.1 CONCLUSION

Esophageal substitution remains one of the highest challenges for the general and pediatric surgeons. Until today it doesn't exist the ideal esophageal substitute because every different autologous segment utilized for this purpose, stomach, ileum or colon, doesn't exhibit the same characteristics in motility and continence of the native esophagus. Moreover, the technical difficulties in taking to the thorax an abdominal colic or ileo-colic segment are elevated and complication rate still remarkable.

In this perspective, tissue engineering approach acquire a notable role in the view of future construction of non rejectable, specifically shaped segments that can easily integrate in the host and avoid major surgical operations. Natural materials seem to be more valuable than artificial ones because they may mimic the ECM environment allowing both host cell ingrowth and neo-vessel formation. In this context, acellular matrices can play a major role, as elicit low inflammatory response, possess suitable shape and physical properties, such as mechanical strength, and can be produced easily at low cost. Moreover, a great bulk of evidences clearly indicates that the presence of autologous cells in the tissue engineered constructs is almost mandatory and strongly improves the outcomes of reconstructive surgery. Nevertheless, experimental data also point out that, in most cases, the successful replacement of long circumferential tract of esophagus remains an unsolved problem. To improve the effectiveness of tissue engineered esophageal substitutes seems to be noteworthy to stimulate also the regeneration from the body's own tissues using combinations of regeneration-permissive molecules and neutralizers of regeneration-inhibiting molecules.

In the present study we attempted to evaluate the adhesion of MSCs on acellular esophageal matrix for esophagus tissue engineering. MSCs were isolated from rabbit bone marrow, characterized, expanded *in vitro*, and seeded onto rabbit acellular esophageal matrix. Our findings demonstrate that esophageal acellular matrix was able to support cell adhesion, and in as much as just after 24 h from seeding, the scaffold appeared completely covered by MSC.

In conclusion, although tissue engineering may represent an attractive promise for esophageal replacement, further work needs to be done and several issues must be solved before becoming a concrete therapeutic option.

REFERENCES

Alcantara PS, Spencer-Netto FA, Silva-Júnior JF, Soares LA, Pollara WM, Bevilacqua RG. Gastro-esophageal isoperistaltic bypass in the palliation of irresectable thoracic esophageal cancer. Int Surg 1997; 82:249-253.

Alhadlaq A , Mao JJ. Mesenchymal Stem Cells: Isolation and Therapeutics. Stem Cells Dev 2004; 13:436-448.

Allman AJ, McPherson TB, Badylak SF, Merrill LC, KallakuryB, Sheehan C, Raeder RH, Metzger DW. Xenogeneic extracellular matrix grafts elicit a Th2-restricted immune response. Transplantation 2001; 71:1631-1640.

Altorki N, Skinner D. Should en bloc esophagectomy be the standard of care for esophageal carcinoma? Ann Surg 2001; 234:581-587.

American Cancer Society. Esophagus Cancer Detailed Guide. www. cancer.org, 2007.

Anjos-Afonso F, Bonnet D. Nonhematopoietic/endothelial SSEA-1 cells define the most primitive progenitors in the adult murine BM mesenchymal compartment. Blood 2007; 109:1298-1306.

Atabek C, Surer I, Demirbag S, Caliskan B, Ozturk H, Cetinkursun S. Increasing tendency in caustic esophageal burns and long-term polytetrafluoroetylene stenting in severe cases: 10 years experience J Pediatr Surg 2007; 42: 636-640.

Atala A, Bauer SB, Soker S, Yoo JJ, Retik AB. Tissue-engineered autologous bladders for patients needing cystoplasty. Lancet 2006; 367:1241-6.

Badylak S, Meurling S, Chen M, Spievack A, Simmons-Byrd A. Resorbable bioscaffold for esophageal repair in a dog model.J Pediatr Surg 2000; 35:1097-1103.

Badylak SF, Vorp DA, Spievack AR, Simmons-Byrd A, Hanke J, Freytes DO, Thapa A, Gilbert TW, Nieponice A.. Esophageal reconstruction with ECM and muscle tissue in a dog model. J Surg Res 2005; 128:87-97.

Badylak SF. Xenogeneic extracellular matrix as a scaffold for tissue reconstruction. Transpl Immunol 2004; 12:367-377.

Bagolan P, Iacobelli Bd B, De Angelis P, di Abriola GF, Laviani R, Trucchi A, Orzalesi M, Dall'Oglio L. Long gap esophageal atresia and esophageal replacement: moving toward a separation? J Pediatr Surg 2004; 39:1084-1090.

Baksh D, Song L, Tuan RS. Adult mesenchymal stem cells: characterization, differentiation, and application in cell and gene therapy. J Cell Mol Med 2004; 8:301-316.

Burge SM, Dawber RPR. Hair follicle destruction and regeneration in guinea pig skin after cutaneous freeze injury. Cryobiology 1990; 27:153-163.

Burra P, Tomat S, Conconi MT, Macchi C, Russo FP, Parnigotto PP, Naccarato R, Nussdorfer GG. Acellular liver matrix improves the survival and functions of isolated rat hepatocytes cultured in vitro. Int J Mol Med. 2004;14:511-515

Caplan AI, Reuben D, Haynesworth SE. Cell-based tissue engineering therapies: the influence of whole body physiology. Adv Drug Deliv Rev 1998 ;33:3-14.

Cha JM, Park SN, Noh SH, Suh H. Time-dependent modulation of alignment and differentiation of smooth muscle cells seeded on a porous substrate undergoing cyclic mechanical strain. Artif Organs 2006; 30:250-258.

Chen MK, Badylak SF. Small bowel tissue engineering using small intestinal submucosa as a scaffold. J Surg Res 2001; 99:352-8.

Conconi MT, De Coppi P, Bellini S, Zara G, Sabatti M, Marzaro M, Zanon GF, Gamba PG, Parnigotto PP, Nussdorfer GG. Homologous muscle acellular matrix seeded with autologous myoblasts as a tissue-engineering approach to abdominal wall-defect repair. Biomaterials 2005; 26:2567-2574.

Conconi MT, De Coppi P, Di Liddo R, Vigolo S, Zanon GF, Parnigotto PP, Nussdorfer GG. Tracheal matrices, obtained by a detergent-enzymatic method, support in vitro the adhesion of chondrocytes and tracheal epithelial cells. Transpl Int 2005; 18:727-734.

Conconi MT, Rocco F, Spinazzi R, Tommasini M, Valfrè C, Busetto R, Polesel E, Albertin G, Dei Tos A, Iacopetti I, et al. Biological fate of tissue-engineered porcine valvular conduits xenotransplanted in the sheep thoracic aorta. Int J Mol Med. 2004; 14:1043-1048

Cook AD, Hrkach JS, Gao NN, Johnson IM, Pajvani UB, Cannizzaro SM, Langer R. Characterization and development of RGD-peptide-modified poly(lactic acid-co-lysine) as an interactive, resorbable biomaterial. J Biomed Mater Res 1997; 35:513-523.

Cywes S, Millar AJW, Rode H, Brown A. Corrosive strictures of the oesophagus in children Pediatr Surg Int 1993; 8:8-13.

Dettin M, Conconi MT, Gambaretto R, Bagno A, Di Bello C, Menti AM, Grandi C, Parnigotto PP. Effect of synthetic peptides on osteoblast adhesion. Biomaterials 2005; 26:4507-4515.

Edwards, R.G. Stem cells today: A. Origin and potential of embryo stem cells. Reproductive biomedicine 2004; 8;275-306.

Ellis FH Jr. Standard resection for cancer of the esophagus and cardia. Surg Oncol Clin N Am. 1999; 8:279-294.

Engelmayr GC Jr, Sales VL, Mayer JE Jr, Sacks MS. Cyclic flexure and laminar flow synergistically accelerate mesenchymal stem cellmediated engineered tissue formation: implications for engineered heart valve tissues. Biomaterials 2006; 27: 6083–95.

Freyman TM, Yannas IV, Yokoo R, Gibson LJ. Fibroblast contraction of a collagen-GAG matrix. Biomaterials 2001; 22:2883-2891.

Gardner, R.L. Stem cells and regenerative medicine: principles, prospects and problems. C. R. Biol 2007; 330:465-473.

Gawad KA, Hosch SB, Bumann D, Lübeck M, Moneke LC, Bloechle C, Knoefel WT, Busch C, Küchler T, Izbicki JR. How important is the route of reconstruction after esophagectomy: a prospective randomized study. Am J Gastroenterol 1999; 94:1490-1496.

Gilbert TW, Sellaro TL, Badylak SF. Decellularization of tissues and organs. Biomaterials. 2006 ; 27:3675-3683.

Gonzalez Saez LA, Arnal Monreal F, Pita Fernandez S, Machuca Santa Cruz J. Experimental study using PTFE (Goretex) patches for replacement of the oesophageal wall. Eur Surg Res 2003;35:372-376.

Grikscheit T, Ochoa ER, Srinivasan A, Gaissert H, Vacanti JP. Tissue-engineered esophagus: experimental substitution by onlay patch or interposition. J Thorac Cardiovasc Surg 2003; 126:537-544.

Haga JH, Li YS, Chien S. Molecular basis of the effects of mechanical stretch on vascular smooth muscle cells. J Biomech 2007; 40:947-960.

Hayakawa K, Hosokawa A, Yabusaki K, Obinata T. Orientation of smooth muscle-derived A10 cells in culture by cyclic stretching: Relationship between stress fiber rearrangement and cell reorientation. Zoological Science (VSP International Science Publishers) 2000; 17:617.

Hayakawa K, Sato N, Obinata T. Dynamic reorientation of cultured cells and stress fibers under mechanical stress from periodic stretching. Exp Cell Res 2001; 268:104-114.

Hayashi K, Ando N, Ozawa S, Kitagawa Y, Miki H, Sato M, Kitajima M. A neo-esophagus reconstructed by cultured human esophageal epithelial cells, smooth muscle cells, fibroblasts, and collagen. ASAIO J 2004; 50:261-266.

Holder WD, Gruber HE, Roland WD, Moore AL, Culberson CR, Loebsack AB, Burg K, Mooney DJ. Increased vascularization and heterogeneity of vascular structures occurring in polyglycolide matrices containing aortic endothelial cells implanted in the rat. Tissue Eng 1997; 3:149-160.

In 't Anker PS, Noort WA, Scherjon SA, Kleijburg-van der Keur C, Kruisselbrink AB, van Bezooijen RL, Beekhuizen W, Willemze R, Kanhai HH, Fibbe WE. Mesenchymal stem cells in human second trimester bone marrow, liver, lung, and spleen exhibit a similar immunophenotype but a heterogeneous multilineage differentiation potential. Haematologica 2003; 88:845-852.

Isch JA, Engum SA, Ruble CA, Davis MM, Grosfeld JL Patch esophagoplasty using AlloDerm as a tissue scaffold J Pediatr Surg 2001; 36:266-268.

Kajitani M, Wadia Y, Hinds MT, Teach J, Swartz KR, Gregory KW. Successful repair of esophageal injury using an elastin based biomaterial patch. ASAIO J 2001; 47:342-345.

Kato H, Fukuchi M, Miyazaki T, Nakajima M, Tanaka N, Inose T, Kimura H, Faried A, Saito K, Sohda M, et al. Surgical treatment for esophageal cancer. Dig Surg 2007; 24:88-95.

Khan AZ, Nikolopolous I, Botha AJ, Mason RC. Substernal long segment left colon interposition for oesophageal replacement. Surgeon 2008; 6:54-56.

Knight MA, Evans GR. Tissue engineering: progress and challenges. Plast Reconstr Surg 2004; 114:26E-37E.

Kobayashi N, Yasu T, Ueba H, Sata M, Hashimoto S, Kuroki M, Saito M, Kawakami M. Mechanical stress promotes the expression of smooth musclelike properties in marrow stromal cells. Exp Hematol 2004; 32:1238–45.

Langer R, Tirrell DA. Designing materials for biology and medicine. Nature 2004; 428:487-492.

Law S, Wong J. What is appropriate treatment for carcinoma of the thoracic esophagus? World J Surg 2001; 25:189-195.

Lindberg K, Badylak SF. Porcine small intestinal submucosa (SIS): a bioscaffold supporting in vitro primary human epidermal cell differentiation and synthesis of basement membrane proteins. Burns 2001; 27:254-66.

Livesey SA, Herndon DN, Hollyoak MA, Atkinson YH, Nag A. Transplanted acellular allograft dermal matrix. Transplantation 1995; 60:1-9.

Logan A. The surgical treatment of carcinoma of the esophagus and cardia. J Thorac Cardiovasc Surg 1963; 46:150-161.

Lopes MF, Cabrita A, Ilharco J, Pessa P, Paiva-Carvalho J, Pires A, Patrício J. Esophageal replacement in rat using porcine intestinal submucosa as a patch or a tube-shaped graft. Dis Esophagus 2006; 19:254-259.

Lynen Jansen P, Klinge U, Anurov M, Titkova S, Mertens PR, Jansen M. Surgical mesh as a scaffold for tissue regeneration in the esophagus Eur Surg Res 2004; 36:104-111.

Macchiarini P, Jungebluth P, Go T, Asnaghi MA, Rees LE, Cogan TA, et al. Clinical transplantation of a tissue-engineered airway. Lancet 2008; 372:2023-30.

Mariette C, Piessen G, Triboulet JP. Therapeutic strategies in oesophageal carcinoma: role opf surgery and other modalities Lancet Oncol 2007; 8:545-553.

Marijnissen WJ, van Osch GJ, Aigner J, van der Veen SW, Hollander AP, Verwoerd-Verhoef HL, Verhaar JA. Alginate as a chondrocyte-delivery substance in combination with a non-woven scaffold for cartilage tissue engineering. Biomaterials 2002; 23:1511-1517.

Marzaro M, Conconi MT, Perin L, Giuliani S, Gamba P, De Coppi P, Perrino GP, Parnigotto PP, Nussdorfer GG. Autologous satellite cell seeding improves in vivo biocompatibility of homologous muscle acellular matrix implants. Int J Mol Med 2002; 10:177-182.

Marzaro M, Vigolo S, Oselladore B, Conconi MT, Ribatti D, Giuliani S, Nico B, Perrino G, Nussdorfer GG, Parnigotto PP. In vitro and in vivo proposal of an artificial esophagus. J Biomed Mater Res A 2006; 77:795-801.

Meezan E, Hjelle JT, Brendel K. A simple, versatile, nondisruptive method for the isolation of morphologically and chemicaly pure basement membranes from several tissues. Life Sci 1975; 17:1721-1732.

Miki H, Ando N, Ozawa S, Sato M, Hayashi K, Kitajima M. An artificial esophagus constructed of cultured human esophageal epithelial cells, fibroblasts, polyglycolic acid mesh, and collagen. ASAIO J 1999; 45:502-508.

Mooney DJ, Mikos AG. Growing new organs. Sci Am 1999; 280:60-65.

Nerem RM, Seliktar D. Vascular tissue engineering. Annu Rev Biomed Eng 2001; 3:225-243.

Othersen HB Jr, Parker EF, Smith CD.The surgical management of esophageal stricture in children. A century of progress. Ann Surg 1988; 207:590-597.

Park JS, Chu JS, Cheng C, Chen F, Chen D, Li S. Differential effects of equiaxial and uniaxial strain on mesenchymal stem cells. Biotechnol Bioeng 2004; 88: 359-68.

Parnigotto PP, Gamba PG, Conconi MT, Midrio P. Experimental defect in rabbit urethra repaired with acellular aortic matrix. Urol Res 2000; 28:46-51.

Parnigotto PP, Marzaro M, Artusi T, Perrino G, Conconi MT. Short bowel syndrome: experimental approach to increase intestinal surface in rats by gastric homologous acellular matrix. J Pediatr Surg 2000; 35:1304-1308.

Patrick Jr CW, Mikos AG, McIntire LV. Frontiers in tissue engineering. New York: Elsevier Science; 1998.

Phinney D.G. Building a consensus regarding the nature and origin of mesenchymal stem cells. Journal of Cellular Biochemistry 2002; 38:7-12.

Pittenger MF, Mackay AM, Beck SC, Jaiswal RK, Douglas R, Mosca JD, Moorman MA, Simonetti DW, Craig S, Marshak DR. Multilineage potential of adult human mesenchymal stem cells. Science 1999; 284:143-147.

Prockop DJ, Sekiya I, and Colter DC. Isolation and characterization of rapidly self-renewing stem cells from cultures of human marrow stromal cells. Cytotherapy 2001; 3:393-396.
Priya SG, Jungvid H, Kumar A. Skin tissue engineering for tissue repair and regeneration. Tissue Eng Part B Rev 2008; 14:105-18.

Ring WS, Varco RL, L'Heureux PR, Foker JE. Esophageal replacement with jejunum in children: an 18 to 33 year follow-up. J Thorac Cardiovasc Surg 1982; 83:918-927.

Rosso F, Giordano A, Barbarisi M, Barbarisi A. From cell-ECM interactions to tissue engineering. J Cell Physiol 2004; 199:174-180.

Sato M, Ando N, Ozawa S, Miki H, Kitajima M. An artificial esophagus consisting of cultured human esophageal epithelial cells, polyglycolic acid mesh, and collagen. ASAIO J 1994; 40:389-92.

Shieh SJ, Vacanti JP. State-of-the-art tissue engineering: from tissue engineering to organ building. Surgery 2005; 137:1-7.

Shinhar D, Finaly R, Niska A, Mares AJ. The use of collagen-coated vicryl mesh for reconstruction of the canine cervical esophagus. Pediatr Surg Int 1998; 13:84-87.

Simmons PJ and Torok-Storb B. Identification of stromal cell precursors in human bone marrow by a novel monoclonal antibody, STRO-1. Blood 1991; 1:55-62.

Spitz L. Gastric transposition via the mediastinal route for infants with long-gap esophageal atresia. J Pediatr Surg 1984 ; 19:149-154.

Stone MM, Fonkalsrud EW, Mahour GH, Weitzman JJ, Takiff H. Esophageal replacement with colon interposition in children. Ann Surg 1986; 203:346-351.

Takami Y, Matsuda T, Yoshitake M, Hanumadass M, Walter RJ. Dispase/detergent treated dermal matrix as a dermal substitute. Burns 1996; 22:182-190.

Takimoto Y, Nakamura T, Teramachi M, Kiyotani T, Shimizu Y. Replacement of long segments of the esophagus with a collagen silicone composite tube. ASAIO J 1995; 41:605-608.

Takimoto Y, Nakamura T, Yamamoto Y, Kiyotani T, Teramachi M, Shimizu Y. The experimental replacement of a cervical esophageal segment with an artificial prosthesis with the use of collagen matrix and a silicone stent J Thorac Cardiovasc Surg 1998; 116:98-106.

Urita Y, Komuro H, Chen G, Shinya M, Kaneko S, Kaneko M, Ushida T. Regeneration of the esophagus using gastric acellular matrix: an experimental study in a rat model. Pediatr Surg Int 2007; 23:21-26.

Wen-Chi C. Lee, J. Peter Rubin , Kacey G. Marra Regulation of Smooth Muscle Actin Protein Expression in Adipose-Derived Stem Cells. Cells Tissues Organs 2006; 183:80-86.

Yamamoto Y, Nakamura T, Shimizu Y, Matsumoto K, Takimoto Y, Kiyotani T, Sekine T, Ueda H, Liu Y, Tamura N. Intrathoracic esophageal replacement in the dog with the use of an artificial esophagus composed of a collagen sponge with a double-layered silicone tube. J Thorac Cardiovasc Surg 1999; 118:276-286.

Yamamoto Y, Nakamura T, Shimizu Y, Matsumoto K, Takimoto Y, Liu Y, Ueda H, Sekine T, Tamura N. Intrathoracic esophageal replacement with a collagen sponge--silicone double layer tube: evaluation of omental-pedicle wrapping and prolonged placement of an inner stent. ASAIO J 2000; 46:734-739.

Zuk PA, Zhu M, Mizuno H, Huang J, Futrell JW, Katz AJ, Benhaim P, Lorenz HP, Hedrick MH. Multilineage cells from human adipose tissue: implications for cell-based therapies. Tissue Eng. 2001;7:211-28.